DIGITAL IMPLEMENTATION OF A D.P.S.K. DEMODULATOR

by

P. CONSTANTINOU

A thesis submitted to the School of Graduate Studies

Engineering in partial fulfilment of the

requirements for the degree of

Master of Applied Science

Department of Electrical Engineering

Faculty of Science and Engineering

University of Ottawa

Ottawa, Canada

July, 1976

TO JOANNE

ABSTRACT

The advantages of discrete circuit realization lead one to investigate the possible implementation of the Differential Phase-Shift Keying (D.P.S.K.) detector digitally. This is accomplished by sampling the incoming R.F. signal at the output of the bandpass filter directly with the decision process taking place right after the sampling point. The majority of the circuit can then be constructed digitally. The effects of timing errors at the sampling instants are evaluated as well the Bit Error Rate (B.E.R.) versus E_B/N_o, in the case where white Gaussian noise is added to the signal. The performance of the circuit for different sampling rates has been evaluated including also cases where more than one sample is taken per symbol period T.

ACKNOWLEDGEMENT

The author is greatly indebted to his thesis supervisor Professor Dr. W. Steenaart for his encouragement and constructive criticism at all stages of this research.

The author is also grateful to Professor S.G.S. Shiva for useful discussions during the project.

Special thanks are extended to Mr. M. Master for many hours of assistance and guidance with the computational procedure.

Thanks are also given to the following individuals, Mr. B. Carraro, Mr. M. Dickerson, Mr. R. Le-Hénaff, Mr. R. Scott, Mr. C. Steele, and to Mrs. A. Granger for typing this thesis.

TABLE OF CONTENTS

LIST OF FIGURES

FIGURES (Cont'd)

LIST OF TABLES

1. INTRODUCTION

1.1 DIGITAL PHASE MODULATION SYSTEMS

The need of efficient utilization of various media for transmission of digital data has stimulated the investigation of advanced coding and modulation techniques.

One of these modulation techniques, digital phase modulation, which is referred to as Phase-Shift-Keying (P.S.K.), has been successfully employed to transmit digital data over high frequency channels (in the GHz range) where fading and multipath phenomena are encountered. In P.S.K. systems digital information is conveyed in the form of phase difference successive radio frequency pulses. In the case of two phase P.S.K. system, one phase of the carrier frequency is used to represent one binary state, and another phase, usually 180^{o}C apart is used for the second state Figure 1.1.

The two phases are generally detected by multiplying the received signal with a reference signal which is of the same frequency as the incoming carrier and of known phase with respect to it. This type of detection is referred to as Coherent Detection [1], [2], [3], [4]. The binary decision is based on the algebraic sign of the detector output. A simplified block diagram of coherent detection of P.S.K. signal is shown in Figure 2.

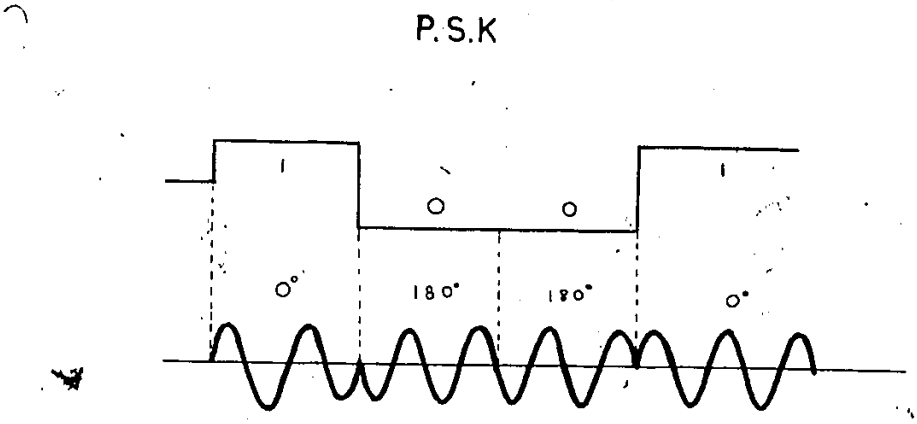

Fig. 1.1. Representations of a P.S.K. signal

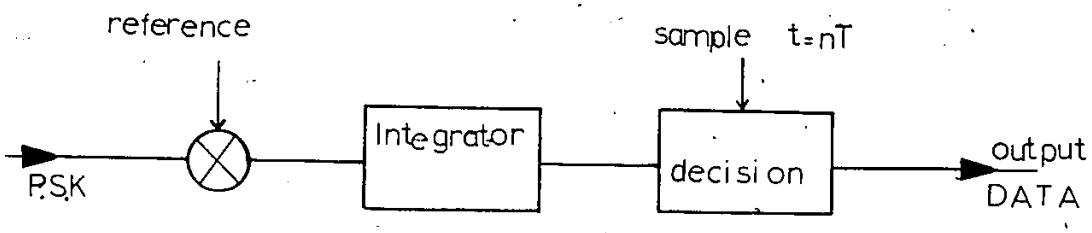

Fig. 1.2. P.S.K. Detector

1.2 DIFFERENTIAL PHASE-SHIFT KEYING (D.P.S.K.) SYSTEMS

Because of the difficulties of establishing and maintaining the absolute phase reference at the receiver, it is common practice to encode the information in terms of phase changes and to detect the signal by comparing phases of adjacent symbols. This is called differential phase-shift keying (D.P.S.K.) which is also known under the name <<KINEPLEX>> as incorporated by Collins Radio Co. [1], [2], [3], [4].

In this technique, information is encoded not by absolute identification of say, 0° phase with Mark and 180° with space, but rather by differentially encoding the informations in terms of the phase change between successive pulses. For example, no phase shift from the previous pulse could designate Mark (+) and 180° phase shift could designate a space (-). The generation of D.P.S.K. signal is shown in Figure 1.3.

The binary encoded message is represented by the sequence a_n, a differentially encoded sequence b_n is generated from it. Note that the sequence b_n requires one more digit than the sequence a_n. The first digit is arbitrary, and we have assumed it to be a 1. Succeeding digits in b_n are determined on the basis of the rule

$$b_n = a_n \oplus b_{n-1} \tag{1.1}$$

where $\oplus$ is the modulo-2 (operator)

A method of generating the bit stream b_n from the bit stream a_n is shown in Figure 1.4. The logic circuit has two inputs: the bit stream a_n and the bit stream b_n delayed by the time T allocated to a single bit, that is, b_{n-1}. The logical operation is shown in the table.

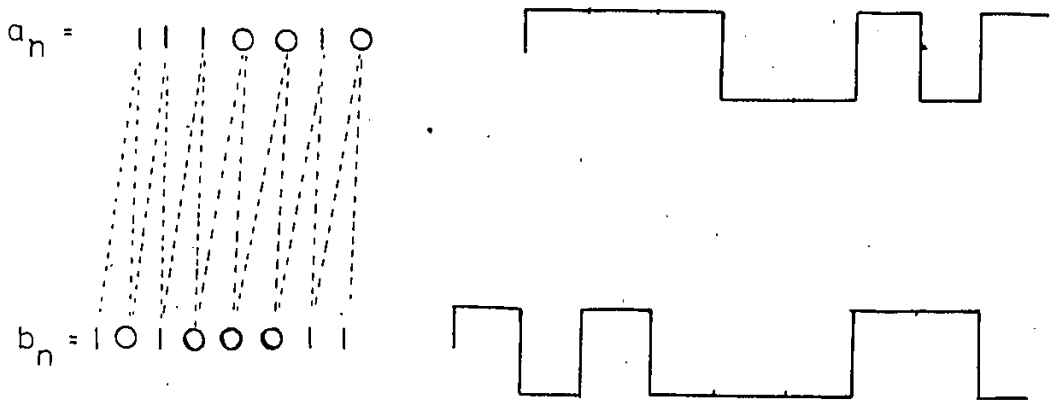

Fig. 1.3. Differential encoded process

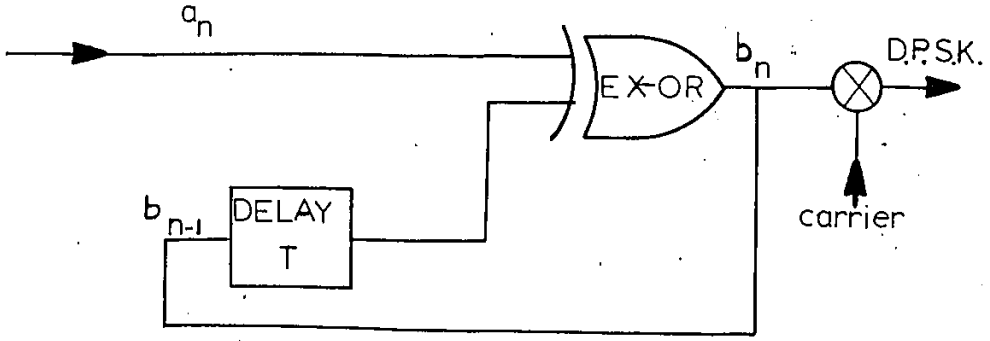

Fig. 1.4. Differential encoder

a_n	b_{n-1}	b_n
0	0	0
1	1	0
1	0	1
0	1	1

Before the appearance of the signal which has been encoded into the bit stream a_n, the voltage on the wire carrying this bit stream will be held constant at some fixed voltage level corresponding either to the binary digit 1 or 0. The arbitrary selection of a 1 as the first bit in b_n is simply equivalent to the assumption that this fixed voltage level corresponds to the bit 1.

Corresponding to the bit stream b_n, a waveform U(t) is generated where say, $U(t) = +V$ for $b_n = 1$ and $U(t) = -V$ for $b_n = 0$.

This waveform is applied as a modulating signal to a balanced modulator to which is applied, as well, a carrier $A \cos 2\pi f_c t$. The modulator output is the D.P.S.K. signal given by:

$$U_n(t) = V_n \cdot A \cdot \cos 2\pi f_c t \qquad (1.2)$$

1.3 D.P.S.K. DETECTION

A method of recovering the message bit a_n from the D.P.S.K. signal is shown in Figure 1.5. The two inputs to the mixer are the waveforms

$$U(t) = V_n A \cos 2\pi f_c t$$

and

$$U(t-T) = V_{n-1} A \cos 2\pi f_c (t-T) \qquad (1.3)$$

The mixer output is then given by

$$U(t) \cdot U(t-T) = V_n \cdot V_{n-1} \cdot A^2 \cdot [\cos 2\pi f_c t \cdot \cos 2\pi f_c (t-T)] \qquad (1.4)$$

Integrating the product for t=o to t=T, and sampling the result at instant T we obtain:

$$S(t) = V_n \cdot V_{n-1} \cdot \text{constant} \qquad (1.5)$$

The product $V_n \cdot V_{n-1}$ represents precisely the original message bit a_n, as is shown in Figure 1.5. This method of detection is known as correlation detection [1]...[7].

1.4 COMPARISON OF D.P.S.K. WITH OTHER DIGITAL MODULATION SYSTEMS

The choice of a modulation method may be based on the relative noise immunity, immunity to channel impairments (such as delay and amplitude distortion, nonlinearities, phase jitter, and frequency offset), or simplicity of instrumentation and compatibility with other equipment. Clearly it would not be realistic to compare modulation systems under all the circumstances cited above. [5]

However, fundamental comparisons based on certain idealizations can be made. For instance, a convenient absolute standard for comparing different modulation methods is obtained through the concept of required signal energy per bit per second in the presence of a given noise spectral density.

A figure of merit for comparing modulation methods based on this concept leads to the emphasis on the minimization of the total transmitted energy required for a given amount of data, which is of particular importance for application in satellite communication systems. [7]

From Shannon's formulation of channel capacity we have that

$$C = B \log_2 \left(1 + \frac{S_i}{N_o B} \right) \qquad (1.6)$$

where C = Channel capacity in bits/sec.

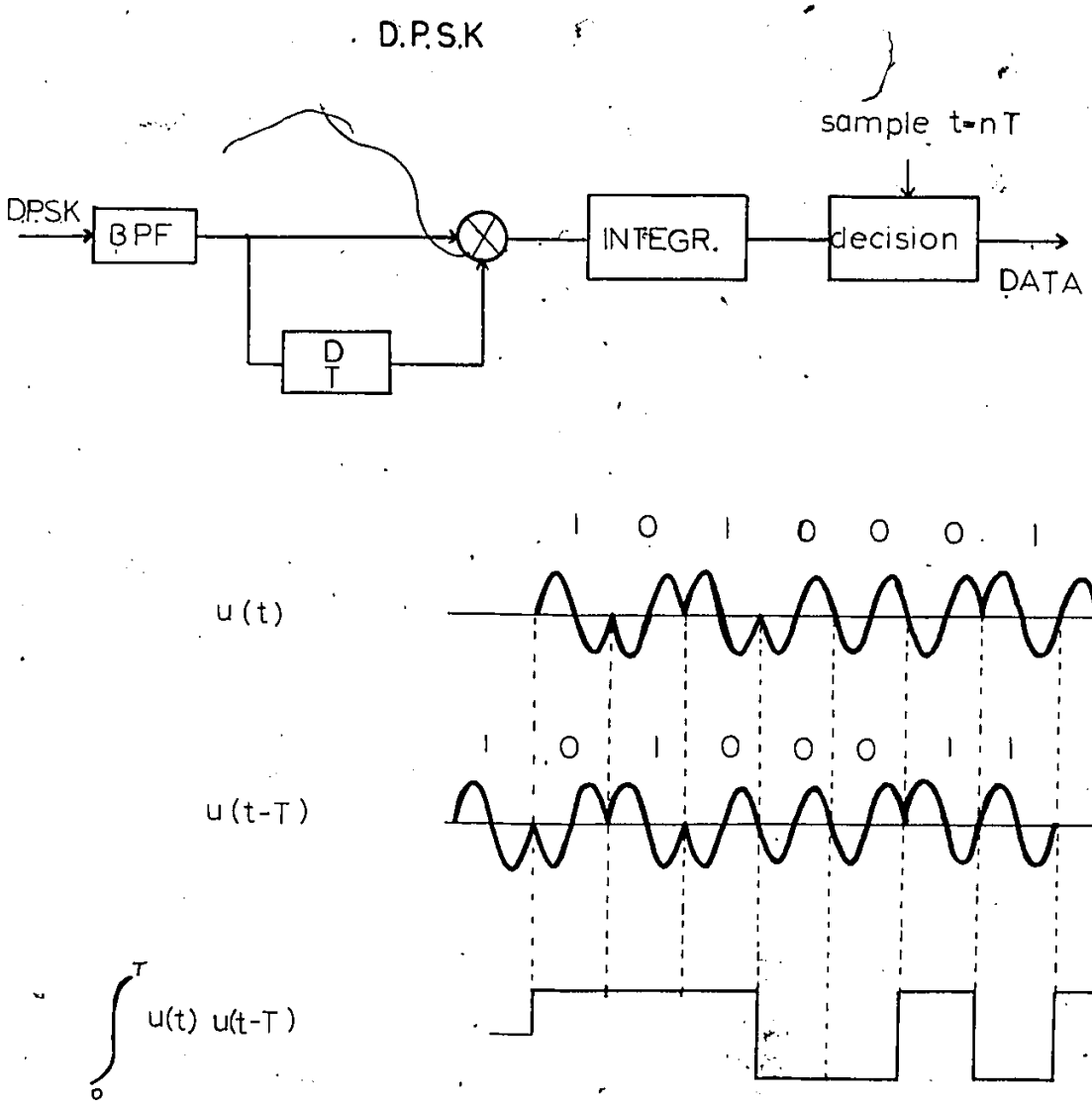

Fig. 1.5. D.P.S.K. Detector

B = Channel bandwidth

N_o = Noise power per cycle of bandwidth

S_i = Signal power.

From eq. 1.6 we have

$$\frac{C}{B} = \log_2 \left(1 + \frac{S_i}{N_o C} \cdot \frac{C}{B} \right) \tag{1.7}$$

or

$$\frac{C}{B} = \log_2 \left(1 + \beta \frac{C}{B} \right) \tag{1.8}$$

where

$$\beta = \frac{S_i}{N_o C} \tag{1.9}$$

The parameter β provides a useful criterion for comparing the efficiency of digital modulation system; it can be interpreted as the minimum input signal power required per bit of information per second in the presence of a given uniform gausian noise-power spectral density of N_o watts/cycle for a given error rate.

Equation (1.8) can be written in the form

$$\beta = \frac{B}{C} (2^{C/B} - 1) = \gamma (2^{1/\gamma} - 1) \tag{1.10}$$

where $\gamma = \frac{B}{C}$, channel bandwidth/bit/sec.

From Eq. (1.10) it follows that the lower bound on β can be obtained by letting $\gamma \to \infty$, which corresponds to systems of unlimited bandwidth. Thus,

$$\lim_{\gamma \to \infty} \beta = \log_e 2 = 0.693 \tag{1.11}$$

The parameter β can be written in the form

$$\beta = \frac{S_i}{N_o C} = \frac{S_i}{N_o B} \cdot \frac{B}{C} = \left(\frac{S}{N}\right)_i \cdot \gamma \tag{1.12}$$

It follows that for any given digital system, β may be computed from the minimum input signal to noise ratio required for a given error rate, and the ratio of bandwidth to information rate. Comparison of binary systems on β factor basis is shown in Figure 1.6 {7}.

Finally, some of the characteristics to be considered in choosing a data transmission system are given relative weighing in Figure 1.7 {6}. Here, in all columns except the second and third, the systems are given numbers indicating the order of preference under each characteristic. The same number given to more than one system indicates either that the systems are equal or that there is insufficient basis for choice.

In the chapters to follow a coverage of those topics in the theory of D.P.S.K. system and the proposed digital implementation of the D.P.S.K. demolulator are presented. Our specific chapter-by-chapter goals are as follows:

Chapter Two. Power spectrum

Despite the fact that the D.P.S.K. system is referred to as digital phase modulation system the circuit implementation, requires analog components. In this chapter we introduce the idea of the digital implementation of the D.P.S.K. demodulator by sampling the RF signal at the output of the B.P.F.

Chapter Three. Digital detector

Despite the fact that the D.P.S.K. system is referred to as digital phase modulation system, the detection process is not digital. In this chapter we introduce the proposed idea of the digital implementation of the D.P.S.K. demodulator by sampling the R.F. signal at the output of the B.P.F.

Chapter Four. Circuit performance

In this chapter the concept of digital implementation of the D.P.S.K. demodulator is analysed by examining in some depth, the bit error rate for two different sampling rates.

Chapter Five. Experimental results

In this chapter experimental results are presented which are bit error rates for the digital D.P.S.K. circuit at various signal rates and noise levels.

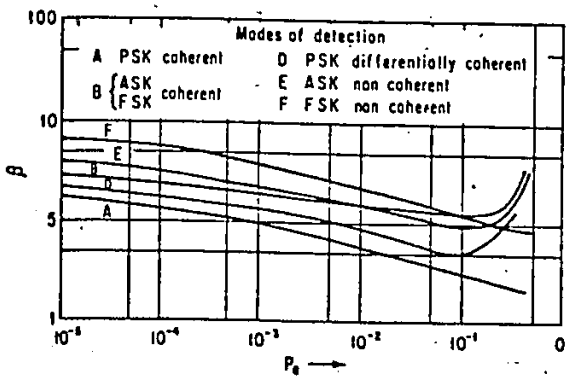

Comparison of binary systems on a β factor basis. Modes of detection: A, PSK coherent; B, ASK coherent and FSK coherent; D, PSK differentially coherent; E, ASK noncoherent; F, FSK noncoherent. (From Hancock,[2] Proc. Natl. Electron. Conf.)

FIG. 1.6

COMPARATIVE ANALYSIS OF MODULATION SYSTEMS {5}

System	Complexity of instrumentation	Bits per cycle of nominal band	Variable speed asynchronous operation	Signal-to-noise performance		Tolerance to parabolic delay distortion	Tolerance to linear delay distortion	Tolerance to amplitude change	Tolerance to frequency offset	Tolerance to phase jumps
				Equal bit rate	Equal bandwidth					
Binary polar baseband ...	1	2	Yes	1	3	2	—	1	—	—
Binary on-off AM ...	2	1	Yes	5	5	2	1	3	1	1
Binary FM	3	1	Yes	4	4	1	2	1	3	2
Binary PM differentially coherent	4	1	No	2	2	3	3	2	3	2
Binary PM coherent	5	1	Yes	1	1	2	1	1	1	4
VSB AM suppressed carrier	6	2	Yes	1	3	3	5	1	2	4
Quaternary PM differentially coherent	7	2	No	3	5	4	4	3	4	3

FIG. 1.7

Characteristics to be Considered in Choosing a Data System {6}

2. POWER SPECTRA OF DIGITAL PHASE-MODULATED SIGNAL

2.1 POWER SPECTRAL DENSITY FUNCTION

The direct way of defining the power spectrum of the signal, is to find the Fourier transform of the signal on a finite time interval T. The magnitude square of this Fourier transform is then divided by T and averaged over all possible values of the signal. The power spectrum is finally obtained by taking the limit of this average. {8}. That is, given a signal U(t), the power spectrum by the direct method is given by:

$$G(f) = \lim_{T \to \infty} \frac{1}{T} < | V(f,T) |^2 > \qquad (2.1)$$

where

$$V(f,T) = \mathcal{F} [U(t)]$$

the Fourier transform of the signal in the interval T and

$$< | V(f,T) |^2 >$$

is the expectation taken over all possible values of the signal in the interval T.

A second method of calculating the power spectrum of a digital phase modulated signal can be obtained from the Fourier transform of the signal autocorrelation function. There is a very simple relationship between the double Fourier transform of the autocorrelation funciton of a given signal and the energy or power spectra density functions as a function of frequency. {9} {14}. That is for a given signal U(t) we have:

$$G(f) = \lim_{T \to \infty} \frac{W(f)}{T} \qquad (2.2)$$

where

$$W(f) = \frac{1}{2\pi} \Gamma(f,f)$$

and $\Gamma(f,f)$ is the double Fourier transform of the autocorrelation function U(t) given by:

$$\Gamma(f,f) = \int_{-\infty}^{+\infty}\int_{-\infty}^{+\infty} R(t_1,t_2) \cdot e^{-j(f_1 t_1 - f_2 t_2)}\, dt_1\, dt_2 \qquad (2.3)$$

We are interested in the effects of the pulse shape and of the probability distribution of the modulating signal on the power spectrum. In section 2.3 the power spectrum of the P.S.K. signal is calculated following the method given by B. GLANCE [3].

2.2 REPRESENTATION OF P.S.K. SIGNAL

A P.S.K. signal generated by modulating the carrier with a binary rectangular waveform, of period T, can be represented by:

$$U(t) = A \cos\left(\omega_c t + b(t)\frac{\pi}{2}\right) = \begin{cases} +A \sin \omega_c t & \text{for } b(t) = -1 \\ -A \sin \omega_c t & \text{for } b(t) = -1 \end{cases} \qquad (2.4)$$

where b(t) is the rectangular waveform, which takes the value +1 or -1 within the time slot T.

From equation (2.4) we can see that the representation of P.S.K. signals needs to be extended to include the shape of the modulating signal and the appearance of the random variable b(t) within the argument complicates the analysis of such a signal. Therefore, we must modify (2.4) in such a way that only the pulse shape function appears within the argument and the random variable outside of it.

For general bipolar waveform modulating the carrier, the P.S.K. signal becomes:

$$U(t) = A \sum_{r=1}^{2} \Gamma_r(t) \left[\cos \omega_c t + g_r(t) \frac{\pi}{2} \right] \tag{2.5}$$

where

$$\Gamma_r(t) = \sum_{k=-\infty}^{+\infty} a_{k,r} \, \delta(t - kT) \tag{2.6}$$

and $a_{k,r}$ is a random variable which takes the values +1, -1, with probabilities p,q respectively and $\delta(t)$ is a window function given by:

$$\delta(t) = \begin{cases} 1, & 0 < t < T \\ 0, & |t| > T \end{cases}$$

and where $g_r(t)$ is a function describing the shape of the modulating waveform within the time slot T and for each level r of the bipolar signal.

Therefore a general expression of the P.S.K. signal is given by:

$$U(t) = A \sum_{k=-\infty}^{+\infty} \sum_{r=1}^{2} a_{k,r} \, \delta(t - kT) \cdot \cos \left[\omega_c t + g_r(t) \frac{\pi}{2} \right] \tag{2.7}$$

where r=1 (level 1) represents the positive part of the bipolar modulating waveform and r = 2 (level 2) the negative part. Equation 2.7 is shown in Fig. 2.1.

2.3 CALCULATION OF THE POWER SPECTRUM

From equations (2.1), (2.2), (2.3) and (2.5) we have

$$F[U(t)] = \int_0^{NT} U(t) \, e^{-j\omega t} \, dt = A \sum_{r=1}^{2} \int_0^{NT} \Gamma_r(t) \cos \left(\omega_c t + g_r(t) \frac{\pi}{2}\right) e^{-jwt} dt$$

or

$$V(f,NT) = \frac{A}{2} \sum_{r=1}^{2} \int_0^{NT} \Gamma_r(t) \, e^{+j \left[(\omega_c - \omega)t + g_r(t) \frac{\pi}{2} \right]} dt + \frac{A}{2} \sum_{r=1}^{2} \int_0^{NT} \Gamma_r(t) \, e^{-j \left[\omega_c + \omega)t + g_r(t) \frac{\pi}{2} \right]} dt \tag{2.8}$$

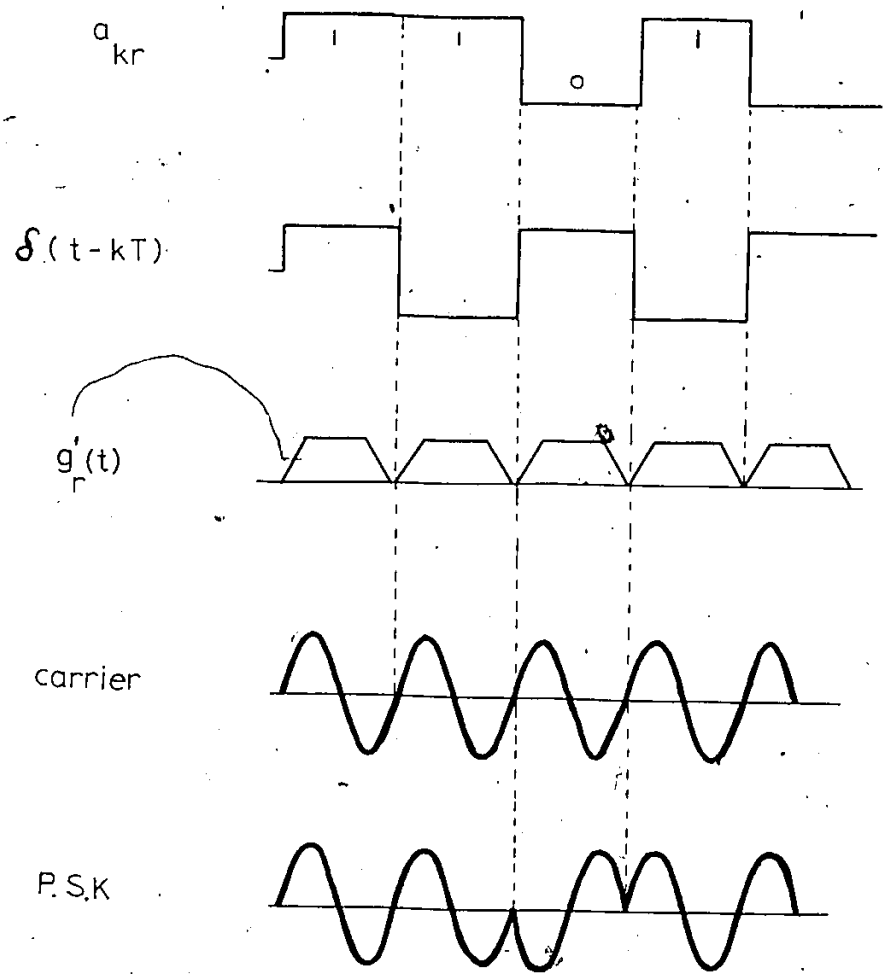

Fig. 2.1. Representations of a P.S.K. signal

The first integral of equation (2.8) represents positive frequencies and the second one negative frequencies. Therefore we can write

$$V(f,NT) = V(f_+, NT) + V(f_-, NT) \qquad (2.9)$$

where

$$V(f_+,NT) = \frac{A}{2} \sum_{r=1}^{2} \int_0^{NT} r(t)\, e^{+j\left[(\omega_c-\omega)t + g_r(t)\frac{\pi}{2}\right]} dt \qquad (2.10)$$

and

$$V(f_-,NT) = \frac{A}{2} \sum_{r=1}^{2} \int_0^{NT} r(t)\, e^{-j\left[(\omega_c+\omega)t + g_r(t)\frac{\pi}{2}\right]} dt \qquad (2.11)$$

Substituting Eq. (2.6) in (2.10), we have for the positive frequencies

$$V(f_+,NT) = A \sum_{k=0}^{N-1} \sum_{r=1}^{2} a_{k,r} \int_0^{T} e^{+j\left[(\omega_c-\omega)\cdot(t+kT) + g_r(t)\frac{\pi}{2}\right]} dt$$

or

$$V(f_+,NT) = A \sum_{k=0}^{N-1} \sum_{r=1}^{2} a_{k,r}\, e^{+j(\omega_c-\omega)kT} \cdot F_r(f_+)$$

where

$$F_r(f_+) = \frac{1}{2} \int_0^{T} e^{-j\left[(\omega_c+\omega)t + g_r(t)\frac{\pi}{2}\right]} dt \qquad (2.12)$$

From Eq. (2.9) and (2.12) we have finally that

$$V(f,NT) = A \sum_{k=0}^{N-1} \sum_{r=1}^{n} a_{k,r} \left[e^{jkT(\omega_c-\omega)} F_r(f_+) + e^{-jkT(\omega_c-\omega)} F_r(f_-)\right] \qquad (2.13)$$

Substituting Eq. (2.13) into (2.1) we have after some calculations that the power spectrum relative to the positive frequencies is given by [8]:

$$G(f_+) = \frac{A^2}{T}\left\{\sum_{r=1}^{2} P_r \left|F_r(f_+)\right|^2 + \left|\sum_{r=1}^{2} P_r F_r(f_+)\right|^2\right\} +$$

$$+ \frac{A^2}{T^2} \sum_{m=\infty}^{+\infty} \left|\sum_{r=1}^{2} P_r F_r(f_+)\right|^2 \delta\left(f_c - f + \frac{m}{T}\right) \qquad (2.14)$$

where P_r are the probability distributions of the levels r.

The first term of Eq. 2.14 gives the continuous power spectrum and the second term the discrete lines. These lines occur at the frequencies

$$f = f_c + \frac{m}{T} \quad , \quad m = 0, \pm 1, \pm 2 \ldots$$

if $$\left| \sum_{r=1}^{2} P_r F_r (f_+) \right|^2 \neq 0 \quad \text{for } f = f_c + \frac{m}{T}$$

otherwise we have only one line at the carrier frequency that is $f = f_c$.

Therefore, to calculate the power spectrum we must have the Fourier transform of the argument of $\cos \left[\omega_c t + g_r(t) \frac{\pi}{2} \right]$, and the probability distribution of the positive and negative pulses, that is $P_1 = p$ and $P_2 = q$

EXAMPLE I

I Consider rectangular pulse of duration $\tau < T$

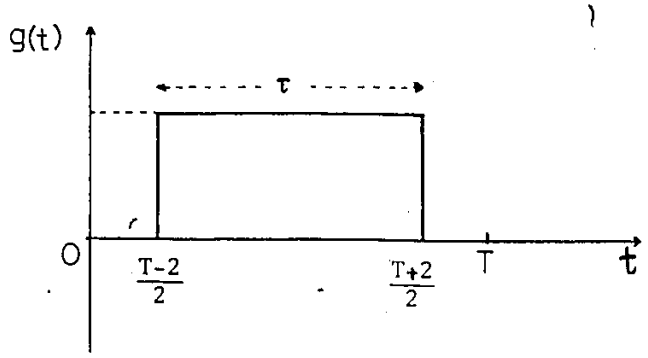

In this case: $$g_r(t) = \begin{cases} 0 & , \ 0 < t < \frac{T-\tau}{2} \\ g_r & , \ \frac{T-\tau}{2} < t < \frac{T+\tau}{2} \\ 0 & , \ \frac{T+\tau}{2} < t < T \end{cases}$$

From Eq. (2.12) we have

$$F_r(f_+) = \frac{1}{2}\int_0^{\frac{T-\tau}{2}} e^{f(\omega_c-\omega)t}\cdot dt + \frac{1}{2}\int_{\frac{T-\tau}{2}}^{\frac{T+\tau}{2}} e^{f(\omega_c-\omega)t} \pm g_r\, dt$$

$$+\frac{1}{2}\int_{\frac{T+\tau}{2}}^{T} e^{f(\omega_c-\omega)t}\, dt$$

which gives a result:

$$F_r(f_+) = -\frac{1}{2j\omega}\left\{(1 - e^{j g_r})\, 2j\left[\sin\frac{\omega\tau}{2}\right] e^{f\frac{\omega\tau}{2}} - 2j\, e^{f\frac{\omega T}{2}} \sin\frac{\omega T}{2}\right\}$$

Substituting $F_r(f_+)$ in Eq. (2.14) we get:

$$G(f_+) = \frac{T}{4}\left\{\left(\frac{\tau}{T}\right)^2\left[\frac{\sin(\omega_c-\omega)\frac{\tau}{2}}{(\omega_c-\omega)\frac{\tau}{2}}\right]^2\left[1 - (P_1 - P_2)^2\right] +\right.$$

$$+\frac{1}{4}\sum_{m=\infty}^{+\infty}\left\{\left[\frac{\sin(\omega_c-\omega)\frac{T}{2}}{(\omega_c-\omega)\frac{T}{2}}\right]^2 - 2\frac{\tau}{T}\,\frac{\cos(\omega_c-\omega)\frac{T-\tau}{2} - \cos(\omega_c-\omega)\frac{T+\tau}{2}}{(\omega_c-\omega)^2\,\frac{T\cdot\tau}{2}}\right.$$

$$\left.\left. + \left(\frac{\tau}{T}\right)^2\left[\frac{\sin(\omega_c-\omega)\frac{\tau}{2}}{(\omega_c-\omega)\frac{\tau}{2}}\right]^2\left[1 - (P_1 - P_2)^2\right]\cdot\delta\left(f_c - f + \frac{m}{T}\right)\right\}\right. \qquad (2.15)$$

Where P_1, P_2 are the probabilities of occurance of 1's and 0's.

From Eq. (2.15) we will consider the following cases:

<u>case A</u> $\tau = T$ $\quad\begin{cases} 1: & P_1 = P_2 = \frac{1}{2} \\ 2: & P_1 \neq P_2 \end{cases}$

and

<u>case B</u> $\tau \neq T$ $\quad\begin{cases} 1: & P_1 = P_2 = \frac{1}{2} \\ 2: & P_1 \neq P_2 \end{cases}$

<u>Case A</u> <u>$\tau = T$</u>

For $P_1 = P_2 = \frac{1}{2}$ from Eq. (2.15) we have

$$G(f_+) = \frac{T}{4}\left[\frac{\sin(\omega_c-\omega)\frac{T}{2}}{(\omega_c-\omega)\frac{T}{2}}\right]^2 \qquad (2.16)$$

That is we have only a continuous spectrum which decreases as $\frac{1}{f^2}$ as $f \to \infty$. Figure (2.2)

If $P_1 \neq P_2$ from Eq. (2.15) we have

$$G(f_+) = \frac{T}{4}\left[\frac{\sin(\omega_c-\omega)\frac{T}{2}}{(\omega_c-\omega)\frac{T}{2}}\right]^2 \left[1-(P_1-P_2)^2\right] + \frac{(P_1-P_2)^2}{4}\,\delta(f-f_c) \qquad (2.17)$$

That is a continuous spectrum and a single line at the carrier frequency.

The power spectra decreases as $\frac{1}{f^2}$ as $f \longrightarrow \infty$. Figure 2.3

Case B $\tau \neq T$, $(\tau = kT)$ $k < 1$

For $P_1 = P_2$, from Eq. (2.15) we have

$$G(f_+) = \frac{T}{4}\,k^2\left[\frac{\sin(\omega_c-\omega)\frac{\tau}{2}}{(\omega_c-\omega)\frac{\tau}{2}}\right]^2 +$$

$$+\frac{1}{4}\sum_{m=\infty}^{+\infty}\left[\frac{\sin m\pi}{m\pi} - k\,\frac{\sin m\pi k}{m\pi K}\right]^2 \delta\left(f_c - f + \frac{m}{T}\right) \qquad (2.18)$$

In this case we have a continuous spectra and discrete lines at $f = f_c + \frac{m}{T}$ Figure (2.4)

If $P_1 \neq P_2$ we have from Eq. (2.15)

$$G(f_+) = \frac{T}{4}\left\{k^2\left[\frac{\sin(\omega_c-\omega)\frac{kT}{2}}{(\omega_c-\omega)\frac{kT}{2}}\right]^2\left[1-(P_1-P_2)^2\right] +\right.$$

$$+\frac{1}{4}\left[(1-\quad)^2 - k^2(P_1-P_2)^2\right] +$$

$$\left.+\frac{1}{4}\sum_{\substack{m=\infty\\ m\neq 0}}^{\infty}\left(\frac{\sin \pi m k}{\pi m k}\right)^2 {}^2\left[1-(P_1-P_2)^2\right]\right. \qquad (2.19)$$

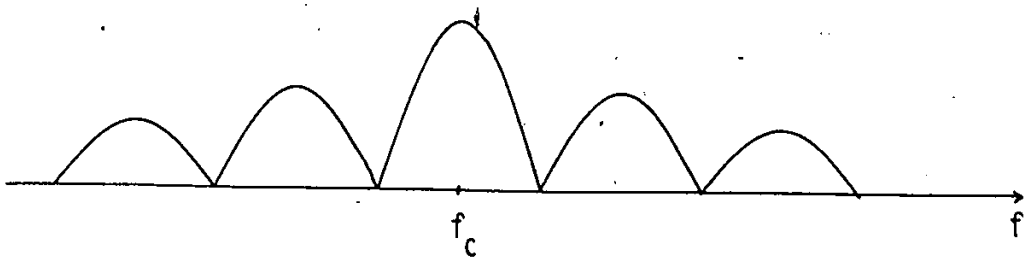

Fig. 2.2. Power spectrum of a P.S.K. signal. For $\tau=T$ and $P_1 = P_2 = \frac{1}{2}$

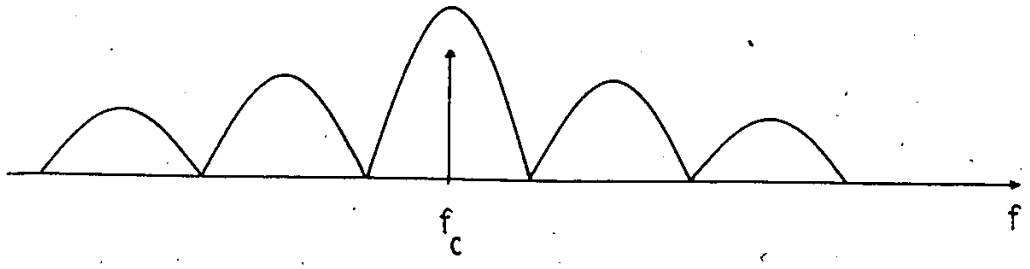

Fig. 2.3. Power spectrum of a P.S.K. signal For $\tau=T$ and $P_1 \neq P_2$

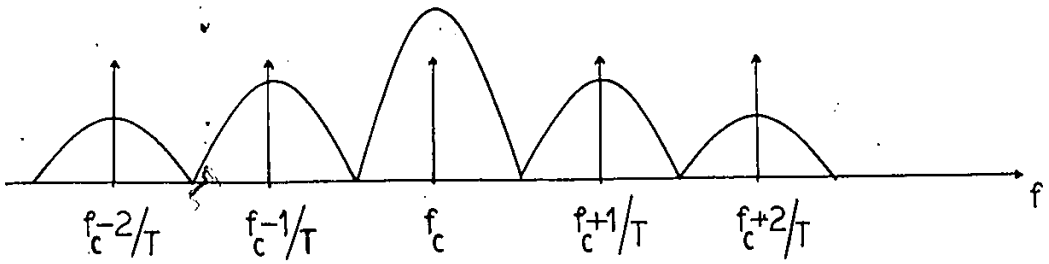

Fig. 2.4. Power spectrum of a P.S.K. signal for $\tau \neq T$ and $P_1 = P_2 = \frac{1}{2}$

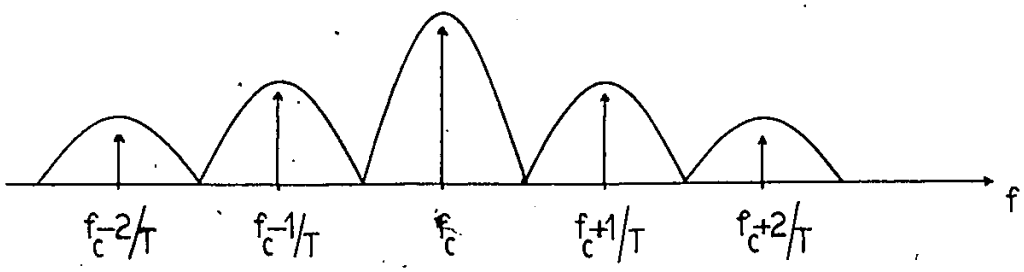

Fig. 2.5. Power spectrum of a P.S.K. signal for $\tau=T$ and $P_1 \neq P_2$

In this case we also have a continuous spectra and discrete lines at $f = f_c + \frac{m}{T}$ with reduced amplitude Figure (2.5).

Example II

A trapezoidal pulse

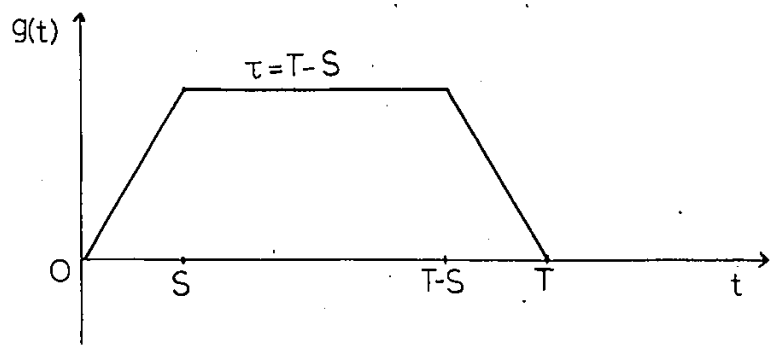

From Eq. (2.12) we have

$$F_r(f_+) = \frac{1}{2}\left\{\int_0^S e^{f\left[(\omega_c-\omega)\,t \pm \frac{\pi}{2S}\right]t}\,dt + e^{\pm f\frac{\pi}{2}}\int_0^{T-S} e^{f(\omega_c-\omega)\,t}\,dt + \right.$$

$$\left. + e^{\pm f\frac{\pi}{2}\,\frac{T}{S}}\int_{T-S}^{T} e^{f\left[(\omega_c-\omega) \mp \frac{\pi}{2S}\right]t}\,.\,dt\right.$$

and Eq. (2.14) gives

$$G(f_+) = \frac{T}{4}\left(\frac{\pi}{4}\right)^2\left\{\frac{\frac{\tau}{T}\,\frac{\sin(\omega_c-\omega)\frac{\tau}{2}}{(\omega_c-\omega)\frac{\tau}{2}} + \frac{S}{T}\cos(\omega_c-\omega)\frac{T}{2}}{\left[(\omega_c-\omega)\frac{S}{2}\right]^2 - \left(\frac{\pi}{4}\right)^2} + \right.$$

$$\left. + \frac{1}{4}\left(\frac{\pi}{4}\right)^2\left(\frac{S}{T}\right)^2 \sum_{m=-\infty}^{+\infty} \frac{\cos^2\left(2\pi m\frac{S}{T}\right)}{\left[\left(\pi m\frac{S}{T}\right)^2 - \left(\frac{\pi}{4}\right)^2\right]^2}\cdot\delta\left(f_c - f + \frac{m}{T}\right)\right.$$

That is we have a continuous and discrete spectra. In this case the power spectrum decreases as $\frac{1}{f^4}$ as $f \longrightarrow \infty$ Figure 2.6.

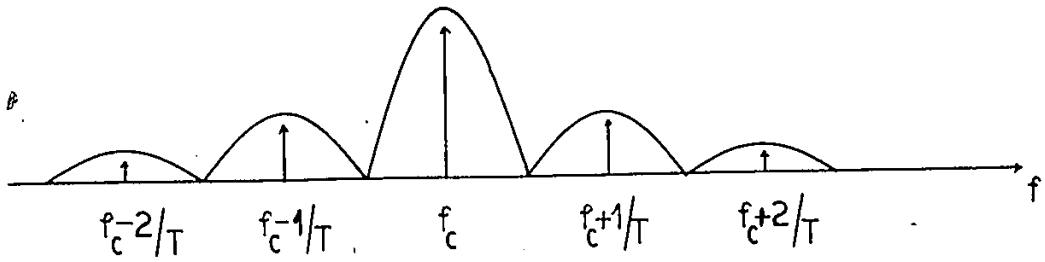

Fig. 2.6. Power spectrum of a P.S.K. signal modulated by a trapezoidal pulse

2.4 POWER SPECTRUM OF D.P.S.K. MODULATED BY PSEUDO-RANDOM BINARY SEQUENCES (P.R.B.S.)

Since pseudo-random sequences are periodic functions of time they have line spectra which may be obtained by a straightforward Fourier series analysis, that is the direct way of defining the power spectrum. However, as the P.R.B.S. become very long the analysis becomes impractical. [10]

Therefor e the power spectrum will be determined from the auto-correlation function by application of the Wiener-Khintchine relations which states that the power spectrum $G(\omega)$ and autocorrelation function $R(t)$ of a periodic signal constitute a Fourier transform pair:

$$G(\omega) = \int_{-\infty}^{+\infty} R(t)\, e^{-j\omega t}\, dt$$

and

$$R(t) = \frac{1}{2\pi} \int_{-\infty}^{+\infty} G(\omega)\, e^{j\omega t}\, d\omega \qquad (2.20)$$

The autocorrelation function of P.R.B.S. is given by the set of correlation values of the sequence with all the cyclic permutations of itself.{10}

$$R = \frac{\text{Number of agreements} - \text{Number of disagreements}}{\text{Number of agreements} + \text{Number of disagreements}} \qquad (2.21)$$

Since a P.R.B.S. is a maximum length sequence, the autocorrelation function is a two level autocorrelation function given by:

$$R_{(\tau)} = \begin{cases} 1 - \left|\frac{t}{\tau}\right| \frac{p+1}{p} & \text{for } -\tau < t < +\tau \\ \frac{1}{p} & \text{elsewhere} \end{cases}$$

Where τ is the digit period and p is the number of digits within one period $T - p\tau$ of the P.R.B.S. The two level autocorrelation function is shown in Figure 2.7.

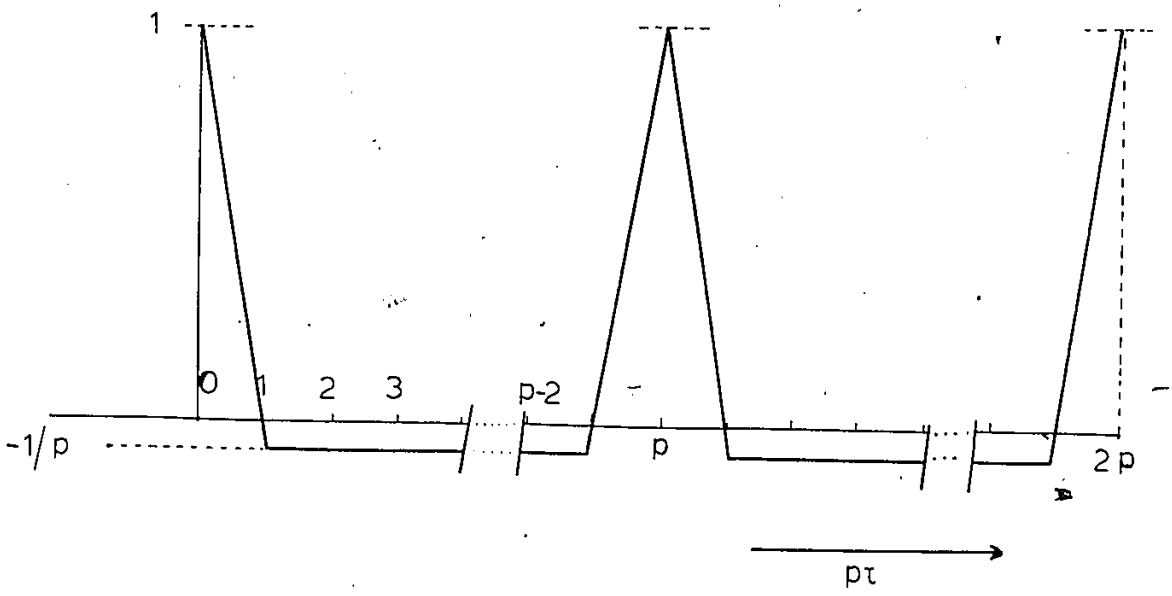

Fig. 2.7. Autocorrelation functions of a P.R.B.S.

To derive Power Spectrum [10] consider a D.P.S.K. signal with phase change of 180^{o} as

$$u(t) = m(t) \cdot A \cos \omega_c t \tag{2.23}$$

where m(t) is a P.R.B.S. with period $p\tau$, and $A \cos \omega_c t$ the carrier.

The power spectrum of u(t) will be:

$$V(f) = \frac{1}{2} M(\omega_c - \omega) + \frac{1}{2} M(\omega_c + \omega) \tag{2.24}$$

where $M(\omega)$ is the spectrum of the modulating P.R.B.S., that is

$$M(f) = \frac{M_o(f)}{p\tau} \cdot \sum_{m=-\infty}^{+\infty} \cdot \delta\left(f - \frac{m}{p\tau}\right) \tag{2.25}$$

where

$$M_o(f) = \int_{-\frac{p\tau}{2}}^{+\frac{p\tau}{2}} R(t)\, e^{-j\omega t}\, dt \tag{2.26}$$

is the Fourier transform of one period of the autocorrelation function. From Eq. (2.26) and (2.20) we have that, since R(t) is an even function

$$M_o(f) = \int_{-\frac{p\tau}{2}}^{+\frac{p\tau}{2}} R(t) \cos \omega t\, dt = 2 \int_0^{+\frac{p\tau}{2}} R(t) \cos \omega t \quad \text{or}$$

$$M_o(f) = 2\left\{\int_0^{+\tau} \left(1 - \frac{t(p+1)}{p\tau}\right) \cos \omega t\, dt + \int_{\tau}^{\frac{p\tau}{2}} \left(-\frac{1}{p}\right) \cos \omega t\, dt\right. \quad \text{or}$$

$$M_o(f) = 2\left\{\int_0^{+\tau} \cos \omega t\, dt - \frac{p+1}{p\tau} \int_0^{\tau} t \cos \omega t\, dt - \frac{1}{p} \int_{\tau}^{\frac{p\tau}{2}} \cos \omega t\, dt\right\} \text{ or}$$

$$M_o(f) = 2\left\{2\, \frac{p+1}{p\tau\omega^2} \sin^2 \frac{\omega\tau}{2} - \frac{1}{p\omega} \sin \omega\, \frac{p\tau}{2}\right\}, \tag{2.27}$$

from (2.27) and (2.26) we have

$$M(f) = \left[\frac{(p+1)}{p^2} \left(\frac{\sin \frac{\omega\tau}{2}}{\frac{\omega\tau}{2}}\right)^2 - \frac{1}{p}\, \frac{\sin \frac{\omega p\tau}{2}}{p\frac{\omega\tau}{2}} \cdot \sum_{m=-\infty}^{+\infty} \delta\left(f - \frac{m}{p\tau}\right), \right. \tag{2.28}$$

Equation (2.28) for $\omega=0$ gives the d.c. value:

$$\frac{p+1}{p^2} - \frac{1}{p} = \frac{1}{p^2} \tag{2.29}$$

From Eq. (2.29) and (2.28) we have

$$M(f) = \frac{p+1}{p^2}\left[\frac{\sin\frac{\omega\tau}{2}}{\frac{\omega\tau}{2}}\right]^2 \sum_{\substack{m=-\infty \\ m\neq 0}}^{+\infty} \delta\left(f - \frac{m}{p\tau}\right) + \frac{1}{p^2}\,\delta(f) \tag{2.30}$$

and from (2.30) and (2.24) the power spectral density function is:

$$V(f) = \frac{1}{2}\,\frac{p+1}{p^2}\left[\frac{\sin\frac{\omega\tau}{2}}{\frac{\omega\tau}{2}}\right]^2 + \sum_{\substack{m=-\infty \\ m=f_c}}^{+\infty} \delta\left(f_c - f + \frac{m}{T}\right) + \frac{1}{p^2}\,\delta(f - f_c) +$$

$$+\frac{1}{2}\,\frac{p+1}{p^2}\left[\frac{\sin\frac{\omega\tau}{2}}{\frac{\omega\tau}{2}}\right]^2 + \sum_{\substack{m=-\infty \\ m\neq f_c}}^{+\infty} \delta\left(f_c + f + \frac{m}{T}\right) + \frac{1}{p^2}\,\delta(f + f_c) \tag{2.31}$$

where f_c is the carrier frequency.

From equation (2.31) we have that the power spectrum in the case of P.R.B.S., is a line spectrum with frequencies at multiples of the fundamental frequency $\frac{m}{p\tau}$ of the P.R.B.S., where $m = \pm 1, \pm 2\ldots$ There is an envelope of the spectrum which is determined by the digit period τ of the modulating signal, i.e. the P.R.B.S. Therefore, the zero points of the envelope are at frequencies given by $\frac{2\pi K}{\tau}$, $K = 1, 2\ldots$ Consequently, the bandwidth required to transmit a D.P.S.K. signal is independent of the length p of the P.R.B.S., is determined solely by the digit period τ, that is how often the modulating signal switches between the two levels. Since the binary waveform has a constant amplitude, the power is also constant with a scale factor inversely proportional to the period p, therefore increasing p the power is reduced and the lines become more dense. The power spectrum of D.P.S.K. signal modulated by a D.P.S.K. signal modulated by a P.R.B.S. is shown in Fig. (2.8), a, b, c, d for different values of p and τ.

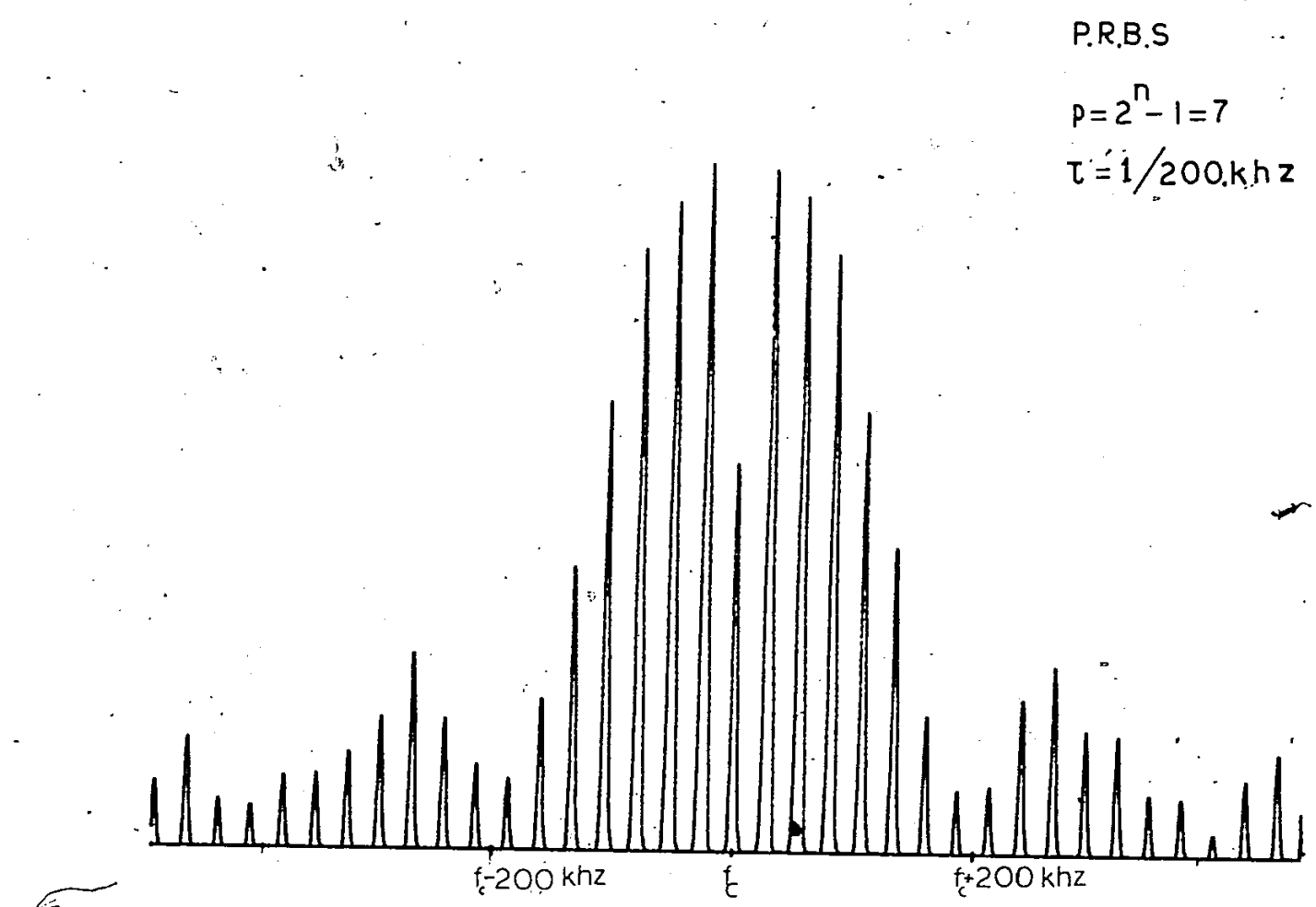

Fig. 2.8a. Power spectrum of a D.P.S.K. signal modulated by a P.R.B.S. with digit period τ=1/200 kHz, and word period p=f bits

P.R.B.S

$P = 2^n - 1 = 15$

$\tau = 1/200.\text{khz}$

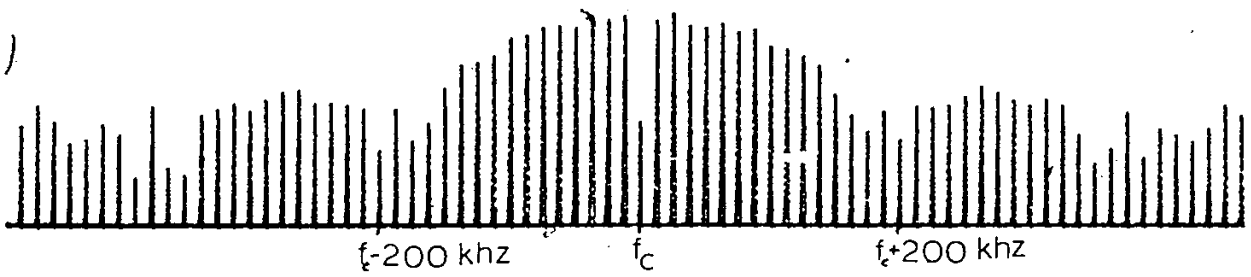

Fig. 2.8b. Power spectrum of a D.P.S.K. signal modulated by a P.R.B.S. with digit period τ=1/200, and word period 15 bits

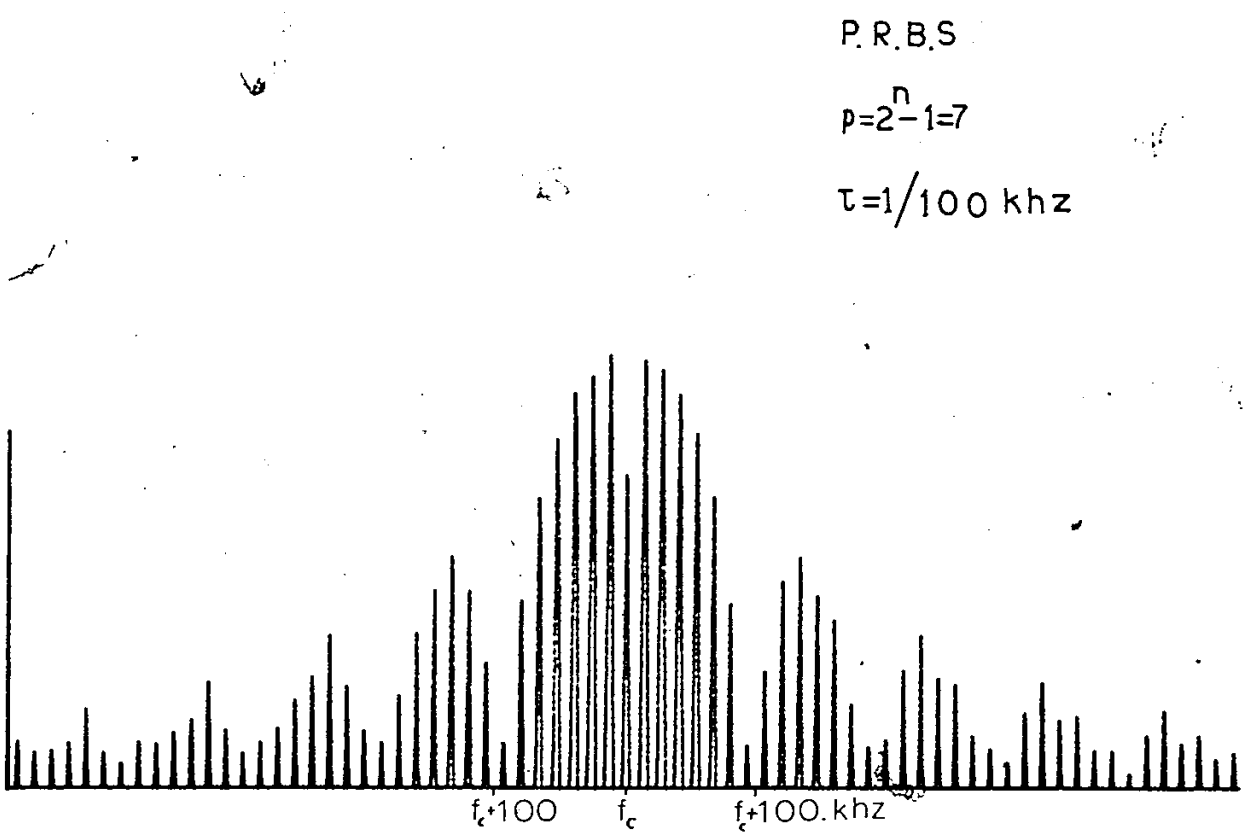

Fig. 2.8c. Power spectrum of a D.P.S.K. signal modulated by a P.R.B.S. with digit period τ-1/100 kHz, and word period 7 bits

P.R.B.S

$p = 2^n - 1 = 15$

$\tau = 1/100$ khz

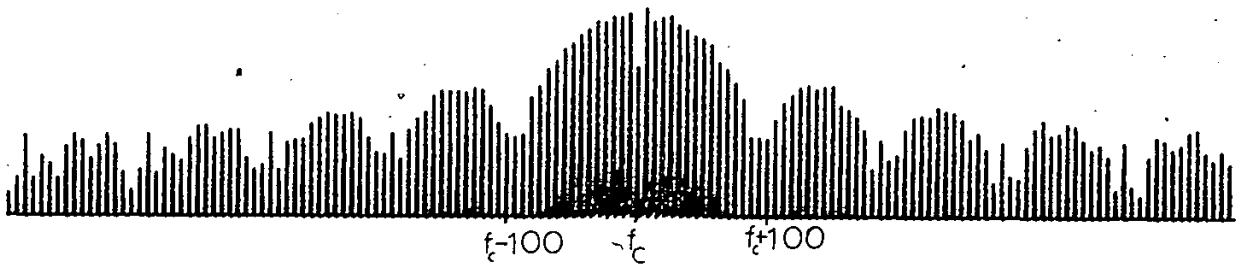

Fig. 2.8d. Power spectrum of a D.P.S.K. signal modulated by a P.R.B.S. with digit period τ=1/100 kHz, and word period 15 bits

3. DIGITAL DETECTOR

3.1 DIGITAL IMPLEMENTATION OF THE D.P.S.K. DEMODULATOR

The D.P.S.K. demodulator, Fig. 1.5, is generally realized with analog circuit components, and only in the last stage of the decision process sampling is used.

The advantages of discrete circuit realization lead us to investigate the possible implementation of the D.P.S.K. demodulator digitally. One approach is to sample the R.F. signal at the output of the bandpass filter directly, which allows for the decision process to take place right after the sampling point, Figure 3.1. The remaining part of the circuit can then be constructed digitally, by means of logic gates and delay flip-flops. For the digital implementation of the D.P.S.K. demodulator we will consider two different sampling periods. First by sampling once within one bit duration, secondly sampling every cycle within a bit duration.

3.2 ONE SAMPLE PER MESSAGE PERIOD

The digital implementation of D.P.S.K. demodulator with one sample within one bit period is represented by the circuit of Figure 3.1.

The D.P.S.K. signal at the output of the B.P.F. has the form

$$u(t) = \pm A \cos 2\pi f_c t - n(t) \qquad (3.1)$$

where n(t) is bandlimited Gaussian noise, and A, f_c are the amplitude and the frequency of the carrier.

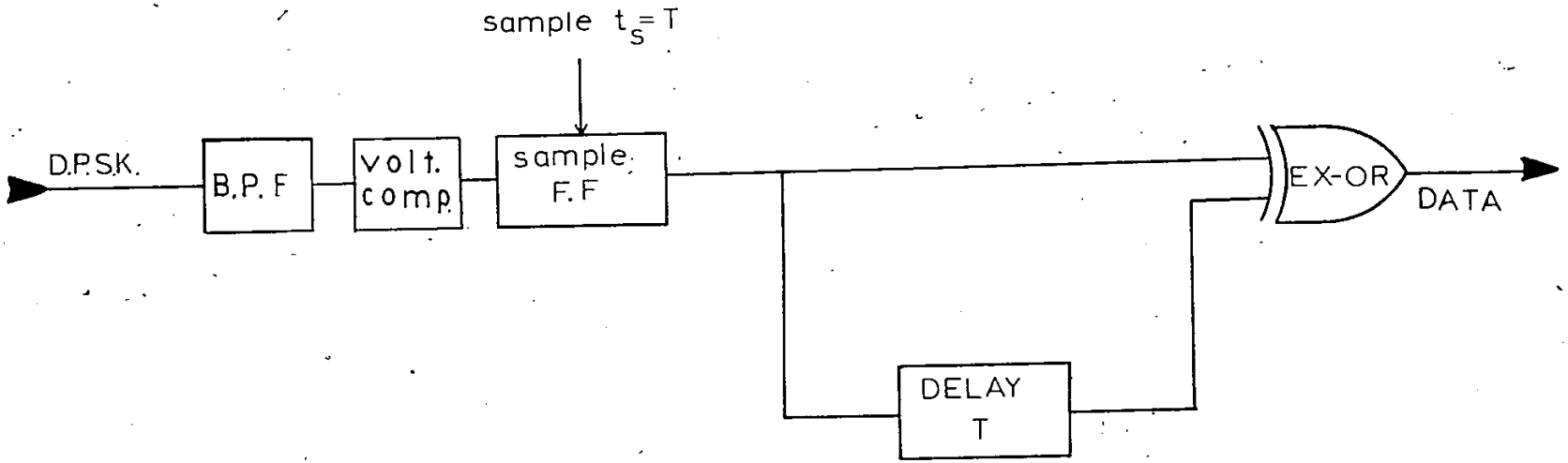

Fig. 3.1. Digital implementation of the D.P.S.K. demodulator with one sample per message bit

At the output of the B.P.F. the R.F. signal is sampled every T seconds, where $T = \frac{N}{f_c}$, cycles within one bit period. Since we are detecting the polarity and not the actual voltage, of the carrier, the sampling operation can be accomplished by the use of a D type flip-flop. At the positive going edge of the clock pulse, when the clock pulse exceeds the threshold value, the sampling instant, the flip-flop is triggered and receives the input signal. If the input signal is greater than the threshold level, required to recognize a positive pulse, it is seen by the flip-flop as a '1', otherwise it is a '0'.

To reduce the threshold level, which in the 74H74 series flip-flop is ≈ 1.5 volts, whereas the required threshold should be at the zero line, we add just before the flip-flop a voltage comparator with one input connected to the ground, as shown in Figure 3.1. The utilization of the comparator removes the threshold ambiquities since if the input to the comparator is greater than 0 volts the output is 3 volts, which is greater than the required 2 volts in the input of the flip-flop to ensure '1'. Similarly if the input to the comparator is less or equal to 0 volts the output is 0 volt which is less than the 0.8 volts, maximum, required by the flip-flop to ensure '0'. The characteristic of the comparator is shown in Figure (3.2). The voltage comparator has no effect in the performance of the D.P.S.K. demodulator [15].

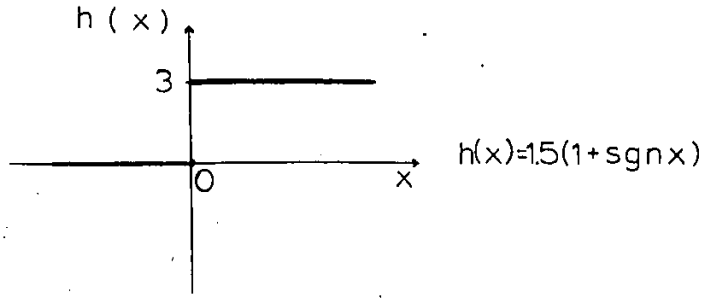

Fig. 3.2. Transfer functions of the voltage comparator

The output of the sample flip-flop is the differentially encoded data.

To compare each data bit with the previous one, as required for the differential decoder, we connect the output from the sample flip-flop which delays the differentially encoded data sequence by T seconds, where T is the period of message bit.

The output of the delay flip-flop, the delayed sequence, is compared with the undelayed sequence by the use of an EX-OR gate. Finally, the output of the EX-OR gate is the required message sequence. The overall operation of the demodulator is shown in Figure 3.3.

3.3 SYNCHRONIZATION REQUIREMENT FOR THE D.P.S.K. DEMODULATOR (Sampling once per symbol bit)

If, within one bit period there are N cycles of the carrier, the sampling point can be chosen at any of the 2N peaks regardless of the cycle, since we have differentially encoded signal where there is no phase knowledge requirement.

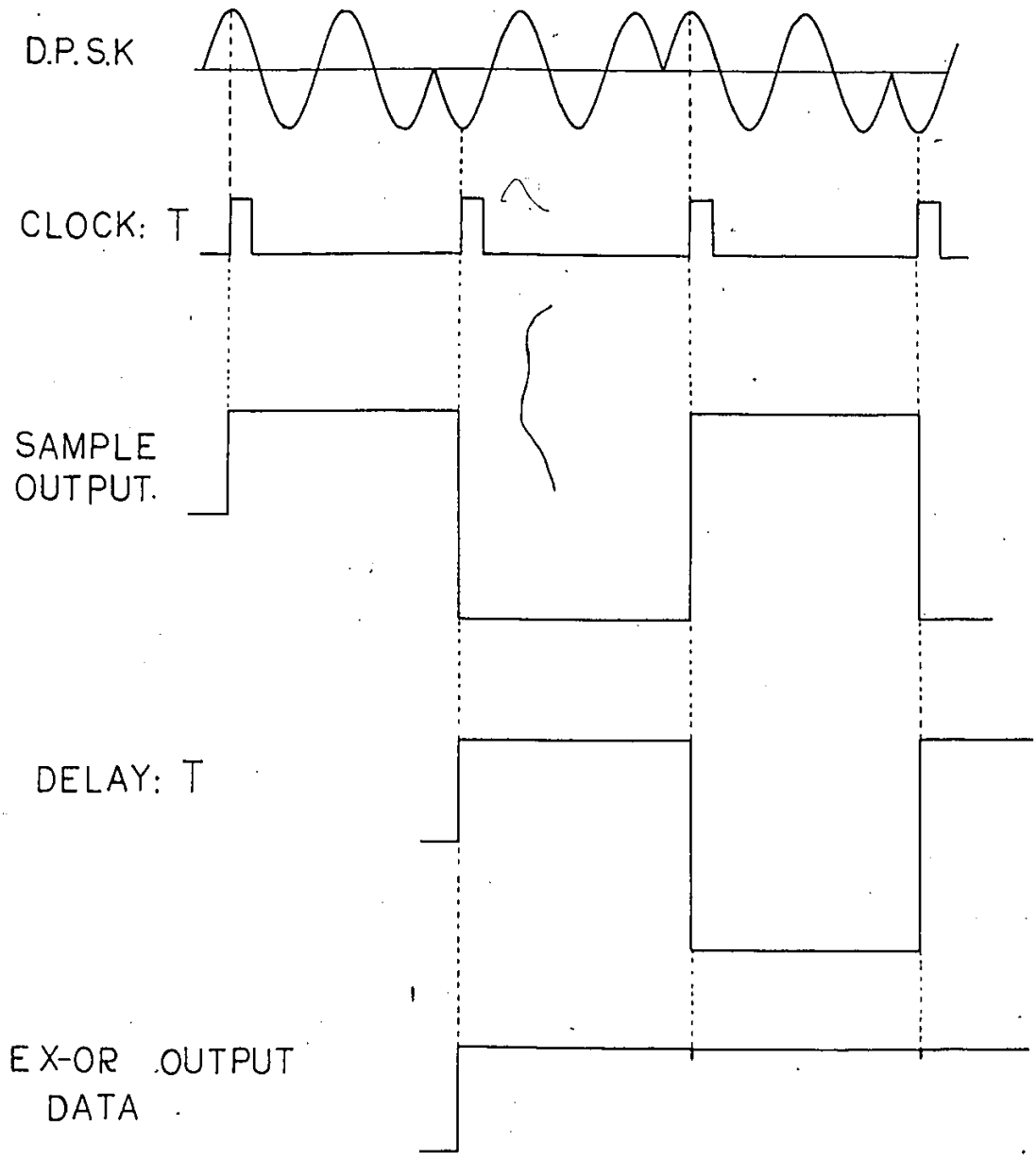

Fig. 3.3. Operation of the digital demodulator, with one sample per message bit

Therefore, we can skip carrier cycles within one bit, by delaying the clock pulse, and sample at the center of the symbol where the phase-change transition time, is eliminated.

From the 74 series, T.T.L. data sheet we have that the input setup time is equal 15 n.s. [16]. Setup time is the interval immediately proceeding the positive going edge of the clock pulse, during which interval the data to be recognized must be maintained at the input to ensure its recognition. Therefore to sample the carrier at the peaks, we must arrange the clock so the peak value appears at the input of the flip-flop at least 15 ns before the positive going edge of the clock pulse.

Given that the carrier period is 1μ sec., the clock edge must occur 265 ns after the zero crossing of the cycle. Figure 3.4

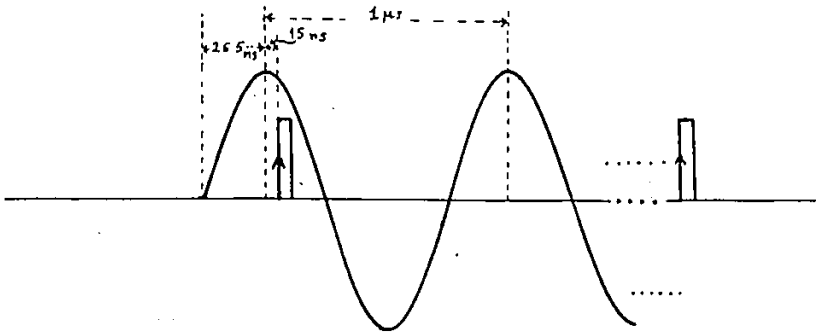

Fig. 3.4. Synchronyzation requirements

Hold time, which is the interval immediately following the positive edge of the clock pulse, during which interval the data to be recognized must be maintained at the input to ensure its continued recognition, for the 74H74 series is zero.

To accomplish the above clocking requirements the measurements were taken using as a clock a pulse generator which has variable delay operation, and was triggered by the P.R.B.S. generator clock output.

3.4 SAMPLING N TIMES PER MESSAGE PERIOD

The digital implementation of the D.P.S.K. demodulator with N samples within one bit period, where N is the number of carrier-cycles within this period, is accomplished by the circuit shown in Figure 3.5. The received signal plus Gaussian noise after filtering through the voltage comparator is entered to a serial to parallel shift register which is triggered by a clock with period $t_c = \frac{1}{f_c}$, where f_c is the carrier frequency. In every shift of the shift-register the data in each storage cell is transferred to the input of the Majority logic gate. When all these inputs belong to the same message bit, the majority gate is enabled by the use of a D type flip-flop which has clock period equal to the bit period $T = \frac{N}{f_c}$.

The output of the enable flip-flop will be the differential encoded message, and is '1', if $\frac{N+1}{2}$ out of N samples are '1', otherwise '0'. The encoded message bit is delayed by another D flip-flop (delayer) and is compared with the undelayed sequence by the EX-OR gate as previously described. The above operation is shown in Figure 3.6.

Synchronization requirements are the same as in the previous case, with the addition of a second clock with period $t_c = \frac{1}{f_c} = \frac{T}{N}$. Given the number of cycles within one bit period, i.e. t_c, the second clock T can easily be obtained by dividing by N the carrier.

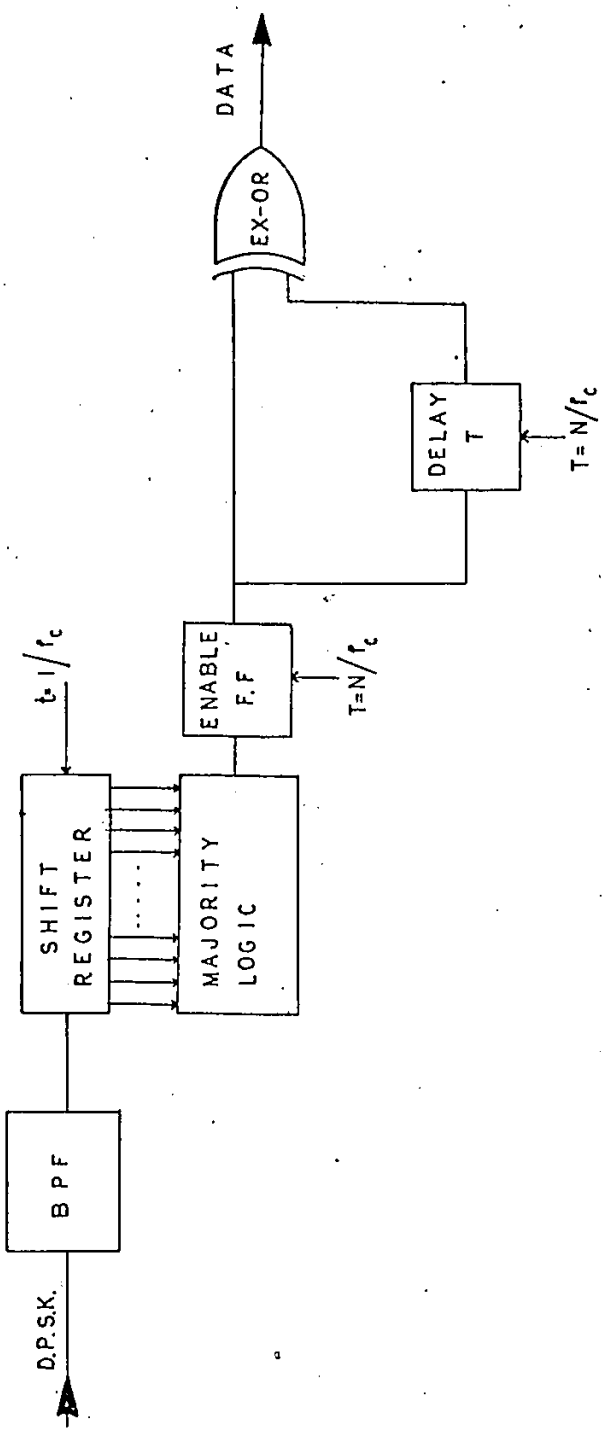

Fig. 3.5. Block diagram of the digital D.P.S.K. demodulator sampling N times within a message bit

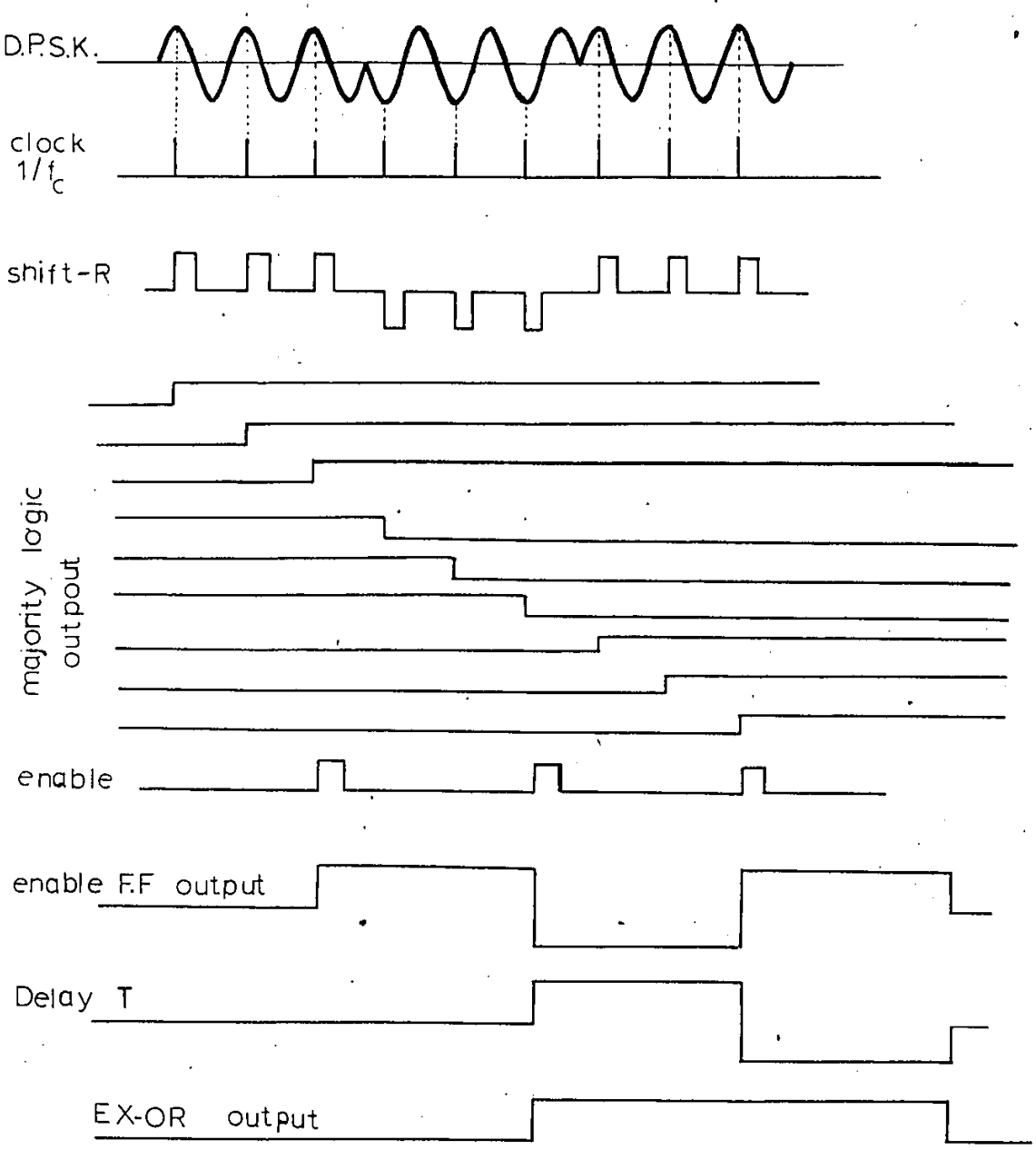

Fig. 3.6. Overall operation of the digital demodulator with three samples per message bit

4. CIRCUIT PERFORMANCE

4:1 PROBABILITY OF ERROR

The final criterion of performance of a digital communication system is the probability of error in the received message. Errors are determined by a comparison of the transmitted and received message. In this chapter we consider the quality of performance of the digital demodulator when while Gaussian noise is added to the signal.

A simplified diagram of the demodulator is shown in Figure (4.1).

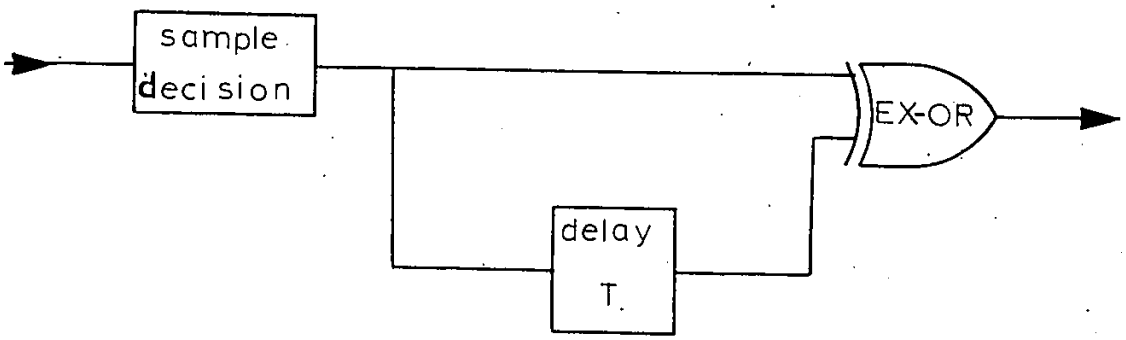

Fig. 4.1. Simplified diagram of the digital demodulator

The received signal and noise at the input of the demodulator, after filtering, is sampled to recover the differentially encoded binary symbols transmitted.

The differential decoding process consists of a delay flip-flop and an EX-OR gate.

An error in the output of the EX-OR gate is a result of an error made by the decision circuit, due to the Gaussian Noise. An error in the decision circuit results in a pair of errors in the output of the EX-OR gate, since the receiver obtains the reference from the preceeding bit. The double error rate performance of the EX-OR gate requires a complete analysis of the probability of error in the output, given the probability of an error in the input.

4.2 PROBABILITY OF ERROR OF THE DIFFERENTIAL DECODER

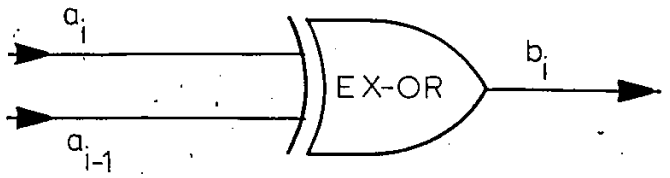

Fig. 4.2. EX-OR GATE

The logic operation of the gate is given by the equation:

$$b_i = a_i \oplus a_{i-1} \tag{4.1}$$

INPUT		OUTPUT
a_i	a_{i-1}	b_i
1	1	0
0	0	0
0	1	1
1	0	1

From Eq. (4.1) we have that:

$$\text{Prob}\,[b_i = \text{wrong}] = \text{Prob}\,[a_i = \text{correct}] \cdot \text{Prob}\,[a_{i-1} = \text{error}] + \text{Prob}\,[a_i = \text{error}] \cdot \text{Prob}\,[a_{i-1} = \text{correct}] \quad (4.3)$$

But

$$\Pr[a_i = \text{correct}] = [\Pr(1,1) + \Pr(0,0)]$$

$$\Pr[a_{i-1} = \text{correct}] = [\Pr(1,1) + \Pr(0,0)]$$

$$\Pr[a_i = \text{error}] = [\Pr(1,0) + \Pr(0,1)] \quad (4.4)$$

$$\Pr[a_{i-1} = \text{error}] = [\Pr(1,0) + \Pr(0,1)]$$

where

$\Pr(1,1)$ = Probability '1' is recovered and '1' was transmitted

$\Pr(0,0)$ = Probability '0' is recovered and '0' was transmitted

$\Pr(1,0)$ = Probability '0' is recovered and '1' was transmitted

$\Pr(0,1)$ = Probability '1' is recovered and '0' was transmitted.

From Eq. (4.3) and (4.4) we have

$$\text{Prob}\,[b_i = \text{wrong}] = [\Pr(1,1) + \Pr(0,0)] \cdot [\Pr(1,0) + \Pr(0,1)] + [\Pr(1,0) + \Pr(0,1)] \cdot [\Pr(1,1) + \Pr(0,0)] \text{ or}$$

$$\Pr[b_i = \text{wrong}] = 2\,[\Pr(1,1) + \Pr(0,0)] \cdot [\Pr(1,0) + \Pr(0,1)] \quad (4.5)$$

But we know that

$$\begin{aligned} \Pr(1,1) &= \Pr(1) \cdot \Pr(1|1) \\ \Pr(0,0) &= \Pr(0) \cdot \Pr(0|0) \\ \Pr(1,0) &= \Pr(1) \cdot \Pr(0|1) \\ \Pr(0,1) &= \Pr(0) \cdot \Pr(1|0) \end{aligned} \quad (4.6)$$

where

$\Pr(1) \triangleq P_1$, probability that 1 is transmitted

$\Pr(0) \triangleq P_0$, probability that 0 is transmitted

$Pr(1|0) \triangleq P_{e_0}$, probability we receive 1 given that 0 was transmitted, or the probability of error, when 0 is transmitted, at the decision circuit due to Gaussian noise. (4.7)

$Pr(0|1) \triangleq P_{e_1}$, probability we receive 0 given that 1 was transmitted, or the probability of error, when 1 is transmitted, at the decision circuit due to Gaussian noise.

From Eq. (4.7)

$$Pr(1|1) = 1 - P_{e_1} \quad \text{and} \quad Pr(0|0) = 1 - P_{e_0} \tag{4.8}$$

From Eq. (4.8), (4.7), (4.6) and (4.5) we have:

$$Pr[b_i = \text{wrong}] = 2\left[P_1 (1 - P_{e_1}) + P_0 (1 - P_{e_0})\right] \cdot \left[P_1 P_{e_1} + P_0 P_{e_0}\right] \tag{4.9}$$

and for $P_{e_1} = P_{e_0} = P_{e_{DECISION}}$, Eq. (4.9) becomes

$$Pr[b_i = \text{wrong}] = 2 P_{e_{DEC.}} (1 - P_{e_{DEC.}}) \quad \text{or}$$

$$P_{e_{EX\text{-}OR}} = 2 P_{e_{DECISION}} (1 - P_{e_{DECISION}}) \tag{4.10}$$

Equation 4.10 is shown in Figure 4.3, where $P_{e_{EX\text{-}OR}}$ and $P_{e_{DEC.}}$ are plotted versus $\frac{E_B}{No}$ From Figure 4.3 we can see the 2 dB degradation because of the use of differential detection.

4.3 PROBABILITY OF ERROR AT THE DECISION CIRCUIT - $P_{e_{DECISION}}$

A) Sampling once per message bit

The R.F. Signal, after bandpass filtering, will be sampled once per bit period.

The decision putput depends on what part of the cycle is sampled. If Gaussian noise is added, the received signal, within one bit period, is given by

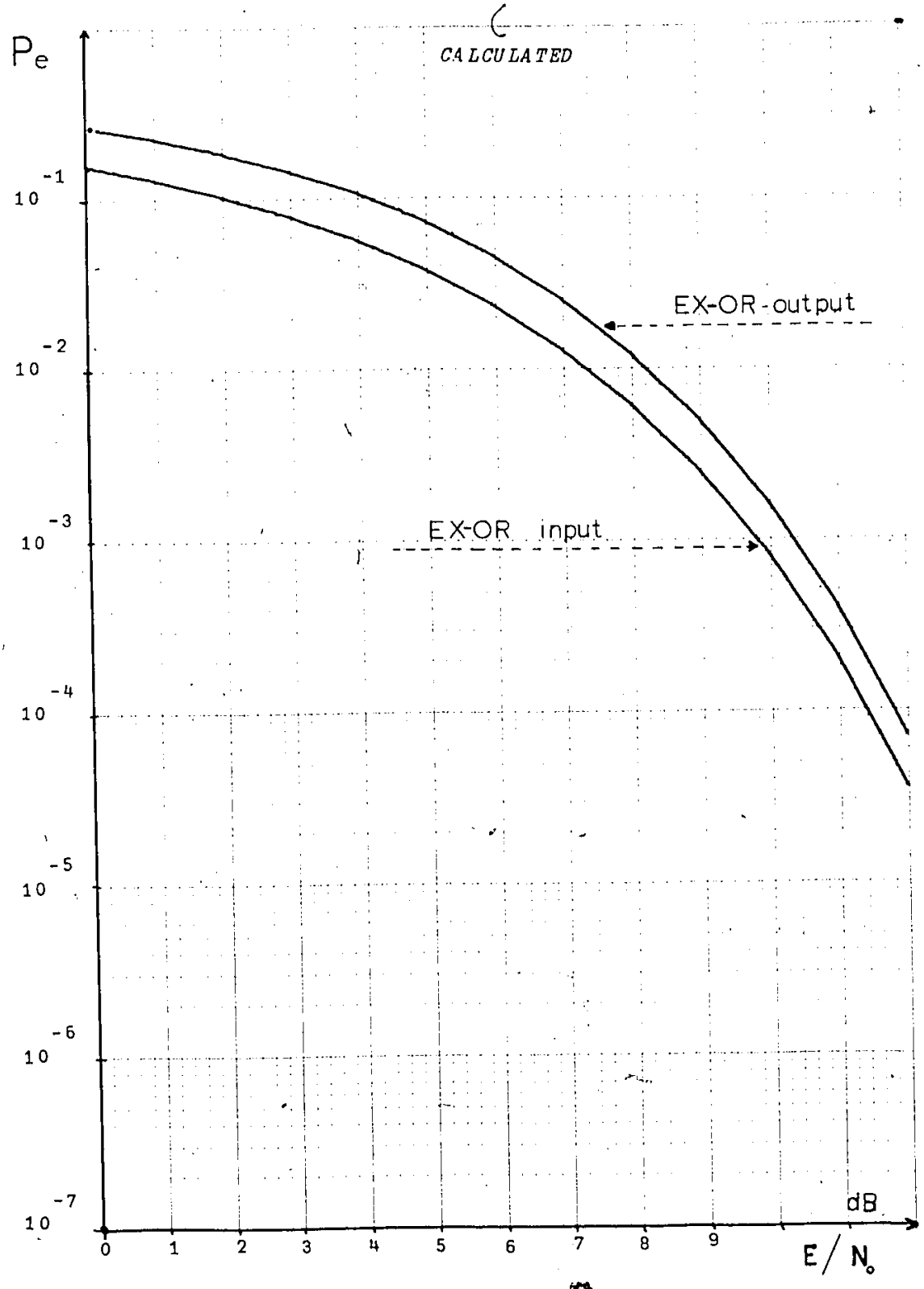

Fig. 4.3. Degradation due to the differential decoder

$$u(t) = \pm A \cos 2\pi f_c t + n(t) \tag{4.11}$$

and at the sampling instant

$$u(t_s) = \pm A \cos 2\pi f_c (t_s + \Delta t) + n(t_s + \Delta t) \tag{4.12}$$

where

A = carrier amplitude

f_c = carrier frequency and $f_c T = N$

t_s = sampling time, equal to T

Δt = timing error due to imperfect clocking.

Expanding (4.12)

$$u(t_s) = \pm A \cos 2\pi f_c \Delta t + n(t_s + \Delta t) \tag{4.13}$$

and if we call

$2\pi f_c \Delta t = \varphi$ and $t_s + \Delta t \triangleq t$, Eq. (4.13) becomes

$$u(t_s) = \pm A \cos \varphi + n(t) \tag{4.14}$$

From Eq. (4.14), the probability of error at the decision output, $P_{e_{DEC}}$, is given by

$$P_{e_{DEC}} = Pr[n > A \cos \varphi \mid A \cos \varphi < 0] \cdot Pr(A \cos \varphi < 0) + \\ + Pr[n < -A \cos \varphi \mid A \cos \varphi > 0] \cdot Pr(A \cos \varphi > 0) \tag{4.15}$$

Since the threshold level is at zero, for Gaussian noise:

$$Pr(n > A \cos \varphi) = Pr(n < -A \cos \varphi)$$

and

$$Pr(A \cos \varphi > 0) = Pr(A \cos \varphi < 0) = \frac{1}{2}$$

therefore (4.15) becomes:

$$P_{e_{DEC}} = Pr(n > A \cos \varphi) \tag{4.16}$$

For Gaussian noise, with zero mean and variance σ_n^2 we have that:

$$Pr(n > A\cos\varphi) = \int_{A\cos\varphi}^{\infty} \frac{1}{2\pi\sigma} e^{-\frac{x^2}{2\sigma^2}} dx$$

$$= 1 \int_0^{A\cos\varphi} \frac{1}{2\pi\sigma} e^{-\frac{x^2}{2\sigma^2}} dx$$

Substitute $\frac{x}{2\sigma} = y$ we get

$$Pr(n > A\cos\varphi) = \frac{1}{2} - \frac{1}{\sqrt{\pi}} \int_0^{\frac{A\cos\varphi}{2\sigma}} e^{-y^2} dy$$

$$= \frac{1}{2}\left[1 - \frac{2}{\sqrt{\pi}} \int_0^{\frac{A\cos\varphi}{2\sigma}} e^{-y^2} dy\right]$$

$$= \frac{1}{2}\left[1 - erf\left(\frac{A}{2\sigma}\right)\cos\varphi\right] \quad \text{or}$$

$$Pe_{DIC} = \frac{1}{2}\left[erfc\left(\sqrt{\frac{A^2}{2\sigma^2}} \cdot \cos\varphi\right)\right] \qquad (4.17)$$

but $\sqrt{\frac{A^2}{2\sigma^2}} = \sqrt{\frac{C}{N}}$, where $\frac{C}{N}$ is the carrier to noise ratio, and Eq. (4.17) becomes

$$P_{e_{DIC}} = \frac{1}{2}\left[erfc\left(\sqrt{\frac{C}{N}}\cos\varphi\right)\right] \qquad (4.18)$$

Substituting Eq. (4.18) in (4.10) we have that, the probability of error of the demodulator, for one sample per bit duration is given by:

$$P_e = erfc\left(\sqrt{\frac{C}{N}} \cdot \cos\varphi\right) \cdot \left[1 - \frac{1}{2} erfc\left(\sqrt{\frac{C}{N}} \cdot \cos\varphi\right)\right] \qquad (4.19)$$

To find P_e with respect of $\frac{E_B}{N_o}$ where

E_B = Energy per bit

N_o = Noise density (Noise power per unit cycle)

we have that:

$$\frac{E_B}{N_o} = \frac{\frac{A^2}{2} T}{\frac{N}{BW}} = \frac{BW}{R} \frac{C}{N} \quad \text{or}$$

$$\frac{C}{N} = \frac{R}{BW} \cdot \frac{E_B}{N_o} \tag{4.20}$$

where

R is the bit rate and

BW is the noise bandwidth.

From Eq. (4.20) and (4.19) we have:

$$P_e = \left[\operatorname{erfc}\left(\sqrt{\frac{R}{BW} \cdot \frac{E_B}{N_o}} \cdot \cos\varphi\right)\right] \cdot \left[1 - \frac{1}{2} \operatorname{erfc}\left(\sqrt{\frac{R}{BW} \frac{E_B}{N_o}} \cos\varphi\right)\right] \tag{4.21}$$

The average probability of error for all possible values of phase-error φ, is given by

$$P_{e\,av} = \int_{\varphi} P_e \cdot p(\varphi)\, d\varphi \tag{4.22}$$

where $p(\varphi)$ is the p.d.f. of the phase-error due to imperfect synchronization.

Assuming uniform distribution for $p(\varphi)$ that is:

$$p(\varphi) = \frac{1}{2a}, \text{ for } -a < \varphi < +a \qquad \text{and } a = \frac{\pi}{2}$$

Eq. (4.22) was evaluated by numerical integration using Simpson's Rule (see Appendix I).

The required bandwidth for 2-φ D.P.S.K. system is known to be equal 1.2 times the data rate R.

Because of the band limited noise, it is given by [23], [27] that the sample values of the noise at the sampling instant in adjacent time slots, in

D.P.S.K. system, are statistically independent random variables only if the noise bandwidth is greater 1.4 times the bit rate R.

J. Jones [28] indicates that to avoid excessive degradation with symmetrical bandwidth limiting, the minimum bandwidth should be no smaller than twice the bit rate R.

Also, A.J. Viterbi [34], in his analysis for frequency acquisition and synchronization system for D.P.S.K. detection in additive noise, assumes that the bandpass filter bandwidth, at the receiver, is made equal six times the data rate R.

Therefore Eq. (4.22) is evaluated for five different noise bandwidths, $B_N = 1.2R, 1.8R, 2R, 3R, 5R$. The results are shown in Fig. (4.4) a, b, c, d, e (solid lines) where $P_e = (\frac{E_B}{N_o})$ is plotted for each noise bandwidth B_N.

The experimental results, dotted lines, were measured assuming noise bandwidth the 3-dB bandwidth of a four pole Butterworth bandpass filter. This assumption introduces systematic errors in the experimental results due to the deviation of the B.P. filter response from the flat response required within the 3-dB bandwidth.

The frequency response of the four pole Butterworth B.P. filter, for the five different 3-dB bandwidths is shown in Fig. (4.5) a, b, c, d, e.

In Fig. (4.6) a,b, the probability of error for the five noise bandwidths, is shown.

In Fig. (4.7), the effect of timing error $\Delta\varphi$ in the system performance is shown.

From Fig. (4.7) we have that to suffer no more than 1-dB loss in performance, as compared to ideal synchronization, i.e. $\Delta\varphi = 0$, requires

$$\Delta\varphi < 36^o$$

$$\Delta t = 10\% \text{ of } \frac{1}{f_c}$$

that is the sampling accuracy should be within 10% of the carrier period.

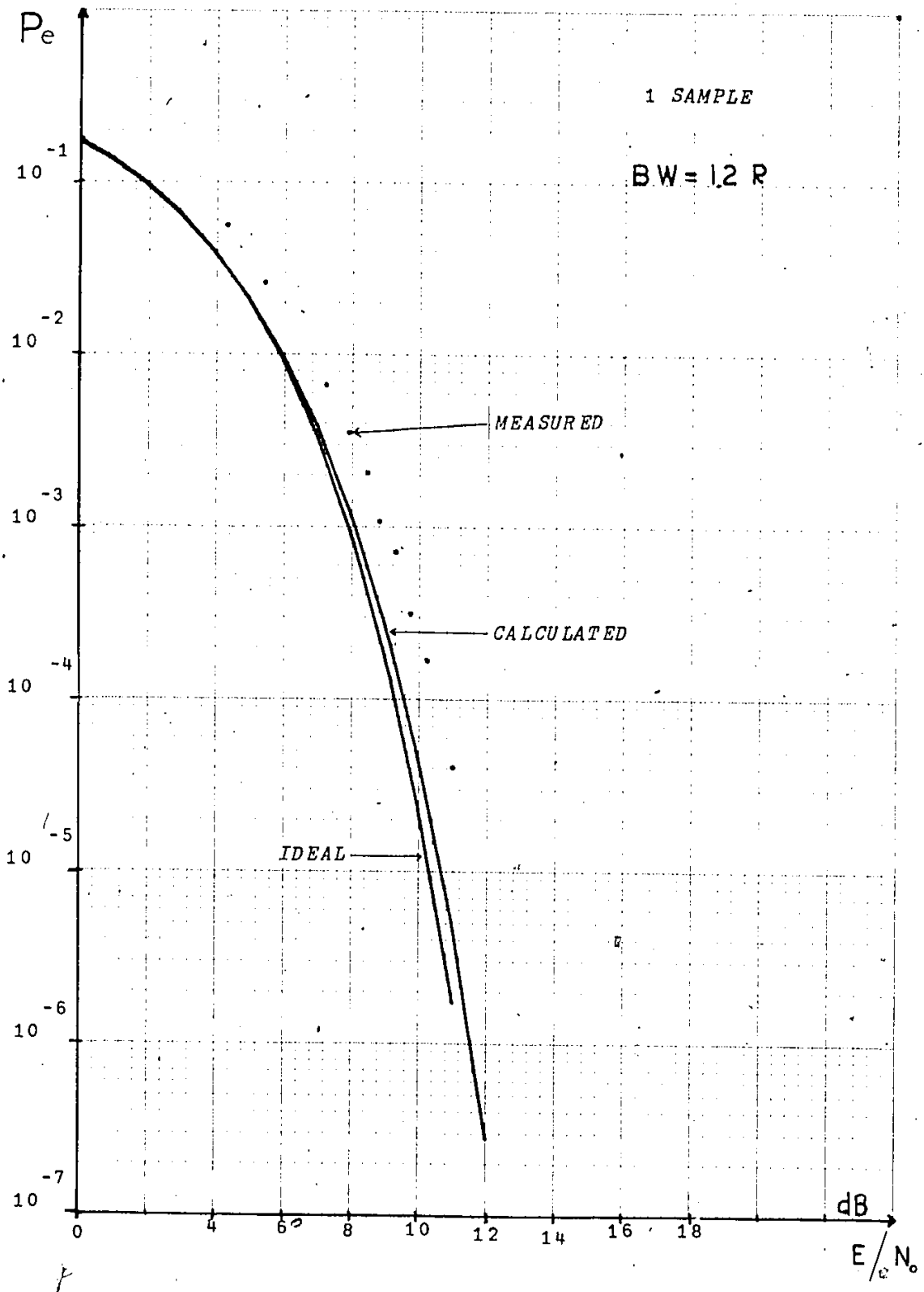

Fig. 4.4a. B.E.R. with noise BW=1.2R

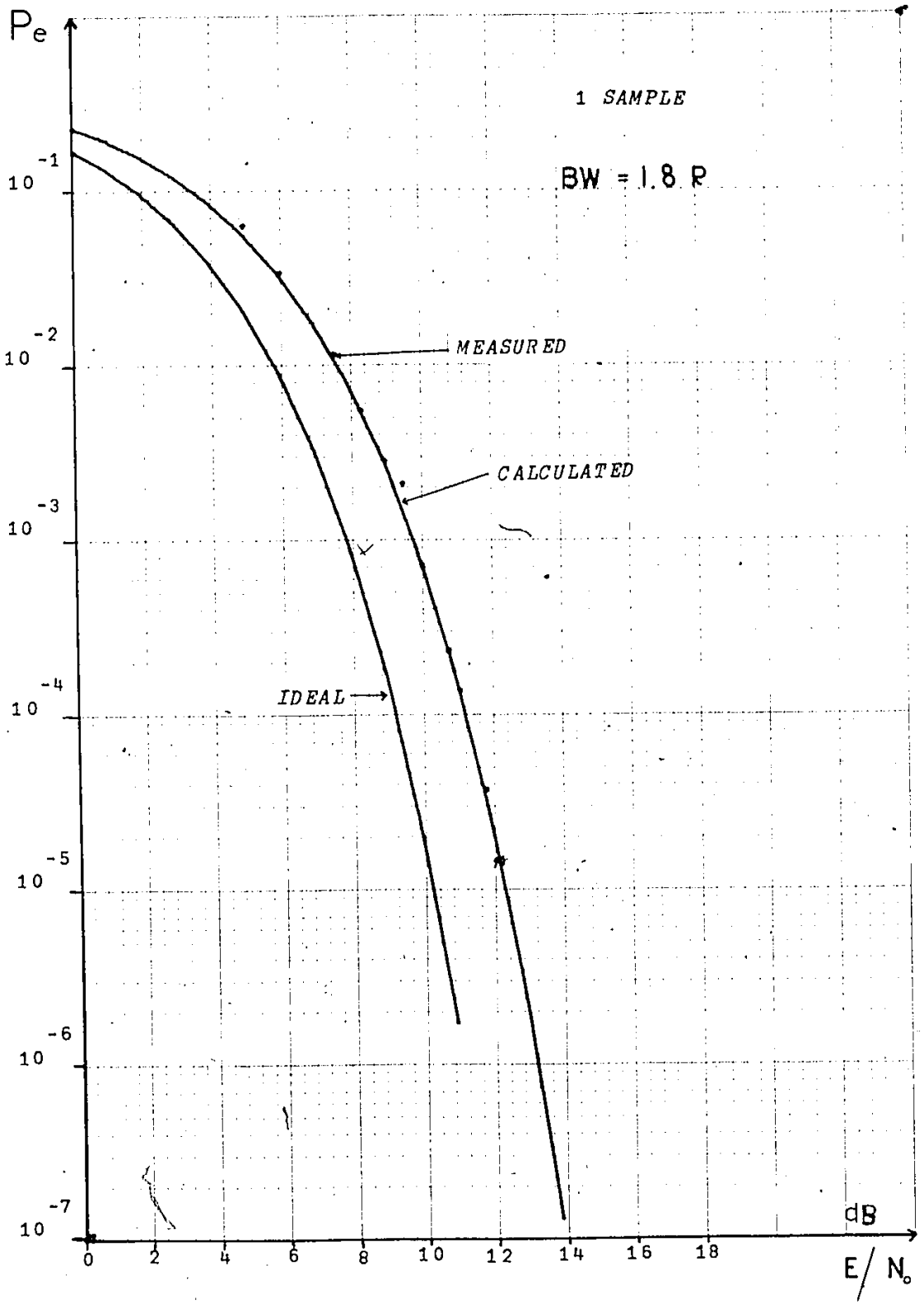

Fig. 4.4b. B.E.R. with noise BW=1.8 R

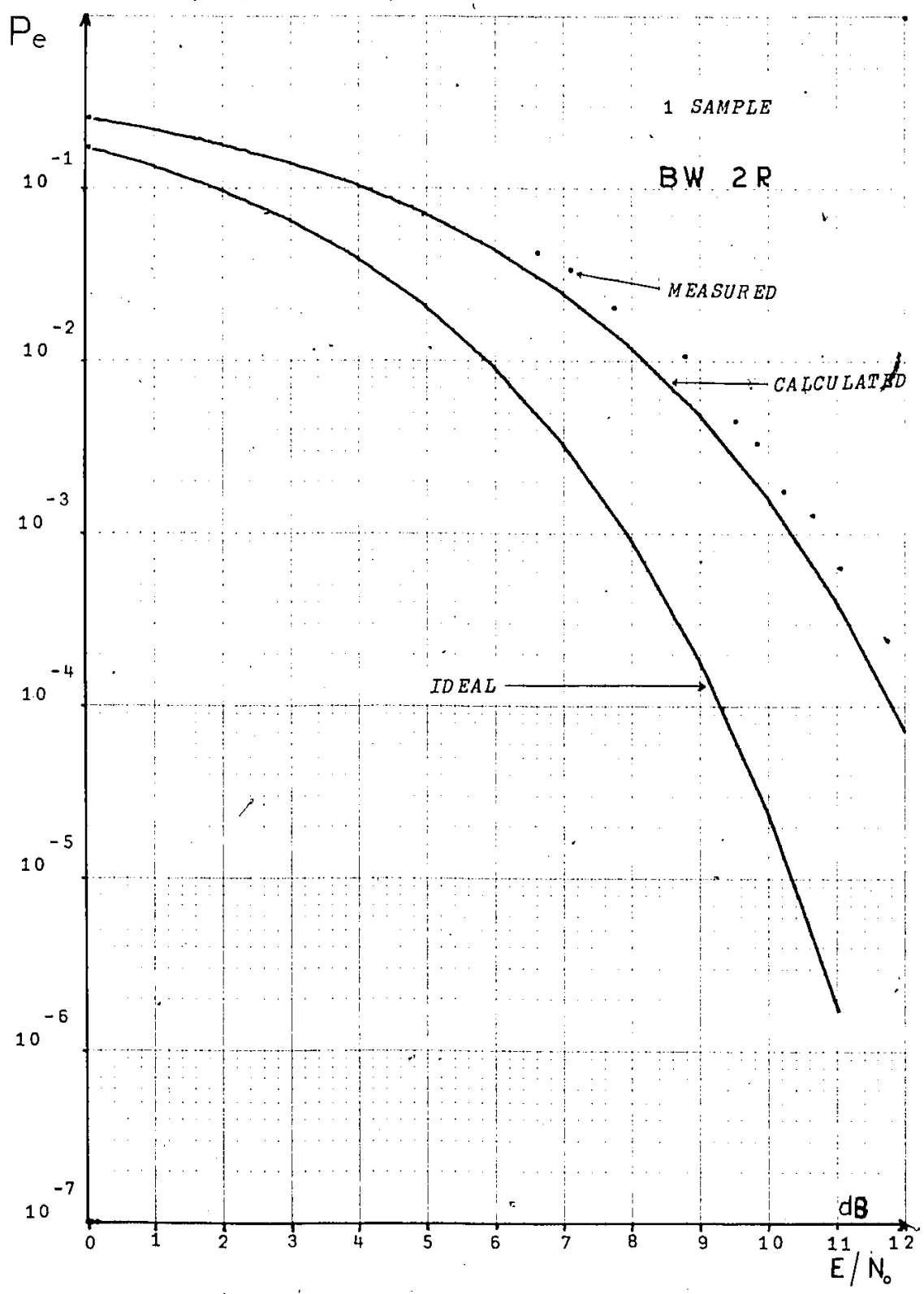

Fig. 4.4c. B.E.R. with noise RW=2 R

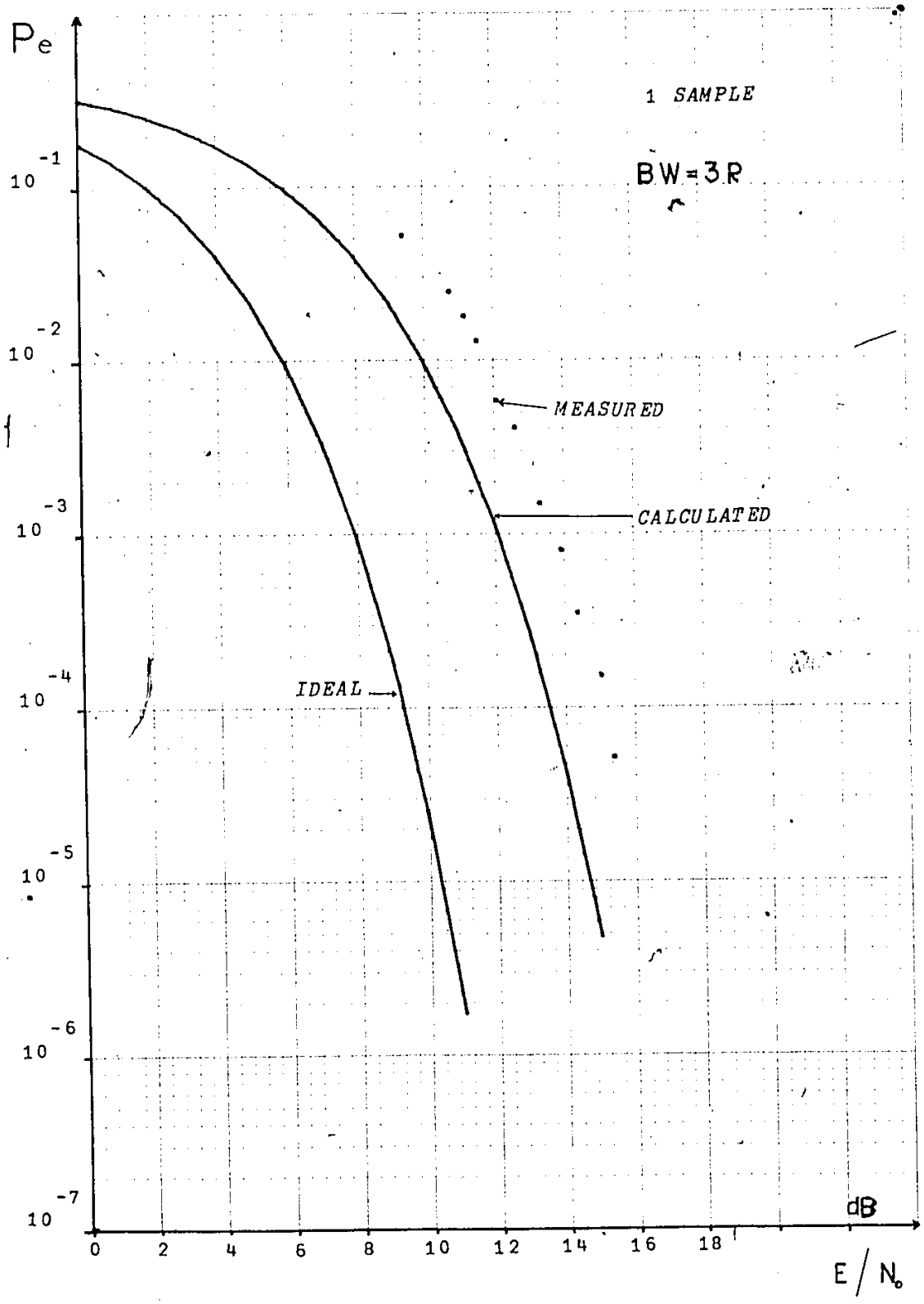

Fig. 4.4d. B.E.R. with noise BW=3R

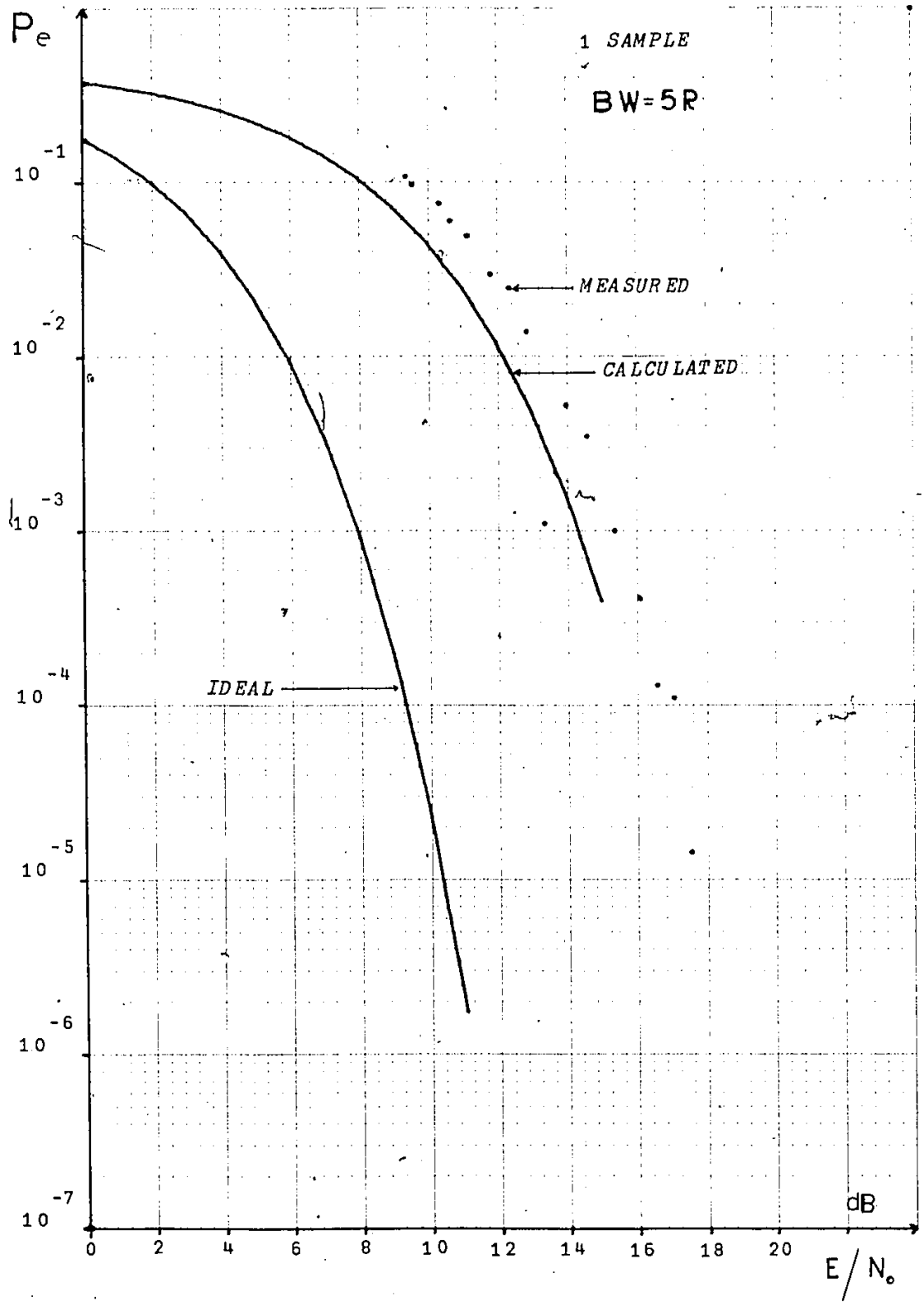

Fig. 4.4e. B.E.R. with noise BW=5 R

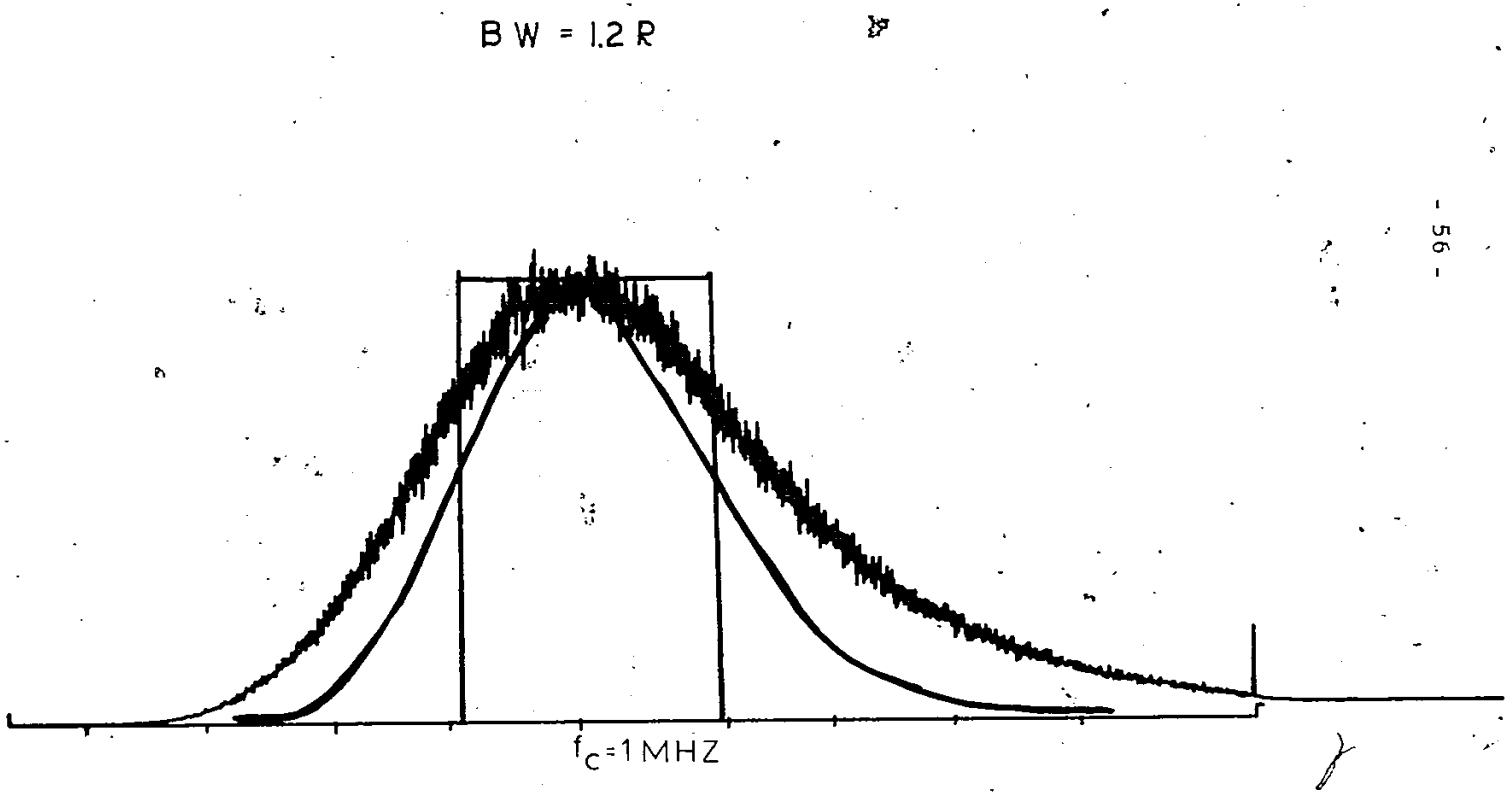

Fig. 4.5a. Filter response with RW=1.2 R

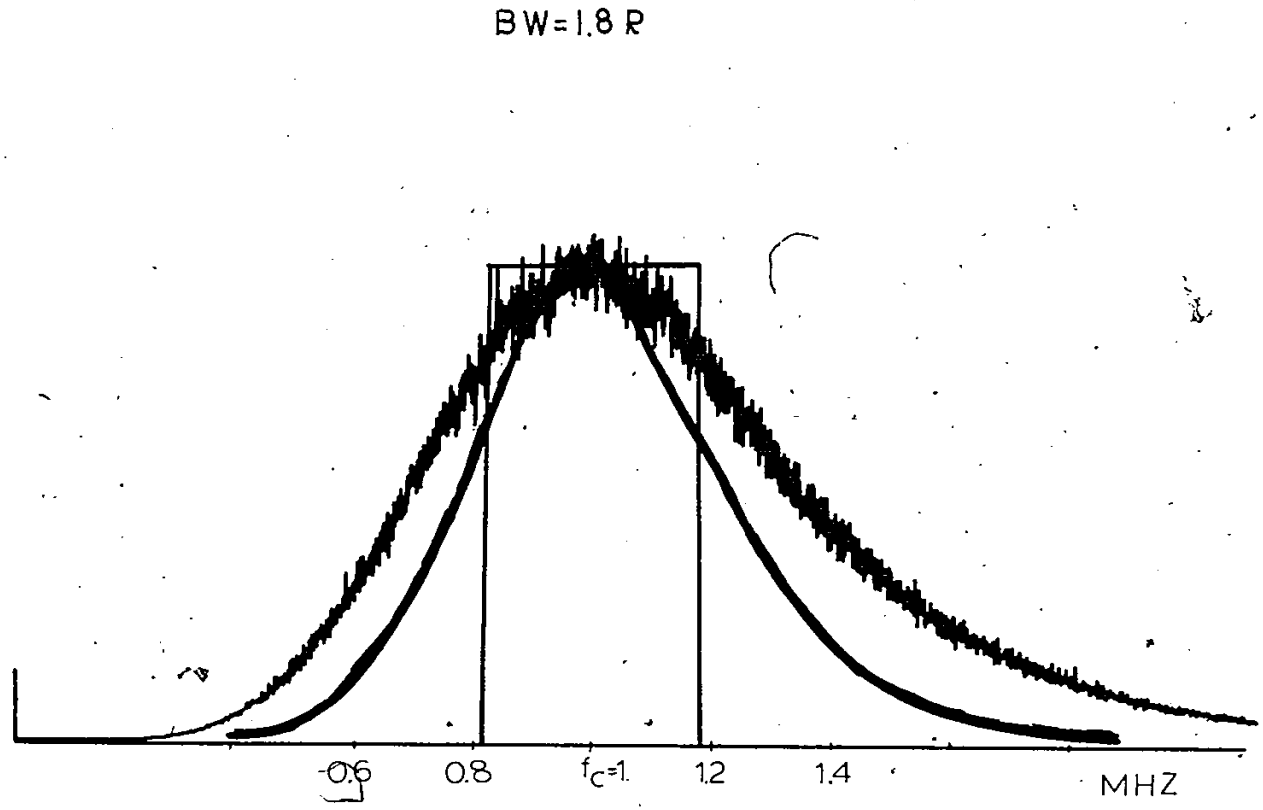

Fig. 4.5b. Filter response with BW=1.8 R

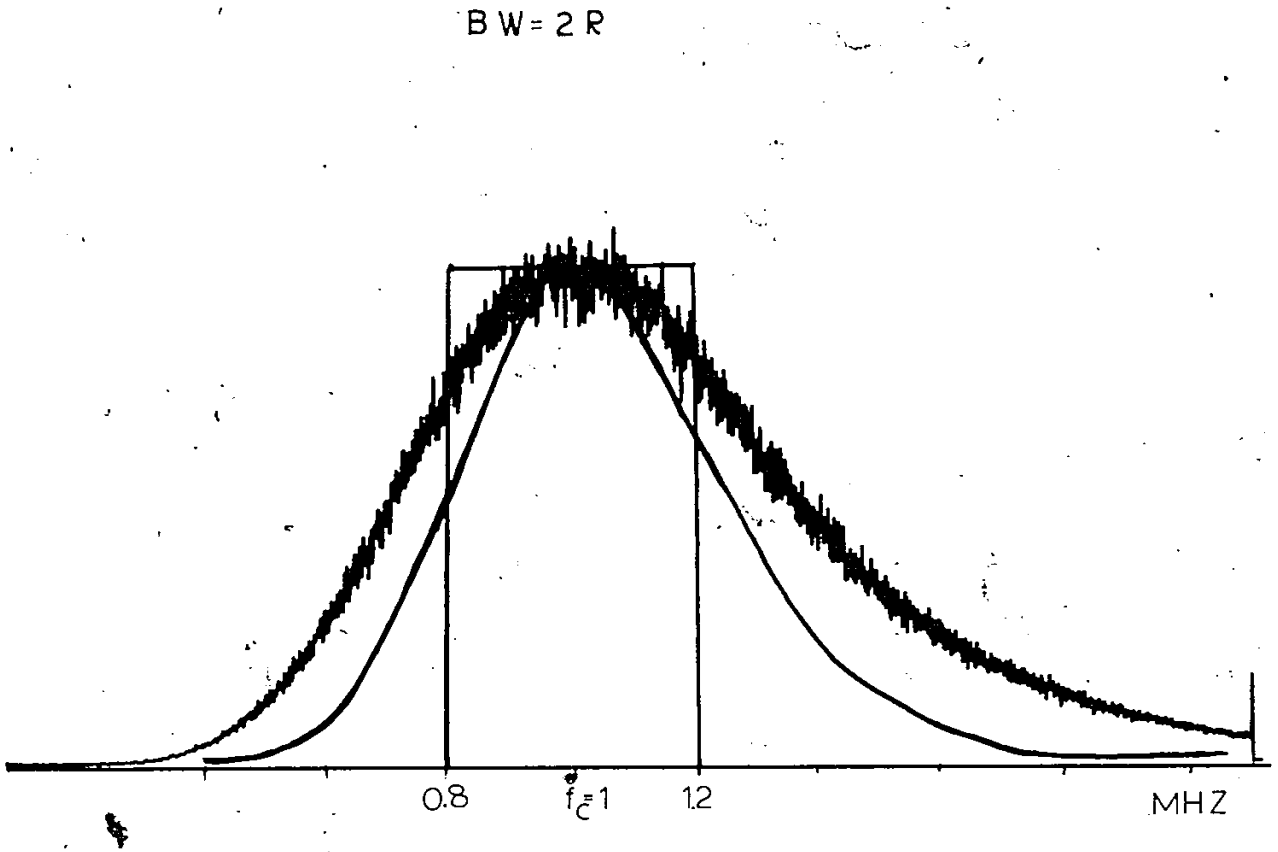

Fig. 4.5c. Filter response with BW=2 R

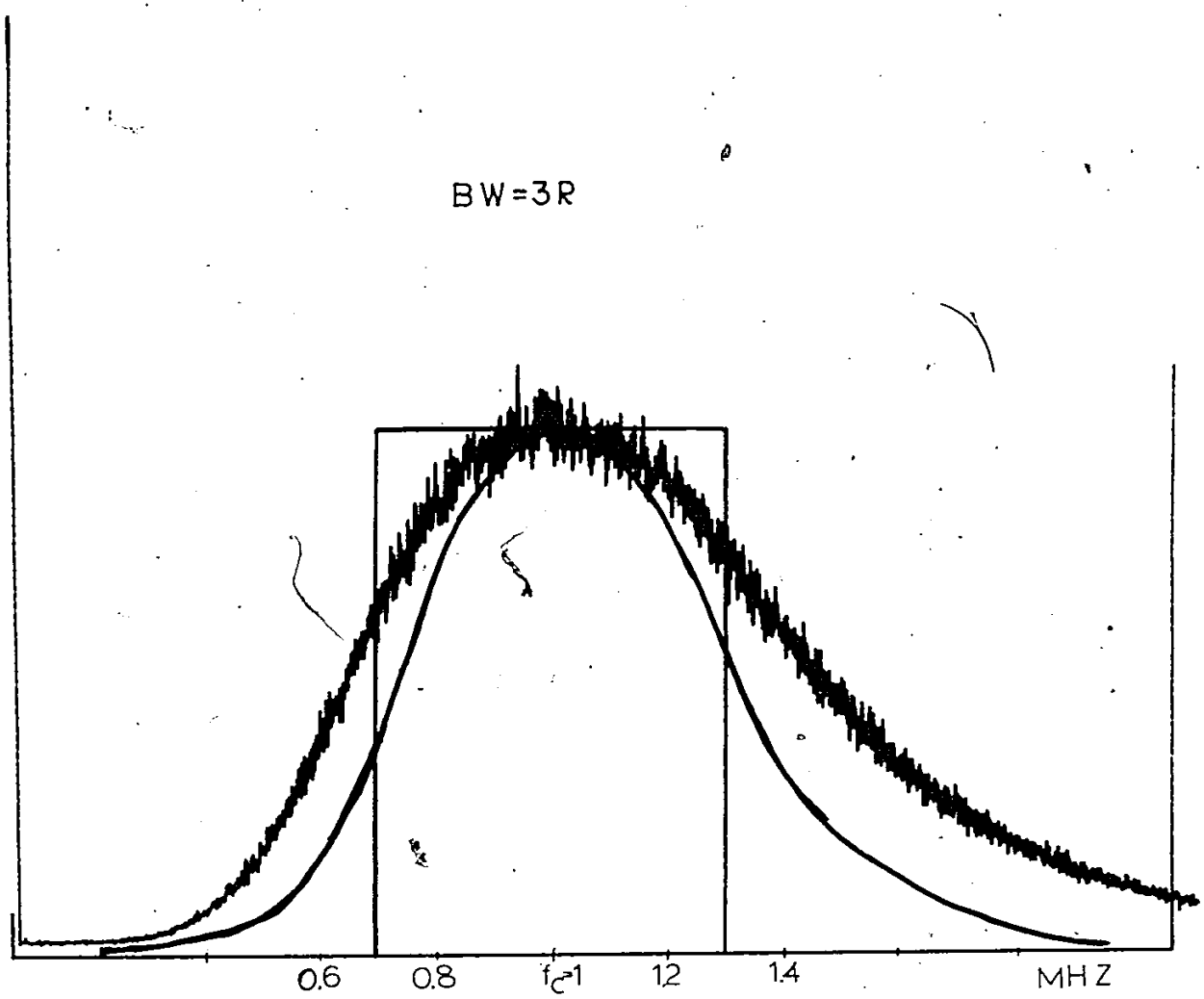

Fig. 4.5d. Filter response with BW=3 R

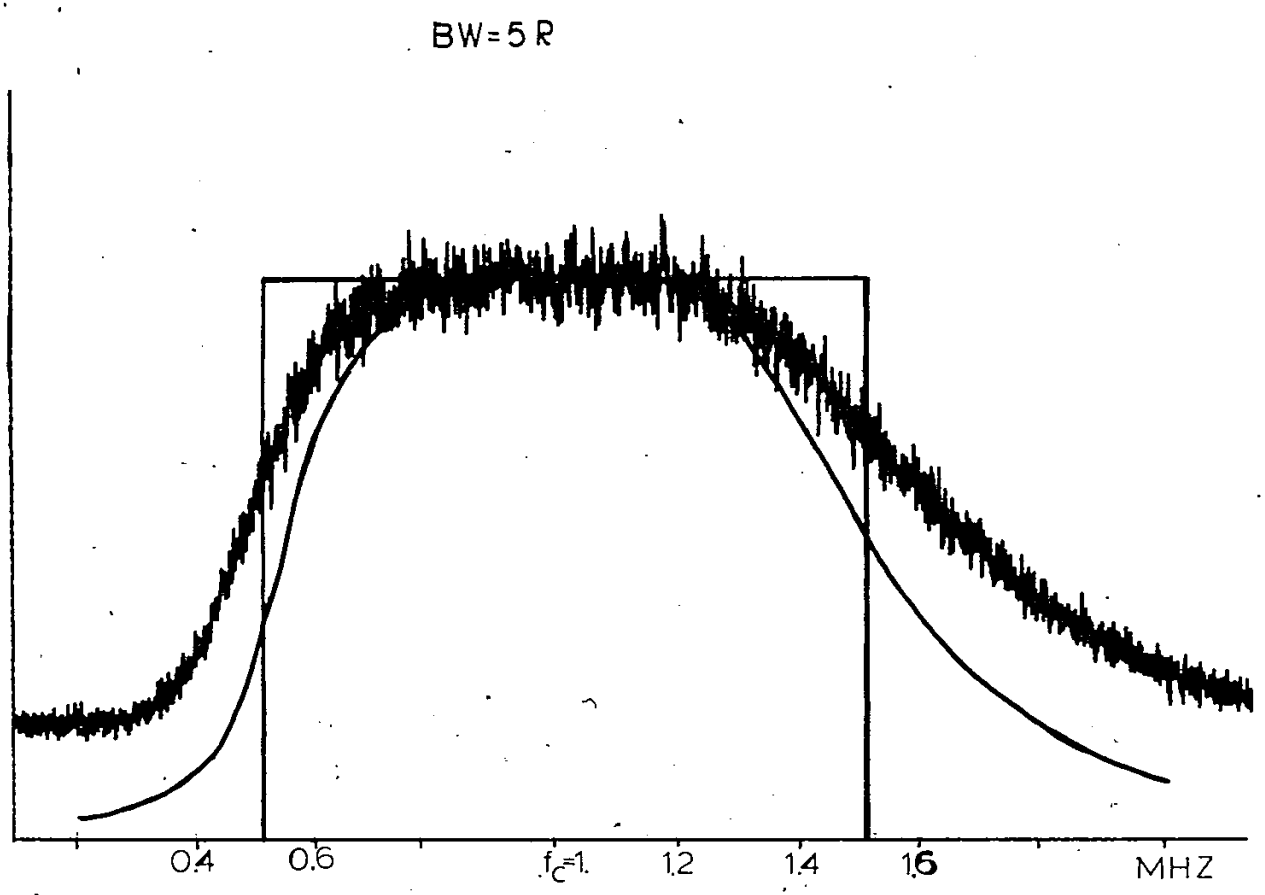

Fig. 4.5e. Filter response with BW=5 R

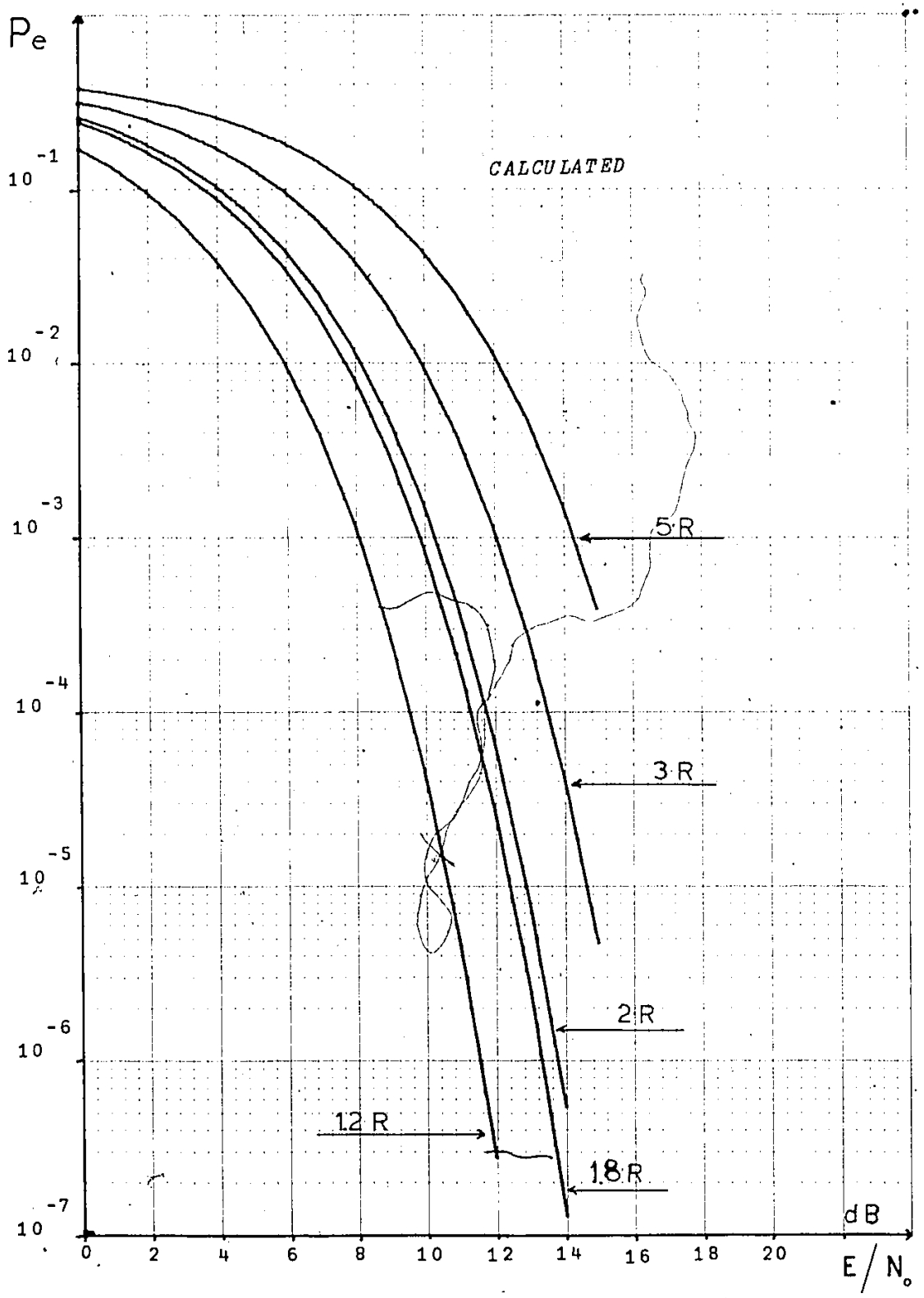

Fig. 4.6a. Calculated B.E.R. for different values of bandwidth BW

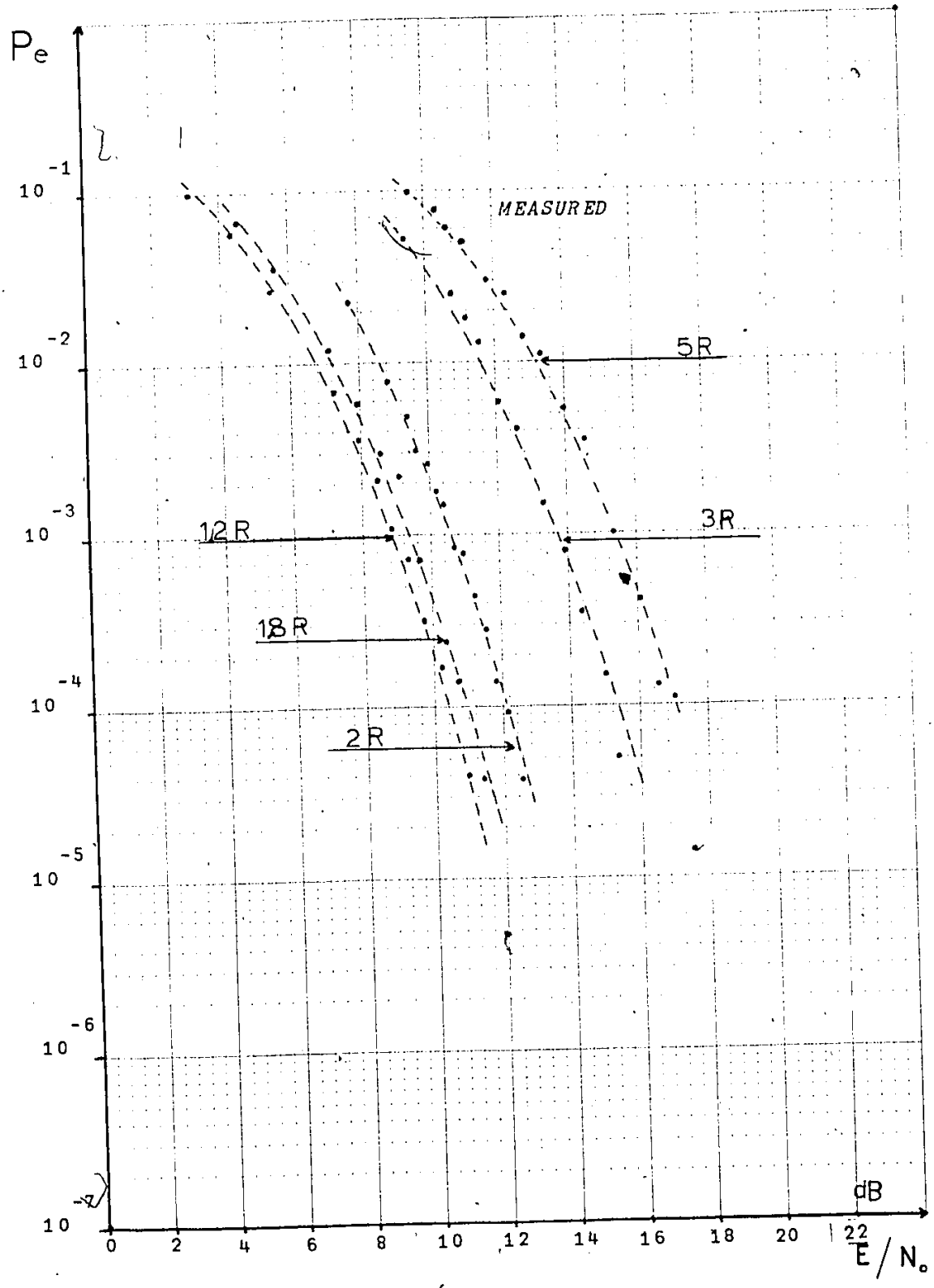

Fig. 4.6b. Measured B.E.R. for different values of bandwidth BW

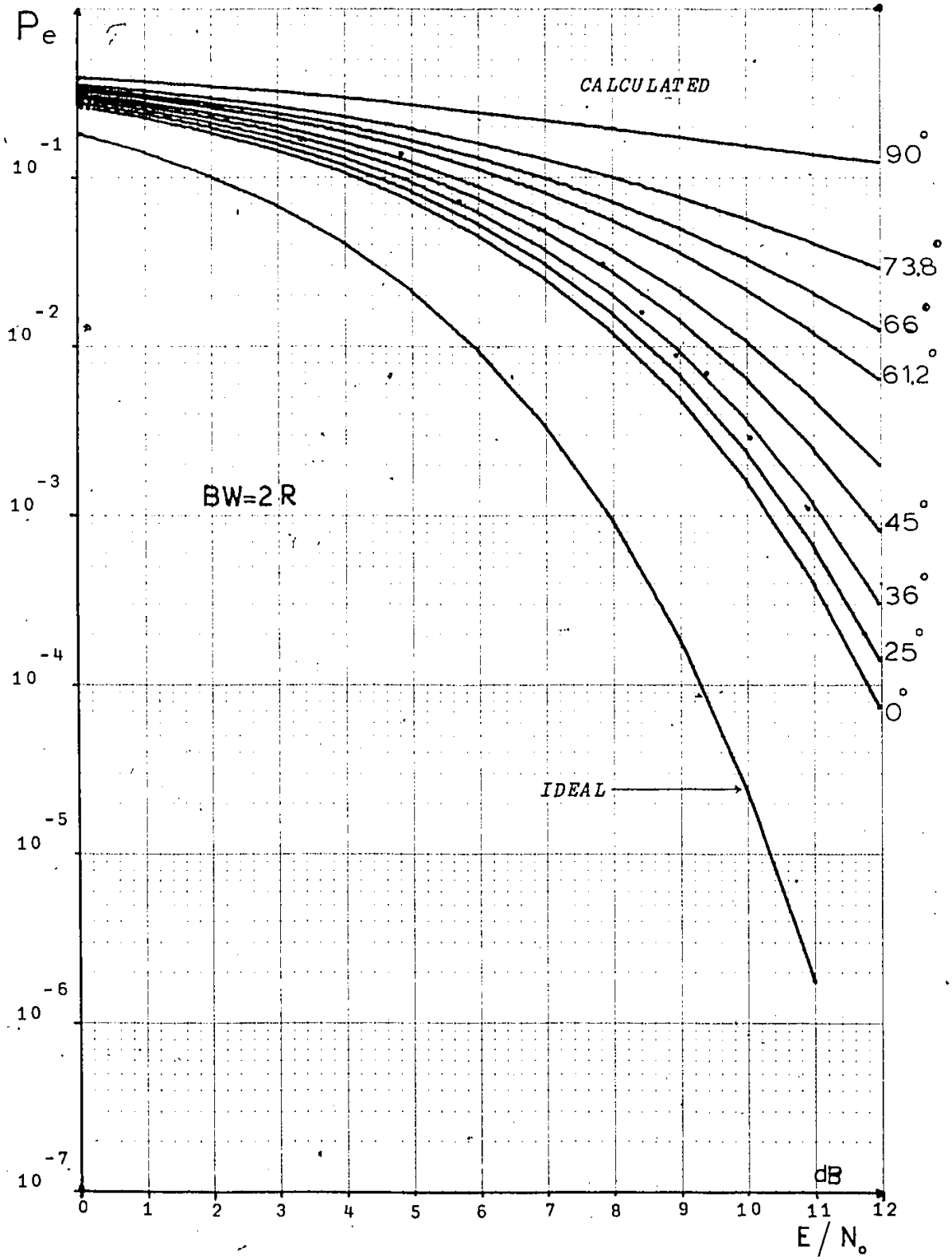

Fig. 4.7. Calculated B.E.R. for different values of timing error

4.4 SAMPLING MORE THAN ONCE PER SYMBOL PERIOD

For sampling more than once per message bit, a simplified diagram of the demodulator is shown in Figure 4.8.

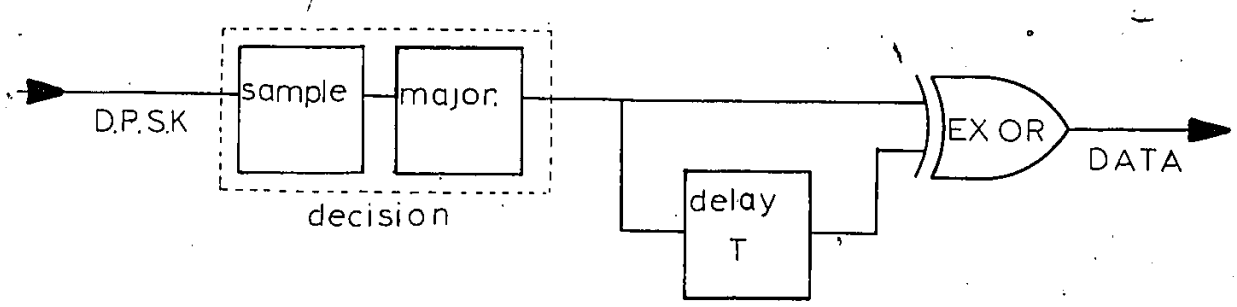

Fig. 4.8. Digital demodulator for N samples per message bit

Assuming zero mean Gaussian noise with variance σ_N^2 and N samples spaced equally throughout the total message bit period T, where $N = T \cdot f_c$, i.e. the sampling interval of $t_s = \frac{T}{N}$, where f_c is the carrier frequency.

We consider two cases: A. Correlated noise samples and B. Independent noise samples.

4.5 A. Correlated Noise Samples

If the noise samples are correlated then the probability of error at the output of the majority logic gate Fig. 4.8 is given by:

Pr(error) = Pr (N samples in error) +

$$+ \Pr\ (N\text{-}1 \text{ samples in error, } 1 \text{ sample correct}) \ +$$

$$+ \Pr\ (N\text{-}2 \text{ samples in error, } 2 \text{ samples correct}) \ +$$

$$+ \ldots\ldots\ldots\ldots\ldots\ldots\ldots\ldots\ldots\ldots$$

$$+ \Pr\ \left(\frac{N+1}{2}\right) \text{ samples in error, } \frac{N-1}{2} \text{ samples correct}).$$

Where

Pr (N=i samples in error, i samples correct) is given by:

$$\int\int\int \cdots \int p(y_1, y_2, \ldots, y_N)\, dy_1, dy_2 \ldots dy_N$$

and

$p(y_1, y_2, \ldots, y_N)$ is the joint probability density function of N noise samples given by [30]:

$$p(y_1, y_2, \ldots, y_N) = \frac{\exp\left[-\frac{1}{2|\Lambda|}\sum_{n=1}^{N}\sum_{m=1}^{N} |\Lambda|_{nm}\, y_n\, y_m\right]}{(2\pi)^{N/2}\, |\Lambda|^{1/2}}$$

where $|\Lambda|_{nm}$ is the cofactor of the element λ_{nm} in the determinant $|\Lambda|$ of the covariance matrix of the noise:

$$\Lambda = \begin{bmatrix} \lambda_{11} & \lambda_{12} & \cdots & \lambda_{1N} \\ \lambda_{21} & \lambda_{22} & \cdots & \lambda_{2N} \\ \text{---} & \text{---} & \text{---} & \text{---} \\ \text{---} & \text{---} & \text{---} & \text{---} \\ \lambda_{N1} & \lambda_{N2} & \cdots & \lambda_{NN} \end{bmatrix}$$

in which matrix

$$\lambda_{nm} = E\,(y_n\, y_m) = \sigma_N^2\, \rho_{nm}$$

where ρ_{nm} is the normalized autocorrelation function of the noise samples given by

$$\rho_{nm} = \rho(kt_s) = \frac{R_{nm}}{\sigma_N^2} \qquad (4.24)$$

for band limited guassian noise Eq. (4.24) becomes

$$\rho(kt_s) = \cos 2\pi f_c t_s \cdot \frac{\sin \pi B_N t_s}{\pi B_N t_s} \qquad (4.25)$$

where B_N is the noise bandwidth.

Instead of evaluating the probability of error from Eq. (4.23), which for N=5 requires the solution of 16 integrals each with 5 variables, we will investigate whether, sampling more than once within one message bit, improves the demodulation process or not, i.e. whether it reduces the probability of error given that the noise samples are correlated.

For the assumed zero mean Gaussian noise the variance of the sample mean σ_M^2 is given by [33]:

$$\sigma^2(M) = \frac{\sigma_N^2}{N} + \frac{2}{N} \sum_{k=1}^{N-1} (1 - \frac{k}{N}) R(k t_s) \qquad (4.26)$$

To see the effect of the correlation between noise samples, suppose that the samples are so highly correlated that approximately

$$\rho(k t_s) \approx 1$$

in this case Eq. (4.27) becomes

$$\sigma^2(M) \approx \sigma_n^2$$

That is, when the samples are highly correlated, the variance of the sample mean is approximately equal to the variance of samples. Therefore, a single sample provides just as much information as any other number of samples.

However, with $\rho(k\,t_s) < 1$ for $k = 1, 2, \ldots, N-1$ we do improve the demodulation process by sampling more than once per symbol period. Since for $\rho(k\,t_s) < 1$ Eq. (4.28) results

$$\sigma^2(M) < \sigma_N^2$$

To show the improvement in the case where $\rho(k\,t_s) < 1$ we consider the following example.

Example

Given carrier frequency f_c = 1 MHz and data rate R = 200 k bits/sec. If we sample every $t_s = 1\,\mu s$, i.e. 5 samples per symbol bit period. Detection improvement with respect of noise bandwidth B_N is shown in Table (4.I).

B_N	$\frac{\sigma^2(M)}{\sigma_N^2}$	Improvement	
1.2 R	0.707	1.5 dB	Fig. (4.9) a
1.8 R	0.567	2.4 dB	Fig. (4.9) b
2 R	0.45	3.3 dB	Fig. (4.9) c
3 R	0.31	4.9 dB	Fig. (4.9) d

During the measurements we set the noise bandwidth to the 3-dB bandwidth of a four-pole Butterworth filter. The deviation of the experimental results from the calculated ones is due to the deviation of the ideal rectangular filter with bandwidth B_N from the four pole band-pass filter utilized in the laboratory.

4.6 Uncorrelated noise samples

In the case where the $N = B_N \cdot T$ noise samples are uncorrelated, i.e. $\rho(k\,t_s) = 0$, for Gaussian noise this implies N independent samples.

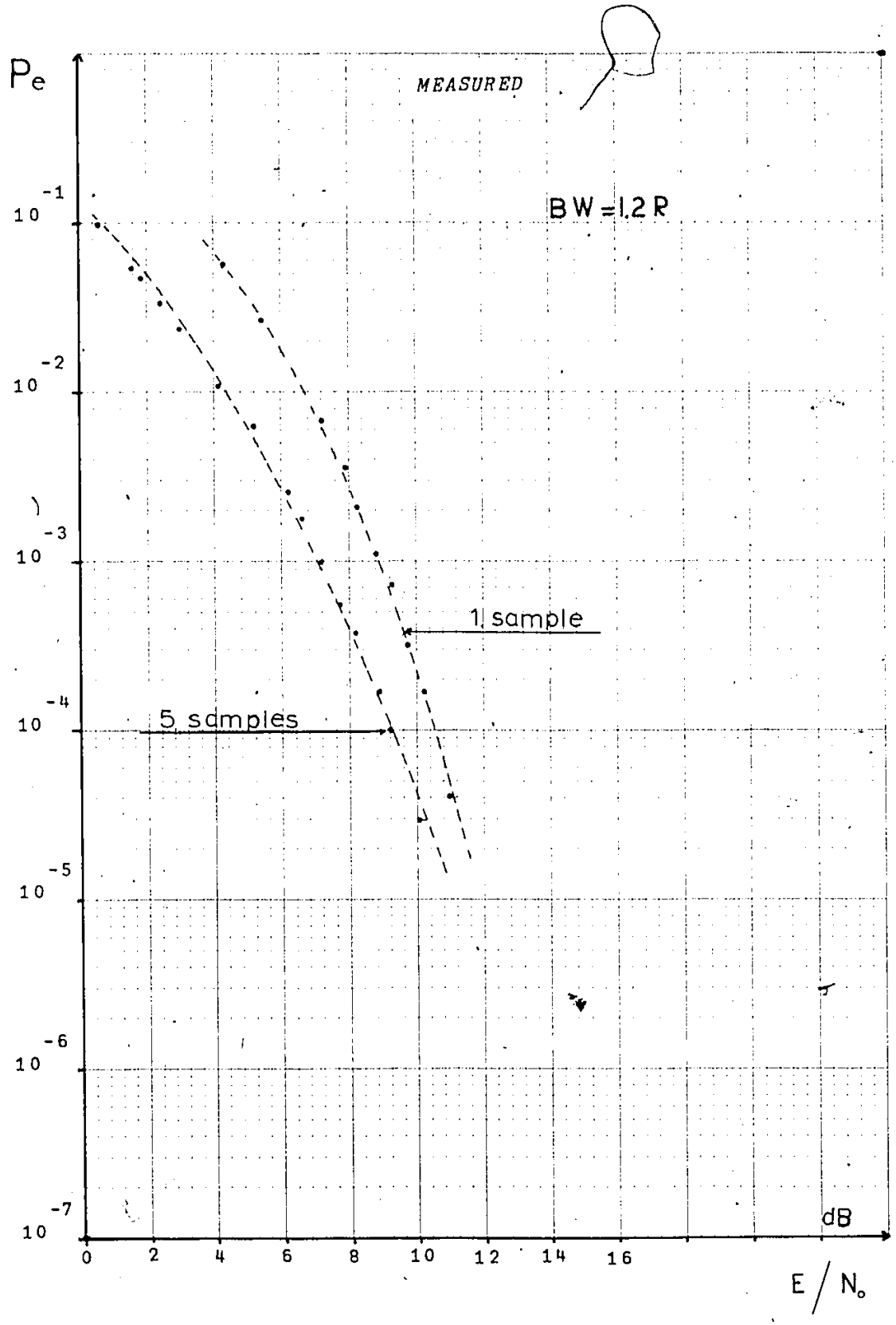

Fig. 4.9a. Measured B.E.R. with BW=1.2 R

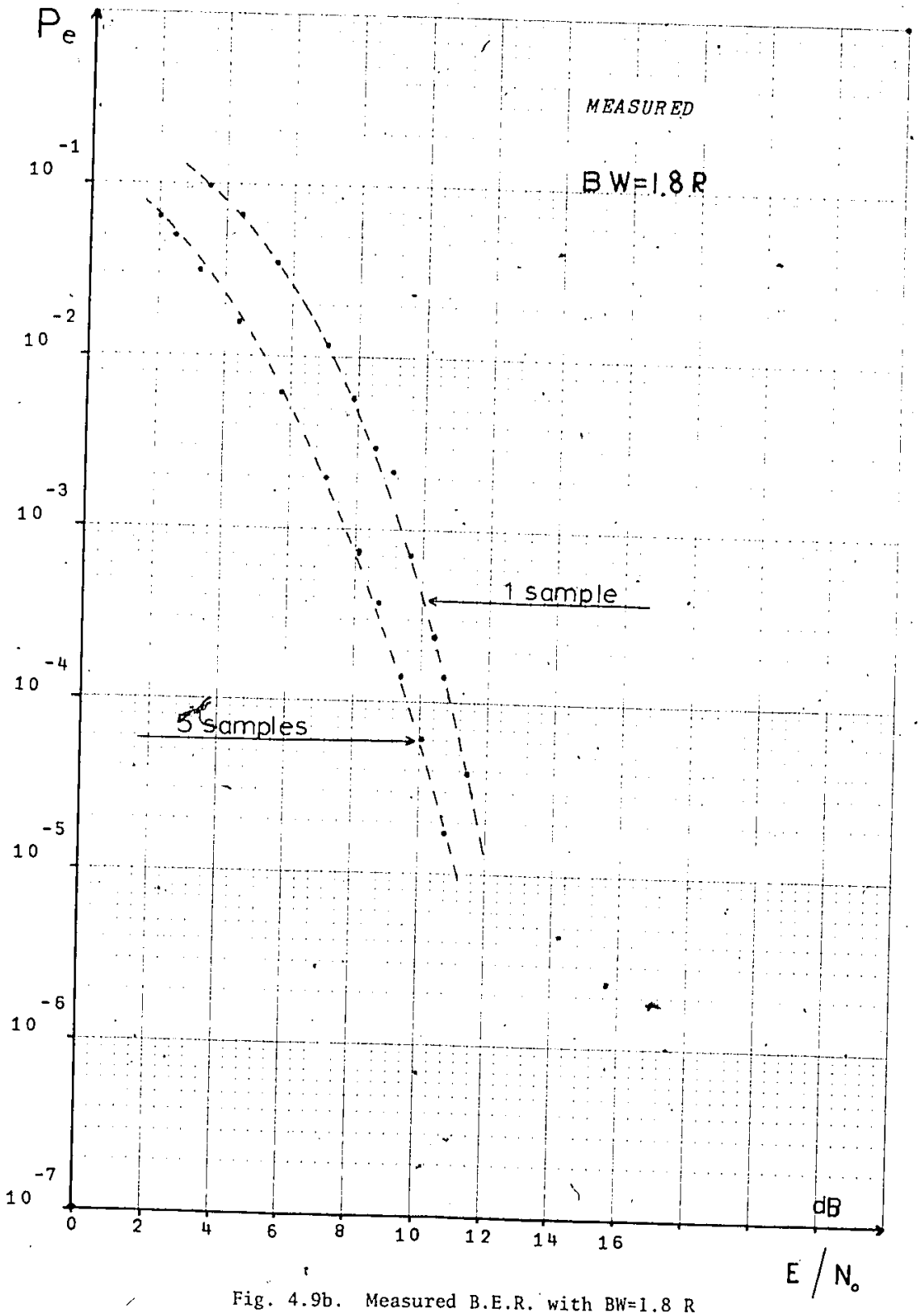

Fig. 4.9b. Measured B.E.R. with BW=1.8 R

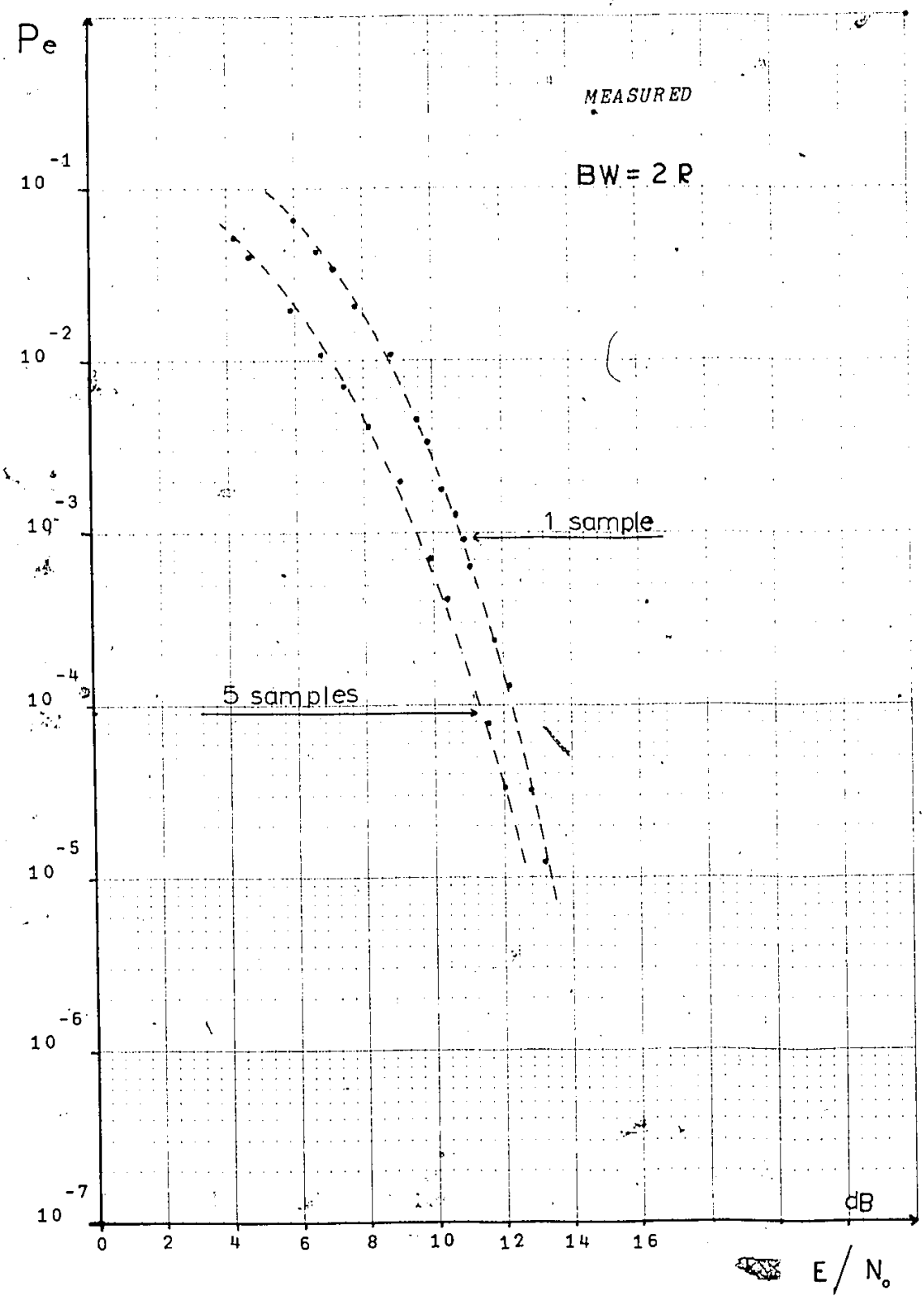

Fig. 4.9c. Measured B.E.R. with BW=2 R

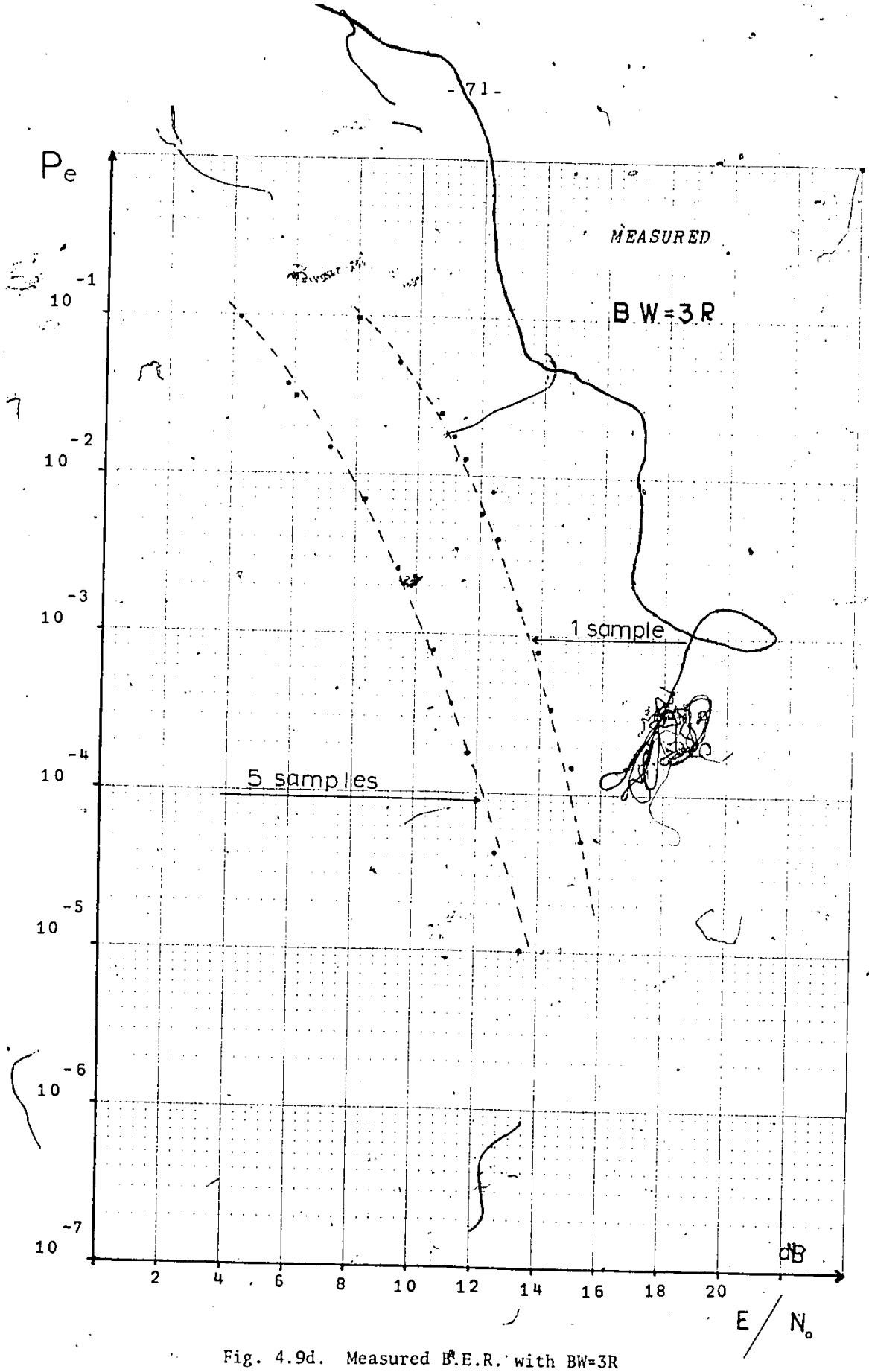

Fig. 4.9d. Measured B.E.R. with BW=3R

The error probability, at the output of the majority logic gate, is then given by the probability that more than half the samples are in error. From the binomial distribution this is given by:

$$Pe_{MAJ} = \sum_{K=0}^{\frac{B_n T-1}{2}} \binom{\frac{B_n T-1}{2}}{K} (1 - Pe_{DEC.})^{K} \cdot (Pe_{DEC.})^{\frac{B_n T-1}{2} K} \quad (4.28)$$

where $B_n T$ = odd and $Pe_{DEC.}$ is the probability of error of one sample at the decision circuit Fig. (4.8) and is given by Eq. (4.22).

Substituting Eq. (4.28) in (4.10) we have

$$Pr\ (b_i = \text{error}) = 2\ Pe_{MAJ}\ (1 - Pe_{MAJ}) \quad (4.29)$$

Equation (4.29) for N = 5 and $B_N = 5R$ was evaluated by numerical integration using Simpson's rule (Appendix II).

The result of integration and the experimental ones, are shown in Fig. (4.10) where $Pe = f\left(\frac{E_B}{N_o}\right)$ is plotted.

From Fig. (4.10) we can see the improvement of about 5 dB by sampling every cycle instead of once, per message bit period, given that the noise samples are uncorrelated.

The effect of timing error was also calculated by numerical integration using Eq. (4.29), (4.28), (4.22) the results are shown in Fig. (4.11). From Fig. (4.11) we have that to suffer no more than 1 dB loss in performance as compared to ideal synchronization case i.e. $\Delta\varphi = 0$, requires

$$\Delta\varphi < 45^{o} \quad \text{or}$$

$$\Delta t = 12.5\% \text{ of } \frac{1}{f_c}$$

that is the sampling accuracy should be within 12.5% of the carrier frequency.

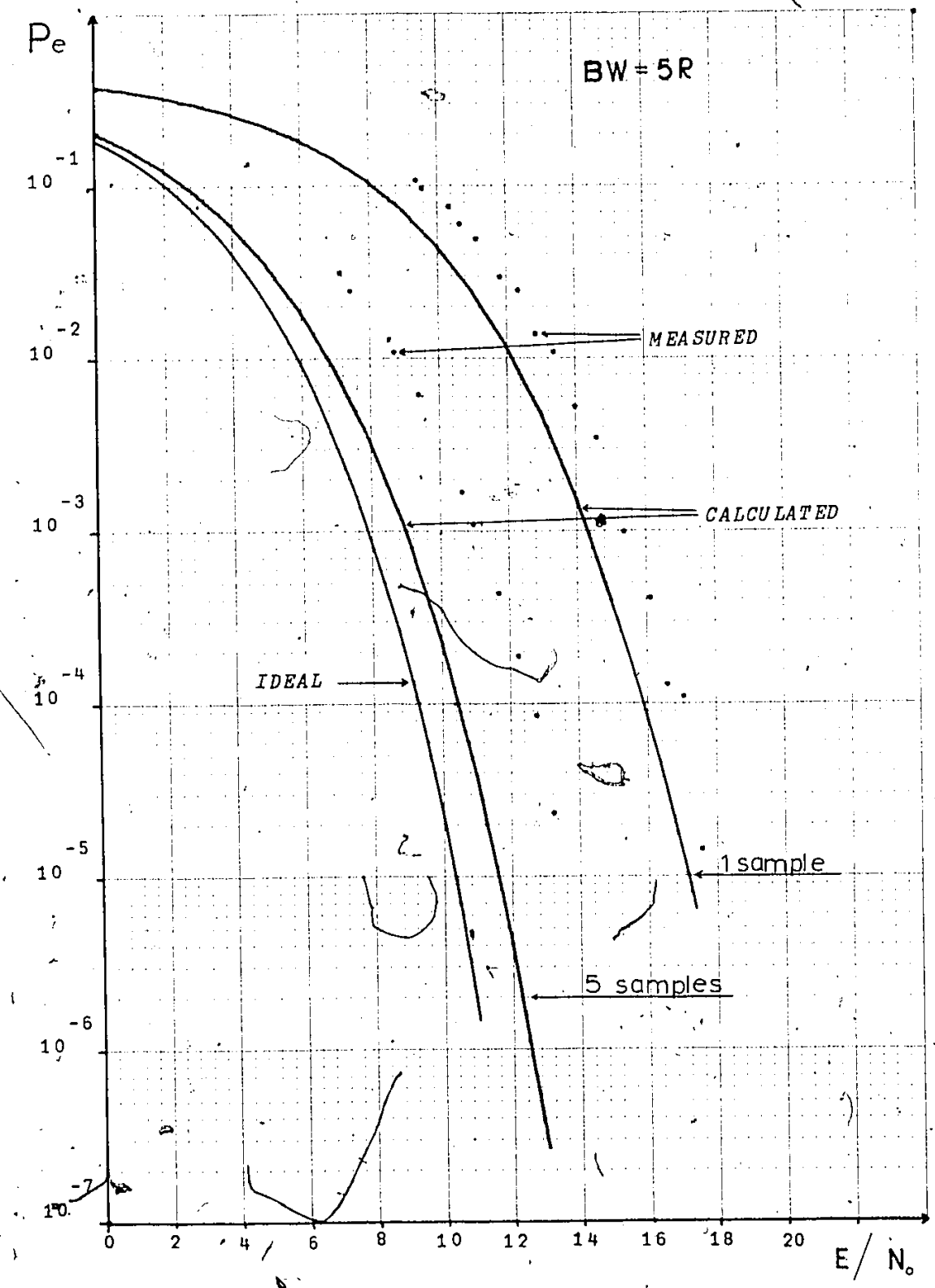

Fig. 4.10. Measured and calculated B.E.R. for two different number of samples uncorrelated noise samples

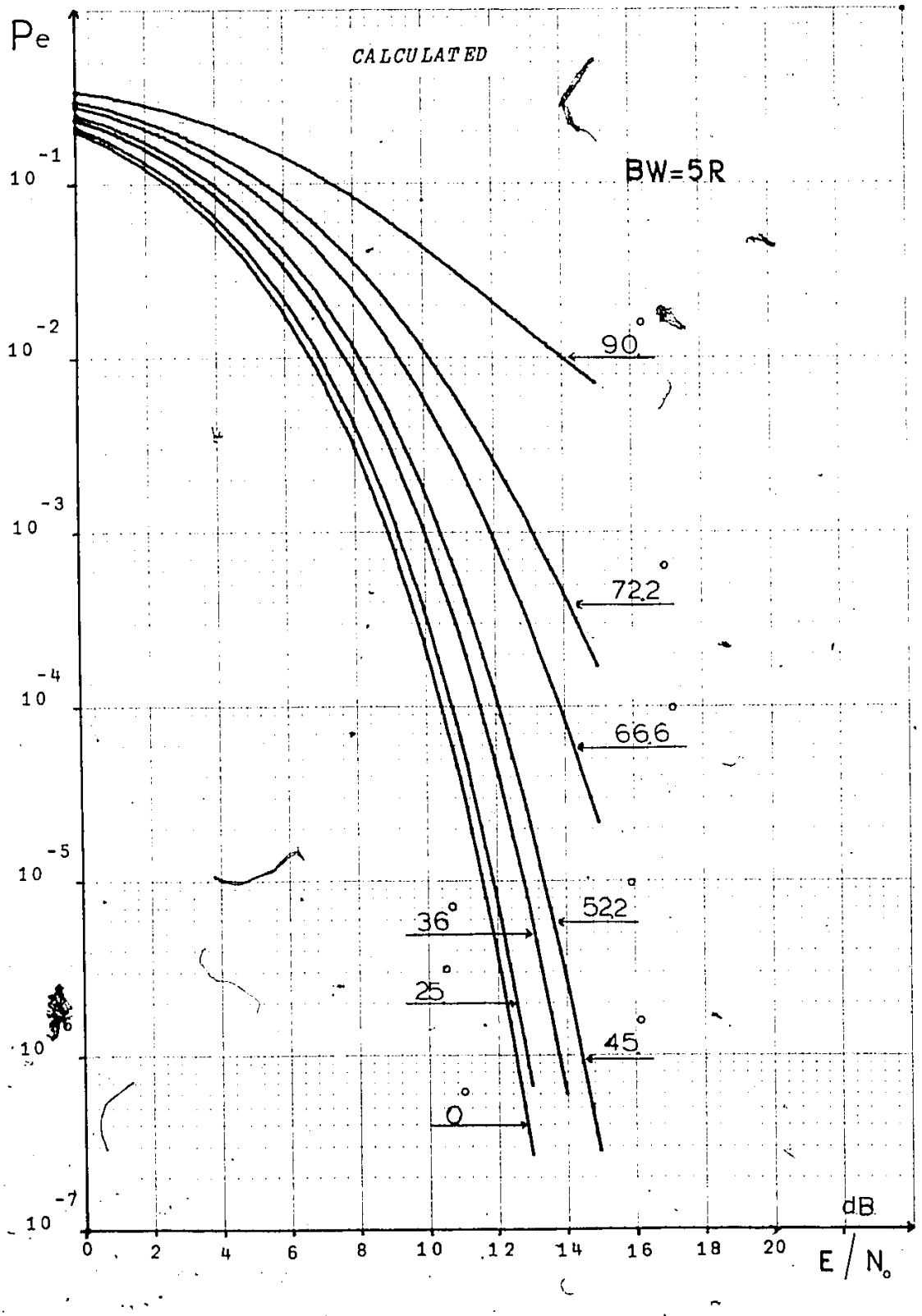

Fig. 4.11. Calculated B.E.R. for different values of timing error

Therefore, in the case where we sample every cycle instead of once within a message bit period, the performance is less sensitive to timing error. However, this margin of 2.5% in synchronization requirements is compensated from the freedom we have, in the case of sampling once per message bit period where we can skip up to N-1 cycles at the beginning of sampling process, whereas in the case of sampling every cycle this freedom is reduced. For example with 5 cycles within one message bit period sampling only once we can skip up to four cycles without any loss, whereas sampling every cycle we can skip no more than 2 cycles.

4.7 CONCLUSION

The required Energy per bit per noise density to obtain probability of error 10^{-4} is shown in Table (4.2), assuming perfect synchronization.

Table 4.2		1 Sample		5 Samples	
Bandwidth	Ideal	Calculated	Measured	Calculated	Measured
N_B	dB for 10^{-4},	dB for 10^{-4}	dB for 10^{-4}	dB for 10^{-4}	dB for 10^{-4}
1.2 R	9.3	9.8	10.7	-	9.4
1.8 R		11.3	11.3	-	9.8
2 R		11.8	12.4	-	11.3
3 R		13.8	15	-	12.2
5 R		15.8	17	10.4	12.5

The improvement by sampling every cycle, instead of once per message bit, is shown in Table (4.3).

Table 4.3

N_B	Calculated	Measured
1.2 R	1.5	(1.3)
1.8 R	2.4	1.5
2 R	3.3	1.1
3 R	4.9	2.8
5 R		4.5

From table 4.2 we have, that for Bandwidth 1.2 times the data rate, i.e. close to 1 x R which is utilized in the analysis of the ideal D.P.S.K. detector, there is no big difference between analog and digital realization of the D.P.S.K. demodulator [15], when we sample every cycle.

For 1 sample per message period [37] the calculated degradation is 0.5 dB and the measured 1,4 dB.

5. EXPERIMENTAL RESULTS

5.1 LABORATORY SIMULATION

The digital demodulator described in Chapter 3 has been tested experimentally as shown in Fig. 5.1.

The transmitter consists of the Pseudo-Random Binary Sequences (P.R.B.S.) generator, generating $2^n - 1$ bits per word period with $n_{max} = 10$. The clock period is controlled by an external clock of period T. The divide by N circuit is used to establish the required relation $T = N/f_c$ between symbol period and carrier, as shown in Fig. 5.2. The binary signal is differentially encoded as shown in Fig. 5.2. The T.T.L. output of the encoder is translated to ± .69 volts, as required to drive the mixer, by means of the level shifter shown in Fig. 5.2. The differentially encoded data, after low-pass filtering, is used to modulate the phase of the carrier by the dual balance mixer to produce the D.P.S.K. signal.

Assuming Gaussian noise as the only disturbance introduced by the channel, we simulate the channel by the circuit shown in Fig. 5.3. A wide band operational amplifier adds the D.P.S.K. output of the balanced mixer with white Gaussian noise. To increase the voltage range of the noise generator (max. 1 volt) a second amplifier is used before the addition process. The noise voltage level is controlled by the voltage level switch on the noise generator.

For the receiver two circuits have been implemented, one for sampling once per symbol period Fig. 5.4 and the second circuit for sampling every cycle, in this case 5 samples per symbol period, Fig. 5.5.

To shift the threshold level of the flip-flop Fig. 5.4, or of the shift register Fig. 5.5 the signal after band pass filtering is entered into a voltage comparator where a potentiometer setting establishes the desired zero level. The voltage comparator is also acting as a driver for the T.T.L. input.

In the case of 1 sample the output of the flip-flop is differentially decoded by the circuit of Fig. 5.4, consists of a D type flip-flop and of an EX-OR gate.

In the case of 5 samples per symbol period, at each clocking the shift register output is transferred to the majority logic gate and is ignored (enable flip-flop low) until all five inputs of the majority gate contain data from the same symbol (enable flip-flop high).

The clock requirements for the flip-flop and the shift register, have been obtained from two different pulse generators, externally driggered from the carrier generator and P.R.B.S. generator. The delay switches of the pulse generator, are used to establish perfect synchronization, i.e. sampling at the peaks of the sine wave.

The recovered signal is compared to the transmitted one by the error detector.

5.2 MEASUREMENTS

The measurements procedure is as follows. With the band pass filter at the desired bandwidth, the peak value of the carrier at the ouptut of the band pass filter is measured, without noise present, the noise voltage is -80 dB down.

Adding noise through the operational amplifier we obtain the readings from the error detector. Without any disconnection, to prevent any impedance distortion, the carrier level is reduced by 130 dBm and the

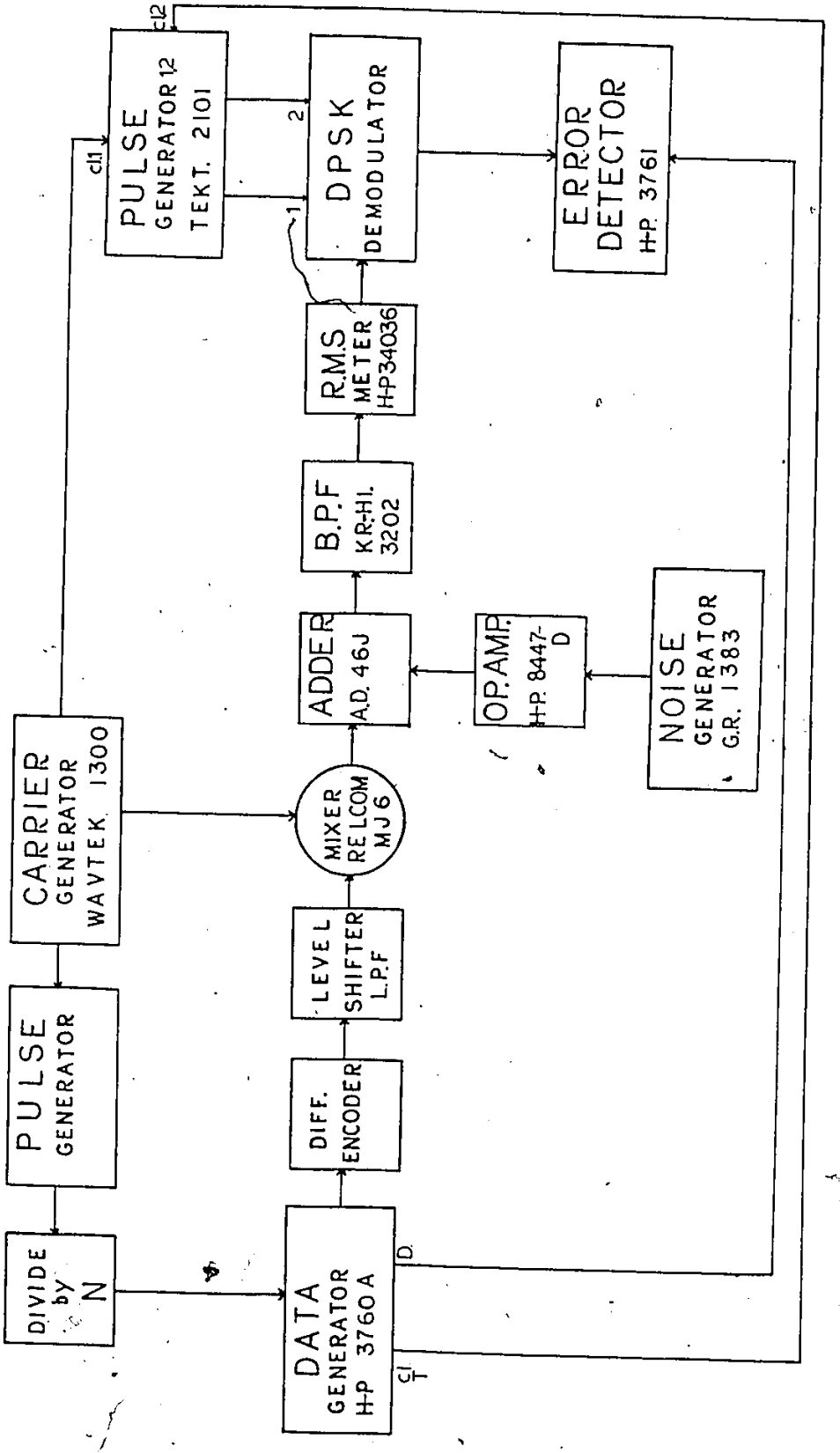

Fig. 5.1. Experimental set-up

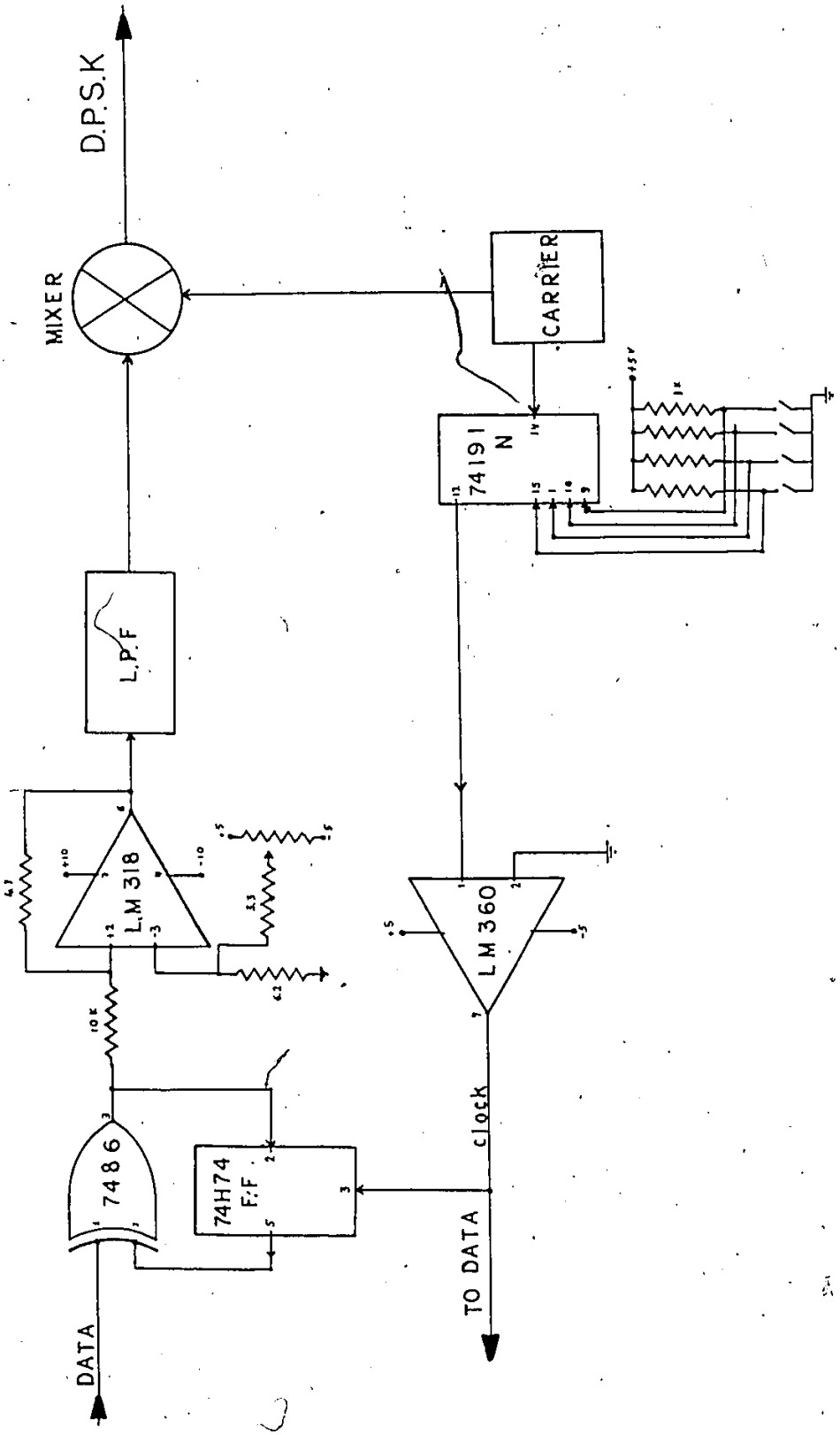

FIG. 52 D.P.S.K MODULATOR

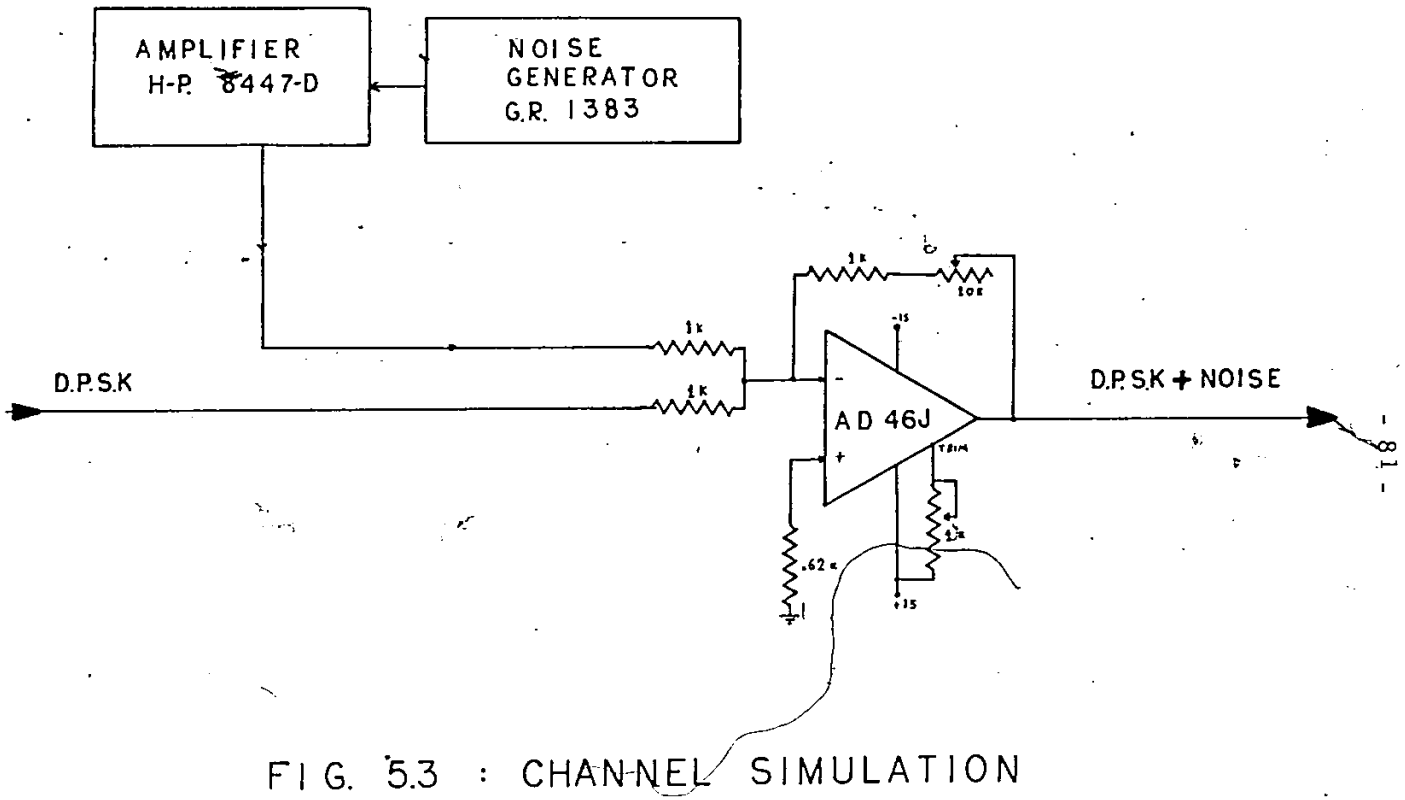

FIG. 5.3 : CHANNEL SIMULATION

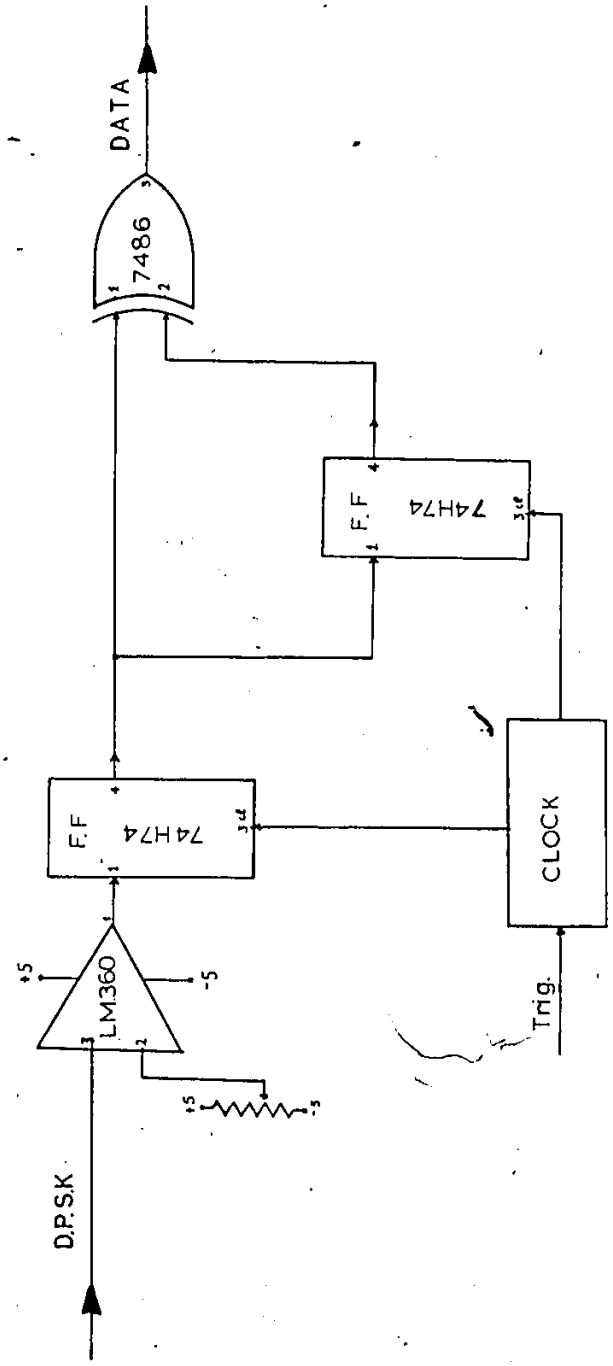

FIG. 5.4 : D.P.S.K DEMODULATOR
1 SAMPLE

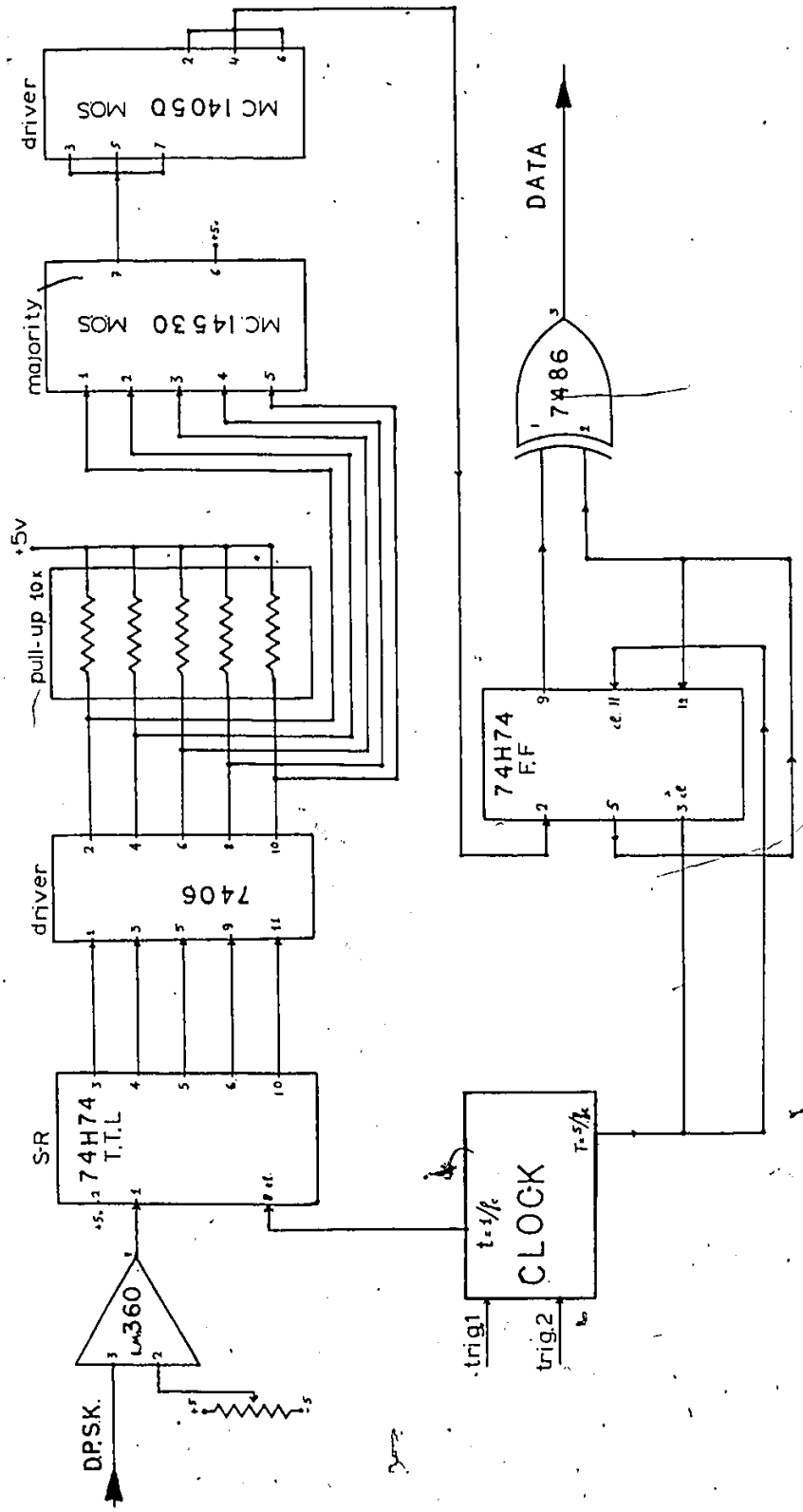

FIG. 5.5: D.P.S.K DEMODULATOR
5-SAMPLES

noise voltage measured at the output of the band pass filter, by a true R.M.S. meter. Increasing the noise voltage and following the above procedure we obtain the experimental results shown in Table 5.1.

The c/N ratio has been transformed to E_b/N_o by multiplying the carrier R.M.S. voltage volume by the square root of the ratio of the filter bandwidth and data rate and divide the square of the product by the square of the noise R.M.S. voltage, according to the relation

$$\frac{E}{N_o} = \frac{BW}{R} \cdot \frac{C}{N} \quad \text{or}$$

$$\frac{E}{N_o} = \frac{\left(\frac{A}{\sqrt{2}} \sqrt{\frac{BW}{R}}\right)^2}{\sigma^2}$$

where A is the carrier peak voltage value and σ the noise R.M.S. voltage.

MEASUREMENTS TABLE. 5.1

1 Sample per Message Period T				
A Peak Volts	Signal $A_{RMS} \cdot \sqrt{BW/_R}$	Noise N_{RMS}	Pe	Comments
1.9	1.47	.417	$4 \quad 10^{-5}$	Carrier 1 MHZ
		.454	$1.7 \quad 10^{-4}$	Data 200 KHZ
		.481	$3.2 \quad 10^{-4}$	
		.506	$7.3 \quad 10^{-4}$	
		.534	$1.1 \quad 10^{-3}$	$BW/_R = 1.2$
		.557	$2.1 \quad 10^{-3}$	
		.593	$3.6 \quad 10^{-3}$	
		.641	$6.8 \quad 10^{-3}$	B.P.F. ±0.888 - 1.12 MHZ
		.788	$2.7 \quad 10^{-3}$	
		.896	$5.8 \quad 10^{-2}$	
		1.032	$1 \quad 10^{-1}$	
2	1.897	.484	$3.8 \quad 10^{-5}$	Carrier 1 MHZ
		.527	$1.4 \quad 10^{-4}$	Data 200 KHZ
		.547	$2.4 \quad 10^{-4}$	
		.594	$7.2 \quad 10^{-4}$	
		.634	$2.2 \quad 10^{-3}$	$BW/_R = 1.8$
		.674	$3 \quad 10^{-3}$	
		.728	$5.8 \quad 10^{-3}$	
		.796	$1.2 \quad 10^{-2}$	B.P.F = .82-1.18 MHZ
		.950	$3.6 \quad 10^{-2}$	
		1.073	$6.8 \quad 10^{-2}$	
		1.202	$1 \quad 10^{-1}$	

A peak Volts	Signal $A_{RMS}\sqrt{BW/_R}$	Noise N_{RMS}	Pe	Comments
2.2	2.19	.517	$3.8\ 10^{-5}$	
		.542	$9.3\ 10^{-5}$	Carrier 1 MHZ
		.563	$1.4\ 10^{-4}$	Data 200 KHZ
		.579	$2.8\ 10^{-4}$	
		.601	$4.4\ 10^{-4}$	$BW/_R = 2$
		.623	$7.8\ 10^{-4}$	
		.642	$8.5\ 10^{-4}$	B.P.F. = 0.8 - 1.2 MHZ
		.663	$1.5\ 10^{-3}$	
		.679	$1.8\ 10^{-3}$	
		.698	$2.6\ 10^{-3}$	
		.726	$3.1\ 10^{-3}$	
		.746	$4.9\ 10^{-3}$	
		.795	$7.8\ 10^{-3}$	
		.902	$2.3\ 10^{-2}$	
2.8	3.42	.583	$5\ 10^{-5}$	Carrier 1 MHZ
		.606	$1.5\ 10^{-4}$	Data 200 KHZ
		.654	$3.5\ 10^{-4}$	
		.689	$8\ 10^{-4}$	$BW/_R = 3$
		.738	$1.5\ 10^{-3}$	
		.801	$4.1\ 10^{-3}$	B.P.F. = 0.7 - 1.3 MHZ
		.851	$5.9\ 10^{-3}$	
		.906	$1.3\ 10^{-2}$	
		.945	$1.8\ 10^{-2}$	
		.991	$2.5\ 10^{-2}$	
		1.159	$5.3\ 10^{-2}$	
		1.352	$1.\ 10^{-1}$	

A peak Volts	Signal $A_{RMS}\sqrt{BW/_R}$	Noise N_{RMS}	Pe	Comments
2.5	3.95	.528	$1.4\ 10^{-5}$	Carrier 1 MHZ
		.559	$1.1\ 10^{-4}$	Data 200 MHZ
		.590	$1.3\ 10^{-4}$	
		.623	$4.1\ 10^{-4}$	$BW/_R = 5$
		.678	$1\ 10^{-3}$	
		.741	$3.5\ 10^{-3}$	
		.794	$5.3\ 10^{-3}$	B.P.F = 0.5 - 1.5 MHZ
		.853	$1.1\ 10^{-2}$	
		.904	$1.4\ 10^{-2}$	
		.957	$3.5\ 10^{-2}$	
		1.018	$3\ 10^{-2}$	
		1.102	$5\ 10^{-2}$	
		1.164	$6.1\ 10^{-2}$	
		1.208	$7.7\ 10^{-2}$	
		1.322	$9.9\ 10^{-2}$	
		1.349	$1.1\ 10^{-1}$	

5 Samples per Message period T				
A Peak Volts	Signal $A_{RMS}\sqrt{BW/R}$	Noise N_{RMS}	Pe	Comments
1.9	1.47	.461	$2.9\ 10^{-5}$	Carrier 1 MHZ
		.510	$1\ 10^{-4}$	Data 200 KHZ
		.535	$1.7\ 10^{-4}$	
		.574	$3.8\ 10^{-4}$	
		.605	$5.6\ 10^{-4}$	$BW/R \simeq 1.2$
		.643	$1\ 10^{-3}$	
		.688	$1.8\ 10^{-3}$	B.P.F = .88 - 1.120 MHZ
		.720	$2.6\ 10^{-3}$	
		.810	$6.4\ 10^{-3}$	
		.913	$1.1\ 10^{-2}$	
		1.041	$2.4\ 10^{-2}$	
		1.115	$3.4\ 10^{-2}$	
		1.192	$4.8\ 10^{-2}$	
		1.229	$5.5\ 10^{-2}$	
		1.381	$1\ 10^{-1}$	
2.1	1.99	.519	$1.7\ 10^{-5}$	Carrier 1 MHZ
		.566	$6.1\ 10^{-5}$	Data 200 KHZ
		.610	$1.4\ 10^{-4}$	
		.660	$3.8\ 10^{-4}$	
		.708	$7.6\ 10^{-4}$	$BW/R = 1.8$
		.795	$2\ 10^{-3}$	
		.928	$6.3\ 10^{-3}$	B.P.F = .82-1.18 MHZ
		1.078	$1.6\ 10^{-2}$	
		1.236	$3.2\ 10^{-2}$	
		1.345	$5.1\ 10^{-2}$	
		1.421	$6.6\ 10^{-2}$	
		1.532	$1\ 10^{-1}$	

A peak Volts	Signal $A_{RMS}\sqrt{BW/_R}$	Noise N_{RMS}	Pe	Comments
2.35	2.34	.587	$3.4\ 10^{-5}$	Carrier 1 MHZ
		.624	$7.9\ 10^{-5}$	Data 200 KHZ
		.672	$2.2\ 10^{-4}$	
		.713	$4.1\ 10^{-4}$	$BW/_R = 2$
		.752	$7.2\ 10^{-4}$	
		.830	$2\ 10^{-3}$	B.P.F = .8-1.2 MHZ
		.921	$4.2\ 10^{-3}$	
		1.0	$7.2\ 10^{-3}$	
		1.079	$1.1\ 10^{-2}$	
		1.194	$2.0\ 10^{-2}$	
		1.375	$4.1\ 10^{-2}$	
		1.443	$5.3\ 10^{-2}$	
2.5	3.18	.677	$1\ 10^{-5}$	Cattier 1 MHZ
		.746	$4.2\ 10^{-5}$	Data 200 KHZ
		.829	$1.8\ 10^{-4}$	
		.881	$3.7\ 10^{-4}$	$BW/_R = 3$
		.946	$8\ 10^{-4}$	
		1.082	$2.6\ 10^{-3}$	
		1.224	$7.1\ 10^{-3}$	B.P.F = .7-1.3 MHZ
		1.394	$1.5\ 10^{-2}$	
		1.583	$3.2\ 10^{-2}$	
		1.632	$3.8\ 10^{-2}$	
		1.95	$1\ 10^{-1}$	

A peak Volts	Signal $A_{RMS}\sqrt{BW/R}$	Noise N_{RMS}	Pe	Comments
2.8	4.42	.895	$2.3\ 10^{-5}$	Carrier 1 MHZ
		.948	$8.6\ 10^{-5}$	Data 200 KHZ
		1.005	$1.9\ 10^{-4}$	
		1.072	$4.4\ 10^{-4}$	$BW/_R = 5$
		1.166	$1.1\ 10^{-3}$	
		1.211	$1.7\ 10^{-3}$	B.P.F.= 0.5 - 1.5 MHZ
		1.398	$6.3\ 10^{-3}$	
		1.514	$1.1\ 10^{-2}$	
		1.75	$2.5\ 10^{-2}$	
		1.81	$3.2\ 10^{-2}$	

REFERENCES

1. Schwartz M., W.R. Bennett, S. Stein: "Communication System and Techniques" McGraw-Hill Book Company 1965.

2. Schwartz M.: "Information Transmission Modulation and Noise" McGraw-Hill Book Company 1970.

3. Taub H., D.L. Schiling: "Principles of Communication Systems" McGraw-Hill Book Company 1971.

4. Stein S., J.J. James: "Modern Communication Principles" McGraw-Hill Company 1967.

5. Lucky B.W., J. Salz, E.J. Weldon: "Principles of Data Communication" McGraw-Hill Book Company 1968.

6. Bennett, W.R., J.R. Davey: "Data Transmission" McGraw-Hill Book Company 1965.

7. Panter P.F.: "Modulation Noise and Spectral Analysis" McGraw-Hill Book Company 1965.

8. Glance B.: "Power Spectra of Multilevel digital phase modulated signals" B.S.T.J. Vol. 50 No. 9, November 1971 pp. 2857.

9. Lundquist L.: "Digital P.M. Spectra by Transform Techniques" B.S.T.J. Vol. 48, No. 2, February 1969, pp. 397.

10. Golomb S.W.: "Digital Communications with Space Applications" Prentice-Hall, Inc. 1964.

11. Golomb S.W.: "Shift Register Sequences" Holden-Day, Inc. 1967.

12. Blackman, N.M.: "The Power Spectrum of a Digital Signal" I.E.E.E. Trans. Commun., Vol. COM-22, March 1974, pp. 349-350.

13. Titsworth R.C., Welch L.R.: "Modulation by Random and Pseudo-Random Sequences" Jet Propulsion Laboratory, California Institute of Technology, Pasadena California, June 12, 1959 Progress Report No. 20-387.

14. Papoulis A.: "Probability, Random Variables and Stochastic Processes" McGraw-Hill Book Company, 1965.

15. Jacobs I.: "The Effects of Video Clipping on the Performance of an Active Satellite P.S.K. Communication System" I.E.E.E. Trans. Commun. Vol. COM-13, June 1965, pp. 195-201.

16. Moris R.L., J.R. Miller: "Designing with T.T.L. Integrated Circuits" McGraw-Hill Book Company 1971.

17. P.C. Jain, N.M. Blackman: "Detection of a P.S.K. Signal Transmitted Through a Hard-limited Channel" I.E.E.E. Trans. Inf. Theory, Vol. IT-19, No. 5, September 1973.

18. Lee J.S., L.E. Miller: "On the binary D.P.S.K. Communication Systems in Correlated Gaussian Noise" I.E.E.E. Trans. Comm., Vol. COM-23, February 1975, pp. 255-259.

19. Watson F. Walker: "The Error Performance of a Class of Binary Communications System in Fading and Noise" I.E.E.E. Trans. Comm. Vol. COM-12, pp. 28-45, March 1964.

20. Shimbo O., M.I. Celebiler, R.J. Fang: "Performance Analysis of D.P.S.K. Systems in both thermal Noise and Intersymbol Interference" I.E.E.E. Trans. Comm., Vol. COM-19, part II, December 1971, pp. 1179-1184.

21. Claire E.J., Claire L.W., S. Kalyanaraman: "Properties of a Class of Signaling Waveforms for Digital Phase Modulation" I.E.E. Trans. Comm., Vol. COM-19, part II, December 1971, pp. 1252-1259.

22. Saltz J., Saltzberg B.R.: "Double Error-Rates in Differentially Coherent Phase Systems", I.E.E.E. Trans. Comm., Vol. COM- , pp. 202-205.

23. Weinstein S.B.: "The White Noise Approximation" I.E.E.E. Trans. Comm. Vol. 17, February 1969, pp. 83-85.

24. Shimbo O., Fang R.J., Celebiler, M.: "Performance of M-ary P.S.K. Systems in Gaussian Noise and Intersymbol Interference" I.E.E.E. Trans. Inf. Theory, Vol. IT-19, No. 1, January 1973, pp. 44.

25. Stein S.: "Unified Analysis of Certain Coherent and Non-coherent Binary Communications Systems" I.E.E.E. Trans. Inform. Th., Vol. IT-10, January 1964, pp. 43-51.

26. Falconer D.D., Werner J.J.: "Comparison Detection of Hard-Limited Digital P.M. Signals" Bell Telephone Laboratories Incorporated Holmdel, New Jersey.

27. Hubbard W.M.: "The Effect of Noise Correlation on Binary Differentially Coherent P.S.K. Communication System" B.S.T.J.

28. James Y.: "Filter Distortion and Intersymbol Interference Effects on P.S.K. Signals" I.E.E.E. Trans. Comm., Vol. COM-19, No. 2, April 1971.

29. A.J. Viterbi: "Principles of Coherent Communication". McGraw-Hill Book Company.

30. Davenport W.B., Root W.L.: "An Introduction to the Theory of Random Signals and Noise" McGraw-Hill Book Company 1958.

31. Lawton J.G.: "Theoretical Error Rate of Differentially Coherent Binary and 'Kineplex' Data Transmission Systems" Proc. I.R.E., Vol. 47, February 1959, pp. 333-374.

32. Cahn C.R.: "Performance of Digital Phase-modulation Communication Systems" I.R.E. Trans. Comm., Vol. C.S.-7, May 1959.

33. Bennett W.R.: "Methods of Solving Noise Problems" Proc. I.R.E. May 1956, pp. 609-638.

34. Rice S.O.: "Statistical Properties of a Sine Wave Plus Random Noise" B.S.T.J., Vol. 27, January 1948.

35. Raemer H.R.: "Statistical Communication Theory and Applications" Prentice-Hall, Inc. Englewood Cliffs, New Jersey 1969.

36. Sunde E.B.: "Communication Systems Engineering Theory" John Wiley and Sons, Inc., 1969.

37. V.O. Hentinen, P.P. Laiho, R.M. Sarkilahti: "A digital Demodulator for P.S.K. Signals", I.E.E.E. Trans. Comm., Vol. COM-21, No. 12, December 1973, pp. 1352-1360.

```
C
C     PROBABILITY OF ERROR OF THE DIGITAL DEMODULATOR
C
C     NO  TIMING  ERROR
C
C     NUMBER OF SAMPLES  N=1,  N=3,  N=5
C
C    FOR BW/R= 1.2, 1.8, 2, 3, 5
C
      REAL*4 GAMA(16),P1(16),DB(16),P2(16),PPSK(16),DPSK(16),PSK(16)
      DO 20 J=1,16
      DB(J)=J-1
      GAMA(J)=10.**((DB(J))*0.1)
      DPSK(J)=0.5*(EXP(-GAMA(J)))
      PSK(J)=0.5*(ERFC(SQRT(GAMA(J))))
20    P1(J)=0.5*ERFC(SQRT((GAMA(J))/BW/R))
      DO 30 N=1,5,2
      N1=((N-1)/2)+1
      WRITE(6,22)N
22    FORMAT('1',10X,'N=',I2,///5X,'DB',10X,'GAMA',10X,'P1',12X,'P2',
     C13X,'PPSK',11X,'DPSK',11X,'PSK',/)
      DO 50 J=1,16
      P2(J)=0
      DO 40 K1=1,N1
      K=K1-1
      NK=1
      IF(K.GT.0) NK=COMB(N,K)
40    P2(J)=P2(J)+NK*((1-P1(J))**K)*((P1(J))**(N-K))
      PPSK(J)=2*P2(J)*(1-P2(J))
      WRITE(6,70)(DB(J),GAMA(J),P1(J),P2(J),PPSK(J),DPSK(J),PSK(J))
70    FORMAT(5X,F5.2,7X,F5.2,5(5X,E10.3))
50    CONTINUE
30    CONTINUE
      END
      FUNCTION COMB(N,K)
      N1=1
      K1=1
      NK1=1
      DO 10 I=1,N
10    N1=N1*I
      DO 25 I=1,K
25    K1=K1*I
      N4=N-K
      DO 27 I=1,N4
27    NK1=NK1*I
      COMB=N1/(K1*NK1)
      RETURN
      END
```

UNIVERSITY OF OTTAWA END JOB 77 16.10 HRS 14 JUL 76

UNIVERSITY OF OTTAWA END JOB 77 16.10 HRS 14 JUL 76

UNIVERSITY OF OTTAWA END JOB 77 16.10 HRS 14 JUL 76

```
C
C     PROBABILITY OF ERROR OF THE DIGITAL DEMODULATOR
C
C     WITH  TIMING  ERROR
C
C     TIMING ERROR IS   FROM  B*(-3.14)   TO   B*(3.14).
C
C     NUMBER OF SAMPLES  N=1,  N=3,  N=5
C
C     FOR BW/R= 1.2, 1.8, 2, 3, 5
C
C
      REAL*4 GAMA(16),P1(16),DB(16),P2(16),PPSK(16),DPSK(16),PSK(16)
      REAL*4 Z(181),DZ(181)
      B=1.0
      DO 201 K7=1,80
      DIST=B*3.141592
      DISTDG=B*90.0
      DO 20 J=1,16
      DB(J)=J-1
      GAMA(J)=10.**((DB(J))*0.1)
      DPSK(J)=0.5*(EXP(-GAMA(J)))
      PSK(J)=0.5*(ERFC(SQRT(GAMA(J))))
      DO 100 I1=1,181
      X1=I1
      X=B*(-3.141592*(91.0-X1))/180.0
  100 DZ(I1)=0.5*(ERFC((SQRT((GAMA(J))/BW/R))*COS(X)))/DIST
      CALL QSF(DIST/180.0,DZ,Z,181)
   20 P1(J)=Z(181)
      DO 30 N=1,5,2
      N1=((N-1)/2)+1
      WRITE(6,252)DISTDG
  252 FORMAT('1',20X,'DISTRIBUTION LIMITS=+,-',F6.2,///)
      WRITE(6,22)N
   22 FORMAT(/,10X,'N=',I2,///5X,'DB',10X,'GAMA',10X,'P1',12X,'P2',
     C13X,'PPSK',11X,'DPSK',11X,'PSK',/)
      DO 50 J=1,16
      P2(J)=0
      DO 40 K1=1,N1
      K=K1-1
      NK=1
      IF(K.GT.0) NK=COMB(N,K)
   40 P2(J)=P2(J)+NK*((1-P1(J))**K)*((P1(J))**(N-K))
      PPSK(J)=2*P2(J)*(1-P2(J))
      WRITE(6,70)(DB(J),GAMA(J),P1(J),P2(J),PPSK(J),DPSK(J),PSK(J))
   70 FORMAT(5X,F5.2,7X,F5.2,5(5X,E10.3))
   50 CONTINUE
   30 CONTINUE
  201 B=B-0.02
      END
      FUNCTION COMB(N,K)
      N1=1
      K1=1
      NK1=1
      DO 10 I=1,N
   10 N1=N1*I
      DO 25 I=1,K
   25 K1=K1*I
      N4=N-K
      DO 27 I=1,N4
   27 NK1=NK1*I
      COMB=N1/(K1*NK1)
      RETURN
      END
```

APPENDIX III

APL PROGRAM FOR GRAPHIC PLOTTER

```
)LOAD PHILIP
SAVED 14.06/ 76.099/ 536
      )FNS PHILIP
∇ PHILIP
 [1] SIG←⍞,0⍴⍞←'SIGNAL'
 [2] NOS←⍞,0⍴⍞←'NOISE'
 [2.5] PEX←⍞,0⍴⍞←'EXPERIMENTAL PROB. OG ERROR'
 [3] RATIO←(SIG×SIG)÷NOS×NOS
 [4] DB←10×10●RATIO
 [5] PE←.5××-RATIO
 [6] 'RATIO'
 [7] RATIO
 [8] 'RATIO IN DB'
 [9] DB
 [10] 'PROBABILITY OF ERROR'
 [11] PE
 [11.1] 'EXPERIMENTAL PROB. OF ERROR'
 [11.2] PEX
 [11.3] 'EXPERIMENTAL'
 [11.4] DB DPLT (10●PEX)
 [11.5] 'CALCULATED'
 [12] DB DPLT (10●PE)
∇
```

VITA

NAME: Philip CONSTANTINOU

DATE OF BIRTH: December 4, 1946

PLACE OF BIRTH: Alexandria, Egypt

I. HIGH SCHOOL: Kifissia, Public High School
Athens, Greece

II. UNIVERSITIES: National University
Athens, Greece

University of Ottawa,
Ottawa, Canada

DEGREE: DIPLOMA in PHYSICS, 1972